

Atomtronic circuits: from many-body physics to quantum technologies

Luigi Amico

*Quantum Research Centre, Technology Innovation Institute, Abu Dhabi, UAE**

INFN-Sezione di Catania, Via S. Sofia 64, 95127 Catania, Italy

Centre for Quantum Technologies, National University of Singapore, 3 Science Drive 2, Singapore 117543, Singapore and

LANEF 'Chaire d'excellence', Université Grenoble-Alpes & CNRS, F-38000 Grenoble, France

Dana Anderson

Department of Physics and JILA, University of Colorado, Boulder, Colorado, 80309-0440, USA

Malcolm Boshier

MPA Division, Los Alamos National Laboratory, Los Alamos, NM 87545, USA

Jean-Philippe Brantut

Institute of Physics, EPFL, 1015 Lausanne, Switzerland

Leong-Chuan Kwek

Centre for Quantum Technologies, National University of Singapore, 3 Science Drive 2, Singapore 117543, Singapore

MajuLab, CNRS-UNS-NUS-NTU International Joint Research Unit, UMI 3654, Singapore and

Institute of Advanced Studies, Nanyang Technological University, 60 Nanyang View, Singapore 639673, Singapore

Anna Minguzzi

Université Grenoble-Alpes and CNRS, LPMMC, F-38000 Grenoble

Wolf von Klitzing

Institute of Electronic Structure and Laser, Foundation for Research and Technology-Hellas, Crete, Heraklion 70013, Greece

Atomtronics is an emerging field that aims to manipulate ultracold atom moving in matter wave circuits for both fundamental studies in quantum science and technological applications. In this colloquium, we review recent progress in matter-wave circuitry and atomtronics-based quantum technology. After a short introduction to the basic physical principles and the key experimental techniques needed to realize atomtronic systems, we describe the physics of matter-waves in simple circuits such as ring traps and two-terminal systems. The main experimental observations and outstanding questions are discussed. We also present possible applications to a broad range of quantum technologies, from quantum sensing with atom interferometry to future quantum simulation and quantum computation architectures.

Contents

I. Introduction	2	C. Atom optical elements	7
II. Traps and Guides	3	1. Waveguides	7
A. Optical Potentials	3	2. Ring traps	7
1. Static laser beams	3	3. Barriers and beam splitters	8
2. Time-averaged optical potentials	3	III. Coherent effects in mesoscopic matter-wave circuits	9
3. Spatial light modulators and Digital Micro-Mirror Devices	4	A. Model Hamiltonians	9
B. Magnetic potentials	4	1. Bosons	9
1. Magnetic traps	4	2. Fermions	10
2. Atom chips	5	3. Impurities, weak-links and contacts	11
3. Adiabatic Magnetic Potentials	5	B. Persistent currents in atomtronic circuits	11
4. Time-Averaged Adiabatic Potentials (TAAPs)	6	1. The concept of persistent current	11
		2. Experimental observation and read out of persistent current in bosonic toroidal-shape atomtronic circuits	12
		3. Persistent current in fermionic rings	13
		C. Two terminal quantum transport in cold atom mesoscopic structures	14
		1. Double well systems	14

*On leave from Dipartimento di Fisica e Astronomia, Via S. Sofia 64, 95127 Catania, Italy

2. Conductance measurements and incoherent reservoirs	16
3. Two terminal transport through ring condensates	18
IV. Atomtronic Components and Applications	18
A. Matter wave optics in atomtronic circuits	18
B. Transistors, diodes, and batteries	19
C. The atomtronic quantum interference device	20
D. Atomtronic qubit implementations	21
E. Atomtronic interferometers	22
V. Remarks and Future Perspectives	23
Acknowledgments	24
References	24

I. INTRODUCTION

Atomtronics is the emerging quantum technology of matter-wave circuits which coherently guide propagating ultra-cold atoms (Amico *et al.*, 2017, 2021, 2005; Seaman *et al.*, 2007). Developing and applying such circuits has been a goal of cold atom physics for decades: see, for example, the opening paragraphs in Dekker *et al.*, 2000; Dumke *et al.*, 2002; Leanhardt *et al.*, 2002; Müller *et al.*, 1999; Schneble *et al.*, 2003. Realizing this vision was an important motivation for the invention and development of atom chip technology in the early years of this century (Denschlag *et al.*, 1999a,b; Schmiedmayer, 1995b; Schmiedmayer and Scrinzi, 1996a,b). While this approach has not yet demonstrated coherent propagation of guided matter waves, there is an extensive body of work on coherent manipulation of trapped clouds of ultracold atoms on atom chips which provides a foundation for the more recent work discussed here. This research is reviewed in (Folman *et al.*, 2002; Fortágh and Zimmermann, 2007; Keil *et al.*, 2016; Reichel, 2002; Reichel and Vuletić, 2011). In the implementations of atomtronic circuits realized to date, matter waves travel in guides made of laser light or magnetic fields. These approaches offer highly controllable, flexible and versatile platforms at the microscopic spatial scale (Gauthier *et al.*, 2019; Henderson *et al.*, 2009; Rubinsztein-Dunlop *et al.*, 2016). The quantum fluid flowing through atomtronic circuits is provided by ultracold atoms that can be fermions, bosons, or a mixture of the two species. Cold atom quantum technology allows coherent matter-wave manipulations with unprecedented control and precision over a wide range of spatial lengths and physical conditions. (Bloch, 2005; Cornell and Wieman, 2002; Dalfovo *et al.*, 1999; Ketterle, 2002).

Atomtronic circuits are suitable as cold-atom quantum simulators (Bloch, 2005; Buluta and Nori, 2009; Cirac and Zoller, 2012; Dowling and Milburn, 2003; Lamata *et al.*, 2014; Lewenstein *et al.*, 2012) in which matter wave currents are harnessed as probes to explore the physics of the system. In this way, important problems in fundamental quantum science, such as superfluidity, strong correlations in extended systems, topological aspects in

quantum matter, quantum transport, and various mesoscopic effects, can be studied from a new angle (Burchianti *et al.*, 2018; Del Pace *et al.*, 2021; Husmann *et al.*, 2015; Krinner *et al.*, 2016; Stadler *et al.*, 2012; Valtolina *et al.*, 2015).

At the same time, atomtronic circuits play an important role in applied science and technology. Like electronic devices, atomtronic circuits operate over a separation of time and length scales between devices and leads. This permits the construction of standardized functional units connected to each other by waveguides acting as wires. Atomtronic counterparts of known electronic or quantum electronic components have been the first developments in the field. Some examples include atomtronic amplifiers, diodes, switches, batteries, and memories (Anderson, 2021; Caliga *et al.*, 2017, 2016b; Pepino *et al.*, 2009; Pepino, 2021; Seaman *et al.*, 2007; Stickney *et al.*, 2007; Zozulya and Anderson, 2013). Moreover, cold atom realizations of Josephson junctions have led to the fabrication and analysis of atomtronic superconducting quantum interference devices (SQUIDs) (Aghamalyan *et al.*, 2015; Amico *et al.*, 2014; Eckel *et al.*, 2014b; Haug *et al.*, 2018b; Jendrzejewski *et al.*, 2014; Ramanathan *et al.*, 2011; Ryu *et al.*, 2013, 2020; Wright *et al.*, 2013a). Atomtronics can also contribute to the field of quantum sensors (Bongs *et al.*, 2019; Cronin *et al.*, 2009; Degen *et al.*, 2017). Building on the pioneering demonstrations of compact atom interferometers using trapped Bose-Einstein condensates (BECs) (Böhi *et al.*, 2009; Günther *et al.*, 2007; Jo *et al.*, 2007; Riedel *et al.*, 2010; Schumm *et al.*, 2005), several solutions for compact atomtronic interferometers with enhanced sensitivity to inertial forces and electromagnetic fields have been studied (Akatsuka *et al.*, 2017; Burke and Sackett, 2009; Kim *et al.*, 2022; Krzyzanowska *et al.*, 2022; McDonald *et al.*, 2013a, 2014; Moan *et al.*, 2020; Qi *et al.*, 2017; Ryu and Boshier, 2015; Wang *et al.*, 2005; Wu *et al.*, 2007). Finally, we observe that the aforementioned specific properties of coherence, control and flexibility characterizing ultracold matter-wave circuits can enable devices with no direct analog in electronics or photonics technology. Proofs of concept built on features inherent to specified microscopic implementations and combined with specifically suited enabling technologies have been considered recently (Aghamalyan *et al.*, 2013; Amico *et al.*, 2014; Chetcuti *et al.*, 2022a; Kim *et al.*, 2022; Krzyzanowska *et al.*, 2022; Lau *et al.*, 2022; Naldesi *et al.*, 2022).

In this Colloquium, we provide a short and accessible review of the atomtronics field for a broad educated audience of researchers. For a more technical discussions of some of the most recent developments, we refer the reader to the roadmap article Amico *et al.*, 2021. The Colloquium is organized as follows: In Sec. II, we discuss the state of the art in optical and magnetic trapping technologies that lead to a variety of circuits. In Sec. III, we focus on the coherent flow in simple atomtronic networks of mesoscopic size. In this section, we bridge many-body models with persistent currents and two-terminal trans-

port through a mesoscopic channel. In Sec. IV we describe some of the components that have been studied and developed so far. Finally, we conclude and provide an outlook in Sec.V.

II. TRAPS AND GUIDES

Atomotronics has been made possible by the ability to trap matter waves of coherent cold atoms in complex smooth potentials in which matter waves can be feasibly created, guided, and manipulated in controllable and flexible fashion. These potentials are produced either by optical fields that exert forces on atoms through their polarizability or by magnetic fields that create forces on atomic magnetic dipoles.

A. Optical Potentials

The formation of optical potentials through static or dynamic laser beams is a mature technology for the realization of atomtronic circuitry. The flexible potentials can have almost arbitrary complexity in both space and time domains.

Optical manipulation of ultracold atoms is based on the electric dipole interaction between the atoms and the laser beam. When the laser frequency ω is far-detuned from an atomic transition of frequency ω_0 , the interaction energy takes the form of an optical dipole potential $U(\mathbf{r}) = -\frac{3\pi c^2 \Gamma}{2\omega_0^3 \Delta} I(\mathbf{r})$, where $\Delta = \omega - \omega_0$ is the detuning, Γ is the natural decay rate of the population of the excited state, and $I(\mathbf{r})$ is the position-dependent laser intensity. This dipole force can be attractive ($\Delta < 0$ or “red-detuned”) or repulsive ($\Delta > 0$ or “blue-detuned”) (Grimm *et al.*, 2000). The detuning should be large enough so that spontaneous scattering is negligible on the timescale of the experiment.

1. Static laser beams

Waveguides supporting coherent propagation of matter waves must be smooth to avoid excitations out the guide ground state to higher modes, and stable because fluctuations in the potential cause fluctuations in the phase accumulated by the matter wave. A collimated laser beam is a straightforward solution to this problem. The first guides for cold, non-condensed atoms used the evanescent field of blue-detuned light propagating in a hollow optical waveguide (Müller *et al.*, 2000; Renn *et al.*, 1996; Rhodes *et al.*, 2002). This is followed by the introduction of traps and guides based on hollow blue-detuned laser beams created with doughnut or Laguerre-Gaussian transverse modes that removed the need for a material optical guide (Kuga *et al.*, 1997). This approach enabled creation of the first waveguide for a Bose-Einstein con-

densate (BEC) (Bongs *et al.*, 2001). When the Laguerre-Gaussian beam is tightly focused, the optical dipole potential becomes more like a toroidal trap (Olson *et al.*, 2007) than a waveguide. Waveguide potentials can also be realized with Bessel beams (Arlt *et al.*, 2000).

Red-detuned collimated laser beam is a simpler technology for creating atomtronic waveguides when spontaneous emission is sufficiently small. An early example of this approach is the realization of a simple beamsplitter for propagating cold thermal atoms with a pair of crossed red-detuned laser beams (Houde *et al.*, 2000). Subsequent demonstrations include coherent propagation of BEC matter wavepackets to realize a Mach-Zehnder atom interferometer (Kim *et al.*, 2022; McDonald *et al.*, 2013a), a beamsplitter for BECs (Gattobigio *et al.*, 2012) and a waveguide Sagnac atom interferometer (Krzyzanowska *et al.*, 2022). Red-detuned collimated lasers are also used to guide the matter wave produced by an atom laser (Couvert *et al.*, 2008; Dall *et al.*, 2010; Guerin *et al.*, 2006). A very recent development is the use of clipped gaussian beams to create elongated trapping and guiding potentials (Lim *et al.*, 2021).

Besides the standard approaches mentioned above, microfabricated optical elements (Birkel *et al.*, 2001), arrays of micro-lenses (Dumke *et al.*, 2002) and the application of conical refraction in a biaxial crystal (Turpin *et al.*, 2015) have been proposed as sophisticated routes to realize complex circuits. Standing waves of laser light impressed on a collimated laser waveguide have been shown to form a distributed Bragg reflector (Fabre *et al.*, 2011). Pulsed optical standing waves are also employed as beam splitters (Kim *et al.*, 2022; Krzyzanowska *et al.*, 2022; Wang *et al.*, 2005; Wu *et al.*, 2005).

2. Time-averaged optical potentials

Optical dipole potentials based on static laser beams are cylindrically symmetric and they can have no time dependence beyond a scaling of the trap strength. This shortcoming motivated the development of time-averaged optical potentials. Similar to the guides discussed above, the initial experiments with this approach used non-condensed thermal atoms, confining them to box and stadium potentials with walls formed by a blue-detuned laser beams that is rapidly scanned with a pair of acousto-optic deflectors (Friedman *et al.*, 2001; Milner *et al.*, 2001). While early experiments on trapping Bose-Einstein condensates (BECs) in multiple wells, formed by rapidly switching the position of a single red-detuned laser, find that the condensates are heated (Onofrio *et al.*, 2000), that issue is absent in later work in which a time-averaged tightly-focused laser beam “paints” a desired potential on a canvas provided by a light sheet that confined atoms to a horizontal plane. This “painted potential” (Henderson *et al.*, 2009; Schnelle *et al.*, 2008) is able to realize arbitrary and dynamic 2D matter waveguide structures-see Fig.1a). This includes the important

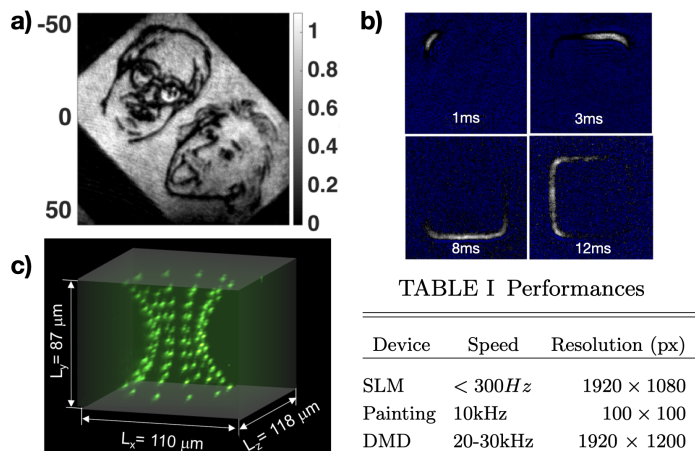


FIG. 1 A Bose-Einstein condensate trapped in potential made by a) DMD, length scales in μm , b) painting technique, dimension of each image is $70 \times 70 \mu\text{m}$, c) SLM. The table compares the performances of the devices in terms of refreshing time, resolution, and diffraction efficiency. Figures a) adapted from Gauthier *et al.*, 2016; b) adapted from Ryu and Boshier, 2015, c) adapted from Barredo *et al.*, 2018.

case of toroidal potentials, (Bell *et al.*, 2016; Henderson *et al.*, 2009; Ryu *et al.*, 2014), where periodically reducing the intensity the laser painting the attractive potential creates movable repulsive barriers that can form Josephson junctions in an atom SQUID geometry (Ryu *et al.*, 2013, 2020). Repulsive barriers can also be imposed on a trap by painting with a blue-detuned laser (Ramanathan *et al.*, 2011; Wright *et al.*, 2013a). A significant advantage of this approach is that a suitable modulation of the tweezer beam intensity as it paints the atomtronic circuit can flatten out any imperfections in the potential (Bell *et al.*, 2016; Ryu and Boshier, 2015), enabling creation of waveguides smooth enough to support single mode propagation and to realize the first coherent beam splitter for propagating matter waves (Ryu and Boshier, 2015).

While painting has the advantages of making efficient use of laser power and enabling fine control of the shape of the potential landscape, it has some limitations. The time averaging requirement that the potential be painted at a rate significantly higher than the guide trapping frequency limits the trapping frequencies attainable with current acousto-optic deflector technology to several kHz. While it is usually a good approximation to regard the painted potential as static, in some circumstances the time-varying phase imprinted by the painting beam can be an issue (Bell *et al.*, 2018).

3. Spatial light modulators and Digital Micro-Mirror Devices

A second technology for creating complex 2D potential landscapes on a light sheet relies on spatial light modulators (SLMs) that can impose amplitude or phase modulation on a laser beam which forms the desired po-

tential after propagation through suitable optics. Two approaches have been demonstrated: a Fourier optics approach in which the SLM acts as a hologram, and a direct imaging of an intensity pattern formed by the SLM. A detailed discussion of the production of arbitrary optical potentials is presented in reference (Gauthier *et al.*, 2021). A recent demonstration for SLM realization of 3d-potentials was reported in Barredo *et al.*, 2018c).

Early work in this direction used liquid crystal modulators to create phase holograms producing arrays of tweezer beams (Curtis *et al.*, 2002) or more complex geometries (Boyer *et al.*, 2004, 2006; Gaunt and Hadzibabic, 2012). Liquid crystal SLMs are now widely used in creating dynamic optical tweezer systems for assembling arrays of Rydberg atoms used for quantum information processing (Nogrette *et al.*, 2014). Advantages of liquid crystal modulators include the ability to impose phase or amplitude modulation on an optical beam and the possibility of using them either as holographic elements or for direct imaging, as well as a high power efficiency. The disadvantages include a limited response time for creating time-dependent potentials, as well as the technical overhead of computing real-time SLM holograms for dynamic potentials, which can be addressed using increasingly powerful GPUs.

An alternative to SLMs are digital micromirror devices (DMDs), producing binary patterns over a matrix of individually switched mirrors. The intensity pattern formed by the DMD can be imaged directly onto an atomic cloud using standard imaging techniques to form intricate potentials in the image plane of the optical system. Fine intensity control overcoming the binary nature of the DMD can then be achieved through half-toning techniques (Gauthier *et al.*, 2021, 2016; Kumar *et al.*, 2016a; Tajik *et al.*, 2019; Zou *et al.*, 2021). DMDs can also be used as programmable diffraction gratings, similar to SLMs, at the expenses of low power efficiency (Zupancic *et al.*, 2016). However, they offer higher refresh rate, allowing for their use in dynamical experiments (Ha *et al.*, 2015). Fig. 1b) illustrates the power of this technique for creating a BEC in the shape of a sketch of Bose and Einstein. DMDs do suffer from flicker modulation due to their intended use in image projectors for the consumer market and so some devices may require customization for optimal use (Hueck *et al.*, 2017).

The performances of painting techniques, SLM, and DMD are summarized in the table of Fig. 1. The three techniques share a diffraction efficiency of $\sim 65 - 80\%$.

B. Magnetic potentials

1. Magnetic traps

Magnetic trapping lies at the heart of many cold atoms quantum technologies. Here, we sketch the logic of the technique. Magnetic traps confine spin-polarized atoms of non-zero magnetic moment to a local minimum of a

static magnetic field \mathbf{B} . If the magnetic field at the center of mass position of an atom is sufficiently large and varies slowly, then its spin follows its change in direction and magnitude. The Zeeman energy of spin polarized atoms ($V = -\boldsymbol{\mu} \cdot \mathbf{B}$) can then be written as $V = m_F g_F \mu_B |\mathbf{B}|$, with $m_F = \{-F \dots F\}$ being the magnetic hyperfine number, g_F the Landé g -factor, and μ_B the Bohr magneton. Unfortunately, Maxwell's equations forbid the generation of a dc-magnetic field maximum in free space. Therefore, one has to trap so-called low-field seeking states, whose energy increases with magnetic field strength. The field strength of the magnetic minimum has to be sufficiently large in order to prevent non adiabatic spin-flip transitions to lower-energy (high-field seeking) states. The latter can cause atoms to be expelled from the trap (Majorana, 1932). The two most common magnetic configurations are the Ioffe-Pritchard (IP) (Baiborodov *et al.*, 1963; Pritchard, 1983) and the time-orbiting potential (TOP) (Petrich *et al.*, 1995) traps.

An IP-trap consists of a radial quadrupole and an axial parabolic field, which together generate an elongated local minimum in the magnetic field. Typical values for the radial trap frequency range from few hundreds for macroscopic traps to few thousands Hz for chip-based traps (Hänsel *et al.*, 2001). Typical axial frequencies are a few tens of hertz. Macroscopic IP traps are usually formed from a combination of large race-track shaped coils for the radial gradient and small 'pinch' coils for the parabolic axial field. It is also possible to use structures from permanently magnetized materials, allowing the creation of larger magnetic gradients and thus steeper traps. They also provide a larger degree of freedom in design when compared to their purely electro-magnetic counterparts albeit at the cost of an inability to dynamically change the strength of the confinement or easily release the atoms from the trap (Davis, 1999; Fernholz *et al.*, 2008; Sinclair *et al.*, 2005; Tollett *et al.*, 1995).

The TOP-trap uses a static magnetic quadrupole field, the center of which is displaced away from the atoms using a rotating magnetic homogeneous offset field (Hodby *et al.*, 2000; Petrich *et al.*, 1995). This oscillating field may be modified locally using inductively coupled conducting structures (Pritchard *et al.*, 2012; Sinuco-León *et al.*, 2014). Care must be taken for the offset field to rotate slow enough for the spin of the atoms to be able to follow, but fast enough for the center of mass of the atoms not to be significantly affected. If this condition is fulfilled, then the atoms will be trapped in the time-average of the magnetic potential. For a static magnetic quadrupole field with an offset field rotating in the symmetry plane this will result in trap with the shape of an oblate sphere and the trapping frequencies $\omega_z = \sqrt{8}\omega_x = \sqrt{8}\omega_y$, with typical trapping frequencies from $\omega_z/2\pi = 40$ Hz to 1 kHz.

2. Atom chips

A simple atom-trap can be produced by applying a transverse homogeneous magnetic field to the one produced by a single wire (Schmiedmayer, 1995a). By shaping the wires on a surface, 'Atom chip' traps (Folman *et al.*, 2000; Hänsel *et al.*, 2001; Reichel *et al.*, 1999) consisting of micro-sized current-carrying wires can be efficiently manufactured using standard semiconductor technologies. Such thin wires can be cooled very efficiently through the substrate and thus permit very large current densities resulting in very large magnetic gradients. Consequently, trapping frequencies of 10 kHz can be achieved. Another advantage is the ability to create in 2D complex wire structures (Folman *et al.*, 2000; Fortágh and Zimmermann, 2007; Keil *et al.*, 2016). Simple H-, T-, U-, Y- and Z-shaped wires can create a wide range of fields. For example, a magnetic IP trap can be formed with an elongated Z-shaped structure, a 3D quadrupole trap with a simple U-shaped wire (Reichel *et al.*, 1999), and a 2D-quadrupole can be formed from three parallel wires, thus creating a matter wave waveguide along which atoms can be propagated (Folman *et al.*, 2000; Long *et al.*, 2005). Cryogenically cooled atom chips have also allowed superconducting devices to be incorporated (Hyafil *et al.*, 2004; Mukai *et al.*, 2007; Nirrengarten *et al.*, 2006; Salim *et al.*, 2013). Atom chips have thus become compact hybrid platforms to trap, prepare, manipulate, and measure cold atoms. They provide the route for miniaturization and interfacing different atomtronic components in more complex devices (Birkl *et al.*, 2001; Gehr *et al.*, 2010; Salim *et al.*, 2013).

Corrugation and noise currents in the conducting wires of an atom chip represent an important challenge to atom-chip based atomtronic circuits that allow a coherent flow of atoms over macroscopic distances (Folman *et al.*, 2002; Henkel *et al.*, 2003). These noises can emerge from diverse causes, ranging current scattering due to unintended changes in flow of direction of the current, noises in the power supplies, or magnetic impurities (David *et al.*, 2008; Kraft *et al.*, 2002; Krüger *et al.*, 2007; Leanhart *et al.*, 2002) to thermal (Johnson) noise (Dikovskiy *et al.*, 2005). Routes to reduce the corrugations in the wave guides have been studied in (Schumm *et al.*, 2005; Trebbia *et al.*, 2007). However, the mere fact that the shape of the atom chip potentials is defined by wire structures means that any imperfections in the wires cause defects and roughness in these potentials and make the single mode propagation over long distance very difficult to achieve.

3. Adiabatic Magnetic Potentials

Adiabatic magnetic potentials offer a very interesting alternative to chip-based structures. They can be used to create a limited number of perfectly smooth trapping structures such as bubbles, rings and sheets. They

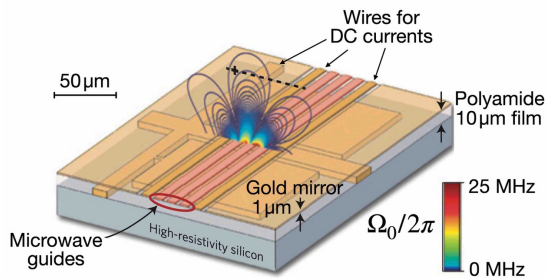


FIG. 2 A schematic drawing of an atom-chip including its magnetic potentials: Atom chips can be used for double well physics in 1D and crossover regimes, which is enabled by the ability to create robust double-well potentials using rf dressing of the atoms (Adapted from Böhi *et al.*, 2009).

occur when a radio-frequency field (\mathbf{B}_{rf}) strongly couples magnetic hyperfine states and are readily described in the dressed dressed-atom picture (Cohen-Tannoudji and Reynaud, 1977). When the radio frequency field is resonant with the magnetic field, i.e. $\omega_{\text{rf}} = \omega_L$, then the coupling strength can be expressed as the Rabi frequency $\Omega_0 = g_F \mu_B B_{\text{rf}}^\perp / \hbar$, where B_{rf}^\perp is the amplitude of the circularly polarized component of \mathbf{B}_{rf} that is orthogonal to \mathbf{B} and couples the m_F states. For an arbitrary detuning ($\delta = \omega_{\text{rf}} - \omega_L$) of the rf-field from the resonance the dressed potential can be expressed as $U(\mathbf{r}) = m'_F \hbar \sqrt{\delta^2(\mathbf{r}) + \Omega_0^2(\mathbf{r})}$. Note that the potential is equal to the non-dressed Zeeman states with $m'_F = m_F$ for $\delta \gg \Omega_0$, and inversely that it is equal to the non-dressed Zeeman states with $m'_F = -m_F$ for $\delta \ll -\Omega_0$.

Let us examine the simple case of a magnetic quadrupole field, where the magnitude of the field increases linearly in all directions. In any direction starting from the center outwards, there is some point at which the rf field becomes resonant. The dressed field therefore forms an oblate bubble shaped trap, which has a radius of $r_\rho = \hbar \omega_{\text{rf}} / (|g_F| \mu_B \alpha)$ in the x-y plane and $r_z = \hbar \omega_{\text{rf}} / (|g_F| \mu_B 2\alpha)$ in the z-direction, where α is the quadrupole field of gradient.

The original idea was proposed by Zobay and Garraway, 2001 and first realized in (Colombe *et al.*, 2004). A thorough review of these traps is found in (Garraway and Perrin, 2016; Perrin and Garraway, 2017).

The dressed quadrupole field itself presents the problem that any homogeneous B_{rf} has one or two points on the bubble, where due to the projection of the rf onto the local quadrupole field the coupling field B_{rf}^\perp is zero, leading to Majorana spin-flip losses. This can be avoided using a IP-type trap, where the magnetic field points predominantly in the direction of the z-axis. In the absence of gravity, the quantum fluid can fill the entire bubble (Sun *et al.*, 2018). These hollow Bose-Einstein condensates are currently under investigation at the international space station (Frye *et al.*, 2021). On earth however, gravity deforms the bubble-trap into something more akin to a cup, which can be exploited for 2D quan-

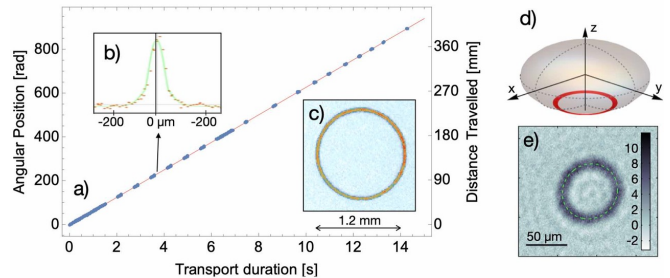


FIG. 3 a) Long distance transport in a ring-shaped TAAF wave-guide. The plot shows the angular position of the condensate and thermal cloud during 14s of transport in the matter-wave guide (blue dots) over a distance of more than 40 cm. The red line depicts the programmed trajectory of $2\pi 10 \text{ rad s}^{-1}$. b) The bi-modal distribution of the BEC after 4.1s of transport and a TOF expansion of 24ms, with the black arrow indicating to the relevant data point. See also Pandey *et al.*, 2019. c) A false-color absorption image of an annular condensate in a TAAF trap. d) A graphical illustration of atoms in a dynamically created ring trap and e) an absorption image of a BEC in it. Adapted from Guo *et al.*, 2020

tum gasses for its strong (weak) confinement in the vertical (horizontal) direction. Using multiple rf-frequencies, multiple shells can be manipulated almost independently (Bentine *et al.*, 2017) and exploited for matter wave interferometry (Mas *et al.*, 2019).

A dressed quadrupole trap can be used to create a matter wave ring simply due to the angular momentum of the trapped atoms and thus approaching a giant vortex state (Guo *et al.*, 2020; Sherlock *et al.*, 2011). Alternatively, one can combine the rf-bubble trap with a red-detuned light-sheet, thus forming a ring-shaped trap (Morizot *et al.*, 2006).

4. Time-Averaged Adiabatic Potentials (TAAPs)

Highly versatile and controllable potentials in a great variety of perfectly smooth shapes can be created by combining the aforementioned adiabatic potentials with an oscillating, homogeneous magnetic field. If the Rabi frequency of the rf dressing field is large compared to the frequency of the oscillating field $\Omega_0 \gg \omega_m$, the resulting trapping potential is the time-average of the adiabatic and modulation potentials (Lesanovsky and von Klitzing, 2007; Navez *et al.*, 2016). Starting with a simple quadrupole field and adding a vertically polarized rf-field, plus a vertical modulation field, one can generate a ring-shaped trap. Typical values are 50 Hz to 100 Hz for the radial and axial trapping frequencies and 50 μm to 1 mm for the radius. The ring can then be adiabatically turned into one or two coupled half-moon shaped traps simply by changing the polarization of the rf or modulation fields. Multiple concentric or stacked rings can be created by using more than one rf-frequency.

The exact shapes of these traps and the barriers be-

tween them depend only on the amplitude and polarization of oscillating magnetic fields, which can be adjusted with extreme precision using standard electronics; making it possible to control the trapping potentials down to the picokelvin level.

Using a suitable choice of polarizations, it is also possible to trap two different spin states in identical effective potentials and even to manipulate them entirely independently (Navez *et al.*, 2016). This technique might be exploited in an atom interferometer, where the atoms are placed in the TAAP in a single hyperfine state and exposed to a suitable microwave pulse. The hyperfine states of the resulting superposition can then be manipulated separately, making them sensitive to gravitation, for instance, and then recombining with a second microwave pulse - resulting in a highly sensitive interferometer (Navez *et al.*, 2016). A similar scheme has been proposed for adiabatic ring-shaped potentials resulting from specially tailored magnetic fields (Stevenson *et al.*, 2015).

Another feature of the TAAP rings is the extreme smoothness of these potentials (Pandey *et al.*, 2019). Its shape is not determined by current carrying structures in proximity but by a quadrupole field and the frequency and amplitude of modulations fields, which are all generated by very distant coils. Therefore, any imperfections in the field-generating coils are exponentially suppressed on the size-scale of the trapping potentials. This is evidenced in Ref. (Navez *et al.*, 2016), where a Bose-Einstein condensate are transported at hypersonic speeds for a distance of 15 cm without loss in spatial coherence.

C. Atom optical elements

In this section, we outline the types of potentials and the optical elements that have been designed to guide the matter-wave in atomtronic circuits.

1. Waveguides

The fabrication of one dimensional guides is important in the atomtronics context, both to control the circuit functionalities and to explore quantum effects in fundamental physics. The coherent regime needs to consider both the tightness of the confinement and any displacement or roughness of the waveguide transverse to the direction of propagation. Operating in the strict one-dimensional regime requires the transverse frequencies to be much larger than both the chemical potential and the temperature of the gas, as well as the kinetic energy originating from the current flowing in the system. This can be achieved using tight optical confinement from optical lattices (Bloch *et al.*, 2008) or projected wires (Kriner *et al.*, 2017). Optical lattices with a typical lattice spacing of few microns have been realized (Rubinsztein-Dunlop *et al.*, 2016). In such structures, in which the

cold atoms can tunnel between the lowest Bloch bands of the adjacent wells, the low temperatures matter-wave effective dynamics is one dimensional.

A rapid modulation of the strength of the transverse confinement or a bend in the waveguide couples the forward motion of the atoms to oscillations of the condensate via its chemical potential. It also causes a shift of the potential energy of the bottom of the waveguide, which can induce scattering, although it is possible to shape a slow bend to avoid this effect (del Campo *et al.*, 2014). As pointed out in section II.B.2, this regime is very difficult to achieve with atom chips. Excitationless matter-wave guides have been demonstrated using single-beam optical dipole beams over distances of 3.5 mm (McDonald *et al.*, 2013a) and using TAAPs over distances of 40 cm for thermal clouds and 15 cm for BECs (Pandey *et al.*, 2019). Waveguide bends and junctions created with painted potentials have demonstrated excitation probabilities of less than 8% (Ryu and Boshier, 2015).

The requirements for precision interferometers are rather stringent. Care must be taken to ensure that the superposition state traverses the interferometer adiabatically and that the trap-induced energy difference between the two paths is extremely well controlled (Kreutzmann *et al.*, 2004; Zabow *et al.*, 2004). For propagating matter wave interferometers this results in extreme requirements on corrugations of the waveguides, since any small lateral deviation tends to couple the forward motion to transverse modes - thus destroying the coherence of the superposition state. In the absence of such coupling the interferometer are expected to be able to operate using multiple transverse modes concurrently (Andersson *et al.*, 2002).

2. Ring traps

Ring traps are the simplest spatially closed atomtronic circuits. They normally consist of a tight harmonic confinement in the vertical and horizontal directions and no confinement along the azimuthal direction. The potential for a ring of radius ρ_0 can be written near the trap minimum as $U = \frac{1}{2}m\omega_\rho^2(\rho - \rho_0)^2 + \frac{1}{2}m\omega_z^2z^2$, with m being the mass of the atoms and ω_ρ and ω_z are the harmonic trapping frequencies in the radial and vertical directions respectively. There are two distinct regimes of interest for ring traps: One where the radius of the ring is small enough for the energy or time-scale of the excitations along the circumference of the ring to become important, and one, where the ring is to be viewed more like a circular waveguide.

Early demonstrations focused on atom propagation in large ring-shaped waveguides. Large-scale magnetic traps have been demonstrated, where the shape of the ring is directly defined by the field generating wires, either using microfabricated ‘atom-chips’ (Sauer *et al.*, 2001) or large wire structures (Arnold *et al.*, 2006; Gupta *et al.*, 2005) and inductively coupled rings (Pritchard

et al., 2012). For polar molecules electrostatic ring-traps have also been demonstrated (Crompvoets *et al.*, 2001).

Small-diameter ring traps can be generated using purely optical dipole potentials. The first toroidal BEC is created with a painted potential (Henderson *et al.*, 2009). Static approaches to creating rings with optical potentials include using a light-sheet in combination with a Laguerre-Gauss beam (Moulder *et al.*, 2012; Ramanathan *et al.*, 2011; Wright *et al.*, 2000). Persistent currents in spinor condensates are detected in (Beattie *et al.*, 2013). In this case, the imperfection in the potential often do not lead to adverse effects since the superfluid nature of the flow smooths them over. Examples include studies of super-currents (Eckel *et al.*, 2014b; Moulder *et al.*, 2012; Ryu *et al.*, 2014) and Josephson junctions (Ryu *et al.*, 2013; Wright *et al.*, 2013a).

Optical ring lattices suitable for trapping cold and quantum degenerate atomic samples have been generated with Laguerre-Gauss laser beams incident on SLM or manipulated by an Acousto-Optical Modulator (Amico *et al.*, 2014; Franke-Arnold *et al.*, 2007; Henderson *et al.*, 2009). By applying computer assisted optimization algorithms using absorption images of BECs in the dipole potentials, smooth potentials of rings radii and lattice spacings in the range of $100\mu\text{m}$ and $30\mu\text{m}$ respectively have been demonstrated. DMD generated rings lattices of $\sim 40\mu\text{m}$ and lattice spacing of $\sim 4\mu\text{m}$ have been achieved (Gauthier *et al.*, 2016). However, in order to achieve any appreciable tunneling among the lattice wells, such numbers need to be scaled down further.

Finally, ultra-smooth ring-shaped waveguides based on Time-averaged Adiabatic Potentials (TAAP)s (Lesanovsky and von Klitzing, 2007) have recently been demonstrated. They support coherent, lossless transport of matterwaves over very macroscopic distances (14 cm) even at hypersonic speeds (Pandey *et al.*, 2019).

3. Barriers and beam splitters

The terms “barrier” and “beam splitters” are primarily distinguished by their intended use rather than by underlying function or principles. Borrowing the term from optics, beam splitters are familiar elements, particularly in the context of interferometers, used for coupling a pair of system modes. Barriers are commonly used to define spatially distinct regions, for example, having different potential structures, temperatures, and chemical potentials as is the case in triple-well transistors, for example (Caliga *et al.*, 2016b). Beam splitters have been implemented using both time-dependent and time-independent potentials, whereas barriers are typically implemented with time independent potentials.

Early work on atomtronic beam splitters split magnetically guided thermal atoms utilizing “Y”- or “X”-shaped conductor junctions, resulting in multi-mode splitting (Cassettari *et al.*, 2000; Muller *et al.*, 2000). Coherent beam splitting on an atom chip has been carried out

using Bragg diffraction from an optical lattice that is exposed to the atoms in a double-pulsed manner (Diot *et al.*, 2004; Wang *et al.*, 2005). Coherent splitting of stationary Bose condensates produced on atom chips has also been carried out utilizing radio-frequency fields that provide an elegant means of evolving in time a single magnetically generated potential well into a double well and vice-versa (Hofferberth *et al.*, 2006; Kim *et al.*, 2017; Schumm *et al.*, 2005). Of note, the earlier successes in coherent beam splitting utilized time-dependent potentials.

In the framework of atomtronic circuitry there is particular interest in beam splitters that are spatially fixed and time independent. The use of “painted potentials” (Henderson *et al.*, 2009) enabled coherent splitting of a propagating condensate in “Y” junction optical waveguides (Ryu and Boshier, 2015) while beam splitting in crossing optical waveguides has also been carried out using an optical Bragg grating produced by a pair of interfering laser beams located at the waveguide junction (Guarrera *et al.*, 2017).

In contrast to the coherent splitting, that is achieved with waveguides coupled by spatial proximity or through optical gratings, barriers act more like the mirrors and beam splitters of optical systems. Barriers produced using projected blue-detuned laser beams feature a smooth Gaussian profile. Coherent splitting occurs due to tunneling and quantum reflection for atoms with energies below or above the top of the barrier, respectively, within an energy range proportional to the inverse curvature of the barrier at its top (Cuevas and Scheer, 2017). Matter wave propagation across arbitrary arrangements of barriers can be numerically calculated utilizing the impedance method (Gutiérrez-Medina, 2013; Khondker *et al.*, 1988), a technique that borrows wave propagation techniques from electromagnetic transmission line analysis.

Projected optical atomic potentials that affect the center-of-mass motion through AC Stark shifts are limited in size-scale by the wavelength of the projected light. Barriers having sub-wavelength size scales down to less than 50nm have been demonstrated using the nonlinear response of the dark state of a three-level system (Lacki *et al.*, 2016; Wang *et al.*, 2018).

Regarding the large variety of approaches in barrier and beamsplitter implementation, it is not evident that a single approach has emerged as best suited for atomtronic systems. Rather, the optimum approach is purpose-dependent. What has emerged, however, is that it has proved quite difficult to achieve coherence-preserving barriers or beam splitters using purely magnetic approaches. Either all optical or hybrid magnetic and optical or radio-frequency systems have met with good success.

III. COHERENT EFFECTS IN MESOSCOPIC MATTER-WAVE CIRCUITS

Like their electronic counterparts (Cuevas and Scheer, 2017), atomtronic devices can operate in a regime where quantum interferences play a dominant role. Such a coherent regime is achieved in situations where the typical transport scale, such as the circumference of a ring trap or the length of a mesoscopic section, is larger than the typical decay length of the particles' correlation function. Phenomena such as Aharonov-Bohm interferences, Bragg reflection on periodic structures or Anderson localization emerge in the transport properties. Quantum coherent transport is deduced from properties of the Hamiltonian describing the atoms inside the conductor, identical to coherent wave propagation in complex media encountered in electromagnetism.

Operating in this regime typically requires low enough temperatures: for Fermi gases, the relevant length scale is $\frac{\hbar v_F}{k_B T}$, where v_F is the Fermi velocity, and for thermal gases it is the thermal de Broglie wavelength. For bosons, the emergence of the condensate below the critical temperature ensures coherence at arbitrarily large distances, making them particularly well suited for the study of coherent transport. The long wavelength dynamics is then efficiently described by superfluid hydrodynamics (see Sec.III.A.1). Many-body fermionic particles are discussed in Secsubsec:fermions. Coherence properties are also affected by many-body effects such as the decrease of quasi-particle lifetime and quantum fluctuations. Furthermore, coherence can be reduced by noise, spontaneous emission from lasers or other external disturbances.

In this section, we bridge microscopic models to simple matter-wave circuits. The various model Hamiltonians describing coherent quantum fluids with different features are introduced. We then focus on the persistent current in ring-shape circuits providing both an important figure of merit for the system's coherence and an elementary building block for atomtronic circuits. Finally we present the two-terminal quantum transport and illustrate the specific features emerging from the coherent quantum dynamics.

A. Model Hamiltonians

The many-body Hamiltonian describing N interacting quantum particles of mass m , subjected to an effective magnetic field described by the vector potential \mathbf{A} and confined in the potential V_{ext} reads

$$H = \int d\mathbf{r} \Psi^\dagger(\mathbf{r}) \left[\frac{1}{2m} (-i\hbar\nabla + \mathbf{A}(\mathbf{r}))^2 + V_{ext}(\mathbf{r}) \right] \Psi(\mathbf{r}) + \frac{1}{2} \int d\mathbf{r} d\mathbf{r}' \Psi^\dagger(\mathbf{r}) \Psi^\dagger(\mathbf{r}') v(\mathbf{r} - \mathbf{r}') \Psi(\mathbf{r}) \Psi(\mathbf{r}') \quad (1)$$

where $\Psi^\dagger(\mathbf{r})$ and $\Psi(\mathbf{r})$ are field operators creating or annihilating a bosonic or fermionic particle at the spatial position \mathbf{r} (Mahan, 2013) and $v(\mathbf{r} - \mathbf{r}')$ is the two-body

inter-particle interactions. We assume contact interactions $v(\mathbf{r} - \mathbf{r}') = g\delta(\mathbf{r} - \mathbf{r}')$, with $g = 4\pi\hbar^2 a_s/m$ and a_s the s -wave scattering length. \mathbf{A} is an effective gauge potential, which plays a crucial role in the description of currents in spatially closed geometries. Both lattice and continuous systems are relevant for atomtronic circuits. The quantum many-body theories will be presented mostly for the one-dimensional case. They will be used to describe quantitatively tightly confined geometries, such as quantum wires and point contacts, but also capture qualitatively the physics of extended systems along the transport direction. Given their relevance for specific atomtronic circuits, the Gross-Pitaevskii mean field theories will also be discussed for higher dimensions.

1. Bosons

In this case the field operators obey the commutation relations $[\Psi(\mathbf{r}), \Psi^\dagger(\mathbf{r}')] = \delta(\mathbf{r} - \mathbf{r}')$. For a recent review on one-dimensional bosons see (Cazalilla *et al.*, 2011). We start with a lattice theory describing atoms localized in potential wells centered in N_s sites, and expand the field operators in Wannier functions, assumed to be a good basis of eigenfunctions of separated local potential wells: $\Psi(\mathbf{r}) = \sum_{j=1}^{N_s} w(\mathbf{r} - \mathbf{r}_j) a_j$, in which the operators \hat{a}_j create a single bosonic particle at the site j , $[a_i, a_j^\dagger] = \delta_{ij}$. With the above expression of $\Psi(\mathbf{r})$, the many body Hamiltonian can be recast to the Bose-Hubbard Model (BHM)

$$\mathcal{H}_{\text{BH}} = \sum_{\langle i,j \rangle}^{N_s} \left[-J (a_j a_{j+1} + a_{j+1} a_j) + \frac{U}{2} n_j (n_j - 1) \right], \quad (2)$$

in which we assumed that only atoms in nearest neighbor local wells can appreciably overlap. A ring geometry is assumed, such that $a_{N_s+1}^\dagger = a_1^\dagger$. The parameters in the Hamiltonian are the hopping amplitude $J = \int d\mathbf{r} w^*(\mathbf{r} - \mathbf{r}_i) \left[\frac{1}{2m} (-i\hbar\nabla + \mathbf{A}(\mathbf{r}))^2 + V_{ext} \right] w(\mathbf{r} - \mathbf{r}_{i+1})$ and interaction strength $U = \pi a_s \int d\mathbf{r} |w(\mathbf{r})|^4/m$. The Hamiltonian (2), originally introduced as a lattice regularization of the continuous theory of bosonic fields (Haldane, 1980), provides a paradigmatic model to study Mott insulator-superfluid quantum phase transitions (Fisher *et al.*, 1989). The BHM is extensively used in mesoscopic physics (Fazio and Van Der Zant, 2001). The conditions for the realization of the the BHM in cold atoms systems are identified in (Jaksch *et al.*, 1998), and since then it provides an important scheme in the cold-atoms quantum technology (Bloch *et al.*, 2008). For neutral matter, the vector potential $\mathbf{A}(\mathbf{x}, t)$ provides an artificial gauge field (Dalibard *et al.*, 2011; Goldman *et al.*, 2014) - see Sect.III.B.1. For sufficiently smooth $\mathbf{A}(\mathbf{x}, t)$ on the atomic scale, the gauge field can be absorbed in the Wannier functions $\tilde{w}(\mathbf{r} - \mathbf{r}_i) = e^{-i\Lambda(\mathbf{r}, t)} w(\mathbf{r} - \mathbf{r}_i) \approx e^{i\Lambda(\mathbf{r}_i, t)} w(\mathbf{r} - \mathbf{r}_i)$ with $\Lambda(\mathbf{r}, t) = \int_{\mathbf{r}_0}^{\mathbf{r}} \mathbf{A}(\mathbf{r}, t) d\mathbf{r}$, where \mathbf{r}_0 is

an arbitrary lattice site. Therefore the hopping parameter results $J = e^{i\Phi} J_0$, $\Phi = \int_{\mathbf{r}_i}^{\mathbf{r}_{i+1}} \mathbf{A}(\mathbf{r}, t) d\mathbf{r}$. The procedure of absorbing the effects of the gauge field into the hopping matrix element is called Peierls substitution (Essler *et al.*, 2005; Peierls, 1933).

In the limit of a large average number of particles per site $\nu = N/N_s \gg 1$ the Bose-Hubbard Hamiltonian effectively reduces to the Quantum Phase Model (QPM) (Fazio and Van Der Zant, 2001)

$$\mathcal{H}_{\text{QP}} = -2J_E \sum_{\langle i,j \rangle} \left[\cos(\hat{\phi}_i - \hat{\phi}_j - \Phi) + \frac{U}{2} \sum_{j=1}^{N_s} \hat{Q}_j^2 \right], \quad (3)$$

where $J_E = JN_s$, $\hat{Q}_j = n_j - N/N_s$ is the on-site particle number fluctuations and $\hat{\phi}_j$ the (Hermitian) phase operators (Amico, 2000; Amico and Penna, 2000). The operators satisfy the commutation relations $[\hat{\phi}_i, \hat{Q}_j] = i\hbar\delta_{ij}$.

In the limit of small filling fractions $\nu = N/N_s \ll 1$ the lattice Hamiltonian Eq.(2) leads to the Bose-gas continuous theory. This statement holds true since the filling is proportional to the lattice spacing Δ : $\nu = D\Delta$, with D being the particle density. In order to have a well defined result in the continuous limit $\Delta \rightarrow 0$, the bosonic operators must be rescaled: $\hat{a}_i = \sqrt{\Delta}\Psi(\mathbf{r}_i)$, $\hat{n}_i = \Delta\Psi^\dagger(\mathbf{r}_i)\Psi(\mathbf{r}_i)$, $\mathbf{r}_i = \mathbf{i}\Delta$. The BHM reads as (Korepin *et al.*, 1997): $H_{BH} = t\Delta^2\mathcal{H}_{BG}$, $\mathcal{H}_{BG} = \int d\mathbf{r} [(\partial_{\mathbf{r}}\Psi^\dagger)(\partial_{\mathbf{r}}\Psi) + c\Psi^\dagger\Psi^\dagger\Psi\Psi]$, with $c = U/(t\Delta)$ (Amico and Korepin, 2004). This coincides with Eq. (1) where $c = mg/\hbar^2$. We note that while the procedure is valid for any U , the attractive case demands smaller values of Δ for the actual mapping of the spectrum (Oelkers and Links, 2007). This feature is due to formation of quantum analog of bright solitons (Naldesi *et al.*, 2019).

The many-body Hamiltonian arising from \mathcal{H}_{BG} in first quantization is known as the Lieb-Liniger model and reads

$$\mathcal{H}_{LL} = \sum_{j=1}^{N_p} \frac{\hbar^2}{2m} \left(-i\frac{\partial}{\partial x_j} - \frac{\Phi}{2\pi N_s} \right)^2 + g \sum_{1 \leq j < k < N_p} \delta(x_j - x_k). \quad (4)$$

We note that, despite the Bose-Hubbard model is not integrable (Amico and Korepin, 2004; Choy and Haldane, 1982; Dutta *et al.*, 2015), the 1D Bose gas is, with exact solution given by Lieb and Liniger using the Bethe Ansatz (Lieb and Liniger, 1963).

With a fully factorized (not-entangled) Ansatz for the many-body wavefunction $\Psi_{GS}(\mathbf{r}_1, \dots, \mathbf{r}_N) = (1/N) \prod_j \phi(\mathbf{r}_j)$ the dynamics entailed by the Hamiltonian (1) reduces to the Gross-Pitaevskii equation (Calogero and Degasperis, 1975; Dalfovo *et al.*, 1999; Leggett, 2006)

$$i\hbar\partial_t\phi(\mathbf{r}, t) = \left[\frac{\hbar^2}{2m} (-i\nabla - \mathbf{A})^2 + V_{ext}(\mathbf{r}) + gN |\phi(\mathbf{r})|^2 \right] \phi(\mathbf{r}), \quad (5)$$

in which we restored the 3D character of the system since many relevant applications of the GPE occur in circuits of higher dimensionality (e.g. toroidal confinements). We note that $\sqrt{N}\phi(\mathbf{r})$ coincides with $\langle \Psi(\mathbf{r}, t) \rangle$, defined by the mean field approximation of the Heisenberg equations of the motion stemming from the Hamiltonian Eq. (1). The reduction of the quantum many body problem to the GPE dynamics is well justified in the dilute regime, i.e. when $a_s^3\rho \ll 1$ (see (Lee *et al.*, 1957) for corrections). In 1D, taking $A = 0$ and $V_{ext} = 0$ the Gross-Pitaevskii equation is integrable, with solitonic solutions (Faddeev and Takhtajan, 2007). Eq. (5), recast in amplitude phase representation $\phi = \sqrt{n}e^{i\theta}$ gives rise to the superfluid hydrodynamics equations for the condensate density n and the phase θ (Dalfovo *et al.*, 1999).

2. Fermions

Here, we refer to a gas of fermions with κ components or colours. In this case, the field operators are characterized by the spin label $\alpha = \{1, \dots, \kappa\}$. They obey the anticommutation rules: $\{\Psi_\alpha(\mathbf{r}), \Psi_{\alpha'}^\dagger(\mathbf{r}')\} = \delta_{\alpha,\alpha'}\delta(\mathbf{r} - \mathbf{r}')$. By employing a similar derivation as described above for the bosonic case, one can obtain the generalization of the Hubbard model. If the physical parameters of the system, like interaction or trapping potentials, turns out independent by the colour then κ -components fermions are known as $SU(\kappa)$ fermions. The Hamiltonian for $SU(\kappa)$ fermions in a ring lattice pierced by an effective gauge field reads (Capponi *et al.*, 2016)

$$\mathcal{H}_{SU(\kappa)} = -J \sum_{j=1}^{N_s} \sum_{\alpha=1}^{\kappa} (e^{i\Phi} c_{\alpha,j}^\dagger c_{\alpha,j+1} + \text{h.c.}) + U \sum_{\alpha \neq \alpha' j} n_{\alpha,j} n_{\alpha',j} \quad (6)$$

where $c_{\alpha,j}^\dagger$ creates a fermion at the site j of a d -dimensional lattice with spin component α , $n_{\alpha,j} = c_{\alpha,j}^\dagger c_{\alpha,j}$ is the local number operator for site j and spin component α . The parameters J and U account for the hopping strength and on-site interaction respectively. They can be expressed in terms of integrals of Wannier functions as discussed for the bosonic case. For $\kappa = 2$, provides a paradigmatic framework to address the physics of itinerant electrons, in d -dimensional lattice (Gutzwiller, 1963; Hubbard, 1963; Kanamori, 1963). See (Baeriswyl *et al.*, 2013; Mahan, 2013; Mielke, 2015) for more recent references. Systems of two spin components (Jördens *et al.*, 2008), and more recently, of κ components fermions (Cappellini *et al.*, 2014; Pagano *et al.*, 2015) have been experimentally realized with the cold atoms quantum technology. For $\kappa = 2$, the Hamiltonian (III.A.2) is integrable by Bethe Ansatz for any values of system parameters and filling fractions $\nu = N/L$ (Lieb and Wu, 1968). For $\kappa > 2$, the Bethe Ansatz integrability is preserved in the continuous limit of vanishing

lattice spacing, (III.A.2) turning into the Gaudin-Yang-Sutherland model describing $SU(\kappa)$ fermions with delta interaction (Sutherland, 1968); such regime is achieved by (III.A.2) in the dilute limit of small fillings fractions. Bethe Ansatz solutions allows the precise understanding both of the ground state and the nature of excitations of the system. The corresponding Hamiltonian reads:

$$H_{GYS} = \sum_{\alpha=1}^{\kappa} \sum_{j=1}^N \frac{\hbar^2}{2m} \left(-i\partial_{x_{j,\alpha}} - \frac{\Phi}{2\pi N_s} \right)^2 + g \sum_{1 \leq i < j \leq N} \sum_{\alpha, \beta=1}^{\kappa} \delta(x_{i,\beta} - x_{j,\alpha}) \quad (7)$$

Another integrable regime of (III.A.2) is obtained for $(\sum_{\alpha} n_{\alpha,j}) = 1 \forall j$ and large repulsive values of $U \gg t$ for which the system is governed by the $SU(\kappa)$ antiferromagnetic Sutherland model (Capponi *et al.*, 2016; Guan *et al.*, 2013; Sutherland, 1975). In the intermediate interactions and intermediate fillings, the model (III.A.2) for $\kappa > 2$ is not integrable and approximated methods are needed to access its spectrum. $SU(2)$ and $SU(\kappa)$ fermions enjoy a different physics. For spin one-half fermions, spin excitations, the so called spinons, are gapless in thermodynamic limit; charge excitations, instead, are gapped at half filling (Mott phase) and gapless otherwise (Andrei, 1995). In the low energy limit, spin and charge excitations separate each other. Notably, the Mott phase is suppressed only exponentially for $\kappa = 2$ (Lieb and Wu, 1968). For $\kappa > 2$, fermions display a Mott transition for a finite value of U/J (Cazalilla and Rey, 2014; Manmana *et al.*, 2011). For incommensurate fillings, a superfluid behavior is found. In the $SU(\kappa)$ case, spin and charge excitations can be coupled (Affleck, 1988).

3. Impurities, weak-links and contacts

Barriers, weak-links, quantum impurities and contacts are essential features for matter-wave circuits. Most, if not all, of these features can be experimentally realized, with a wide range of parameters both in the spatial and time domains. Below, we will sketch on how they can be incorporated in the systems Hamiltonian.

In continuous systems (like Eqs. (4), (5), (7)), ideal localized barriers can be modeled as delta-function potentials. They can be used to stir ring-shape condensates (Hallwood *et al.*, 2007, 2010; Nunnenkamp *et al.*, 2011; Schenke *et al.*, 2011). In numerical simulations describing closely the experimental conditions the delta function is replaced by a suitably peaked Gaussian function (Nunnenkamp *et al.*, 2011). Localized barriers in lattice systems are achieved through weak-links in the hopping amplitudes (Aghamalyan *et al.*, 2016a; Amico *et al.*, 2014) or by suitable offsets of the local potentials (Aghamalyan *et al.*, 2015; Cominotti *et al.*, 2015).

In a typical transport set-up, the effect of a thin localized barrier of large strength can be described by the

tunnel Hamiltonian $\mathcal{H} = \mathcal{H}_L + \mathcal{H}_R + \mathcal{H}_t$ in which \mathcal{H}_L and \mathcal{H}_R are the left and right leads, and \mathcal{H}_t is the tunneling Hamiltonian. A standard expression for \mathcal{H}_t is $H_t = \mathcal{J}(\psi_L^\dagger \psi_R + h.c.)$, ψ_L and ψ_R being single particle operators of the left and right leads respectively (see for example (Nazarov and Blanter, 2009)) and \mathcal{J} the tunnel amplitude. At a semi-classical level, the two leads transport can be described in terms of the atoms transfer among the reservoirs $\Delta N = N_L - N_R$. Specifically, the current is defined as $I = -(1/2)d(\Delta N)/dt$. Such a logic is applied in the two-terminals transport set-ups discussed in the Sect.III.C.

B. Persistent currents in atomtronic circuits

Even though persistent currents are mesoscopic in nature, they are instrumental for atomtronics. They can provide an important tool for quantum simulation, since they can probe quantum phases of matter. At the same time, persistent currents can be used for atomtronic devices such as, e.g. quantum sensing (see Sect.IV.E) or neutral currents-based platforms for qubit implementations (see Sec.IV.D).

1. The concept of persistent current

The persistent current is one of the defining notions of mesoscopic physics (Büttiker *et al.*, 1983; Imry, 2002; Imry and Landauer, 1999): in an electronic ring-shaped gas (a metal for example) pierced by a static magnetic field, a dissipationless current can occur. This is a manifestation of the electron phase coherence all along the ring, implying that the coherence length is larger than the system size. This counter-intuitive phenomenon occurs in the quantum regime, when resistive effects due to interactions, presence of impurities and thermal fluctuations leading to decoherence are negligible. Persistent currents in electronic systems are thoroughly studied both theoretically and experimentally (see eg (Saminadayar *et al.*, 2004; Zvyagin and Krive, 1995) and references therein), with the aim of shedding light on its own mechanism, studying the effect of interactions, understanding the role of the impurities (Chakraborty and Pietiläinen, 1994; Imry, 2002; Matveev *et al.*, 2002; Riedel and von Oppen, 1993).

In superconductors and superfluids, the persistent currents coincide with the supercurrents flowing across the ring and originate from the macroscopic phase coherence of such quantum states. Experimental observations of persistent currents are reported in several condensed-matter systems: normal metallic rings (Bleszynski-Jayich *et al.*, 2009; Lévy *et al.*, 1990; Mohanty, 1999) and superconductors, (Deaver and Fairbank, 1961). Exciton polaritons have also been proposed as platform to study persistent currents under controllable conditions (Gallemí *et al.*, 2018; Li *et al.*, 2015; Lukoshkin *et al.*, 2018; San-

vitto *et al.*, 2010).

By virtue of the control and flexibility of their operating conditions and the possibility to deal with different particles' statistics, ultracold atoms provide an ideal platform to study persistent current with a new scope. The study of persistent currents is first initiated in cold atoms systems confined to ring-shaped potentials and pierced by a synthetic magnetic field by Amico *et al.*, 2005. Indeed, a quantum gas in ring-shaped confinement and subjected to an artificial gauge field with flux Φ (see Sect.III.A) behaves as a charged particle subjected to a magnetic field. The artificial magnetic field can be engineered by a variety of techniques in quantum technology ranging from a simple rotation to the transfer of angular momentum through two-photon Raman transitions or Berry phases and hologram phase imprinting techniques (Dalibard *et al.*, 2011; Goldman *et al.*, 2014). The effective magnetic field imparts a phase gradient on the particles' wave function defining a finite velocity field along the ring. For sufficiently smooth guides (i.e. the most common situation in cold-atom experiments) the particles' flow is dissipationless. The current is obtained from the free energy thanks to a thermodynamic identity deduced from the Hellmann-Feynman theorem $I = -(1/2\pi)\partial F/\partial\Phi$ (Zvyagin and Krive, 1995). In the ground-state, the persistent current is $I = -(1/2\pi)\partial E_{GS}/\partial\Phi$.

In the quantum-coherent regime, the particle current is predicted to be a periodic function of the applied flux $\Phi = \omega R^2$ of the artificial gauge field, R being the ring radius. A theorem due originally to Leggett (Leggett, 1991) shows that for spinless fermions and bosons with repulsive interactions on a clean ring, the persistent currents do not depend on the interaction strength, but merely reflect angular momentum conservation along the ring, so that the ground-state energy is written as $E = E_0(\ell - \Phi/\Phi_0)^2$, with ℓ denoting the z -angular momentum quantum number, i.e. the ground-state energy is piece-wise parabolic and each parabola indicates a different value of angular momentum carried by the circulating particles. The period of oscillation of the currents is the flux quantum $\Phi_0 = \hbar/m$. Inclusion of localized impurities or of a barrier mixes the angular momentum states, thus smoothing the amplitude of the persistent currents (Cominotti *et al.*, 2014; Hekking and Glazman, 1997; Matveev *et al.*, 2002). Such an impurity is felt by the interacting fluid as an effective localized barrier affecting the system in a way that depends on interaction. For repulsive interactions, the Luttinger liquid paradigm (Giamarchi, 2003) holds at intermediate and strong interactions and the effective barrier depends on a power law with the ring size, while for the weak interactions, the barrier is screened by healing length effects (Cominotti *et al.*, 2014). The regime where the barrier effectively splits the ring into two disconnected parts is a universal function of barrier and interaction strength (Aghamalyan *et al.*, 2015). For attractive interactions, the excitation spectrum is quadratic and a universal scaling with a non-

trivial interplay of barrier and interaction strength is observed in some interaction regimes (Polo *et al.*, 2021).

Relying on the enhanced capabilities of DMD's or painting techniques, persistent currents can be engineered by machine learning assisted dynamics of the trapping potential (Haug *et al.*, 2021). Specifically, the engineering can be achieved by training a deep-learning network on the local potential off-sets thereby trapping the atoms in ring-shaped circuit with lumped parameters Eqs. (2), (3). This approach predicts better performances in the state preparation and in the very nature of persistent currents (currents involving three angular momentum can be engineered) can be achieved, compared with the existing protocols based stirring protocols.

Persistent currents have been also studied in bosonic ring ladders (Aghamalyan *et al.*, 2013; Haug *et al.*, 2018a; Polo *et al.*, 2016a; Richaud and Penna, 2017; Victorin *et al.*, 2019). There, discrete vortex structures can occur in the transverse direction, giving rise to a wealth of phases (see eg for a review (Amico *et al.*, 2021)). Josephson oscillations and orbital angular momentum dynamics in two coupled rings in a stuck configuration have been studied in (Lesanovsky and von Klitzing, 2007; Nicolau *et al.*, 2020; Oliinyk *et al.*, 2019). In multi-component mixtures, the criterion of stability of persistent current and the relation with entanglement are addressed in Abad *et al.*, 2014; Anoshkin *et al.*, 2013; Spehner *et al.*, 2021. Transfer of angular momentum between different bosonic species was theoretically addressed in Penna and Richaud, 2017

We close the section, by summarizing the important results based on Gross-Pitaevskii dynamics in two or three spatial dimensions. In most of the protocols studied so far, the matter-wave flow is obtained by stirring. Many sources of decay of persistent currents have been identified: generation of elementary excitations, thermal fluctuations, vortices and vortex rings (Abad, 2016; Mathey *et al.*, 2014; Piazza *et al.*, 2009; Wang *et al.*, 2015; Khani *et al.*, 2020). For a tightly confined toroidal shape condensate, persistent currents may still decay by phase slippage mechanisms, in particular through incoherent or coherent phase slips depending on interaction and temperature regimes (Danshita and Polkovnikov, 2012; Kunimi and Danshita, 2017; Polo *et al.*, 2019). By this approach, stirring the matter wave is studied in in race-track atomtronic circuit (Eller *et al.*, 2020).

2. Experimental observation and read out of persistent current in bosonic toroidal-shape atomtronic circuits

Rotating fluids and persistent currents are observed in ultracold atomic gases on a ring in a donut-shaped ring trap (Moulder *et al.*, 2012; Ramanathan *et al.*, 2011; Ryu *et al.*, 2014; Wright *et al.*, 2013a) - see Fig.4a) and Fig.4b). A challenge to rotate a quantum fluid is the generation of excitations and vortices (Arabahmadi *et al.*, 2021; Dubessy *et al.*, 2012). The threshold for creation

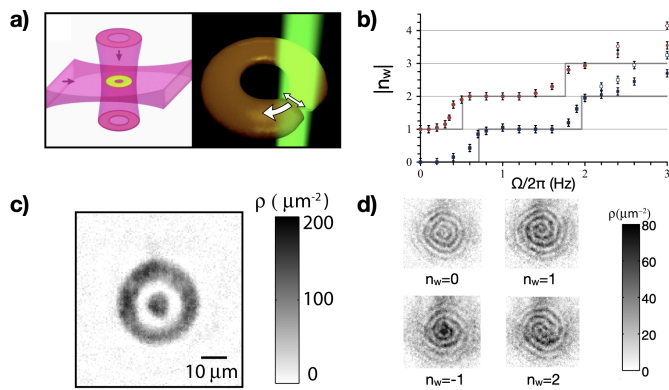


FIG. 4 Experimental realization of BEC rotating in a circular atomtronic circuit. a) Schematics of the fabrication of the optical potential and the stirring protocol; the circular confinement is realized through a Laguerre-Gauss laser field; the transverse confinement is implemented through light sheets; the condensate is stirred with a rotating blue detuned focused laser beam. b) The persistent currents features quantized steps of the angular momentum imparted to the BEC expressed by the winding number n_w . c) displays the ccd-contrast image of ring shaped rotating BEC concentric with a second BEC; d) such a configuration allows to probe direction and strength of the angular momentum through characteristic spiral interferograms. Panels a) and b) adapted from Wright *et al.*, 2013a. Panels c) and d) adapted from Corman *et al.*, 2014.

of excitations has been measured (Wright *et al.*, 2013b). The decay of persistent currents due to thermal fluctuations has been also experimentally studied (Kumar *et al.*, 2017). Recent experiments has also achieved very high rotation quantum numbers, with a rotation speed up to 18 times the sound velocity (Guo *et al.*, 2020; Pandey *et al.*, 2019).

By introducing two moving weak links on the ring in opposite directions, the transition from superfluid to resistive flow is studied (Jendrzejewski *et al.*, 2014). This experiment provides a new technique: the use of a ring to address mesoscopic transport properties (see also Sec.III.C). Along the same line, it is demonstrated that it is possible study the current-phase relation of a superfluid using a ring geometry (Eckel *et al.*, 2014a).

Persistent currents can be explained with the various branches of the energy dispersion relation as a function of the flux or the rotation rate. In Ref. (Eckel *et al.*, 2014b), hysteresis among different branches is observed and proposed as a method to control an atomtronics device.

Readout of the currents in ultracold atomic systems can be done in various ways. The ccd contrast image of the atoms density after long time releasing of the condensate from the trap is called Time Of Flight (TOF). In most of the experiments, the TOF image is achieved after 10 – 20ms releasing time. The theoretical approach to TOF accounts to compute the momentum distribution of the system at the instant of time in which the trap is open

$t = 0$ (Read and Cooper, 2003). For condensate flowing along ring-shaped circuits, TOF displays a characteristic shape in which the density around \mathbf{k} is suppressed. The TOF image (taken from the top of the expanding condensate, along the falling direction) shows a donut shape which is very different from a bell-shaped image in absence of circulation (Amico *et al.*, 2005), see Fig.5. The value of the donut radius results to change in discrete steps corresponding to the quantization of angular momentum of the condensate (Moulder *et al.*, 2012; Murray *et al.*, 2013; Ryu *et al.*, 2014; Wright *et al.*, 2013a)- see Fig.4-b).

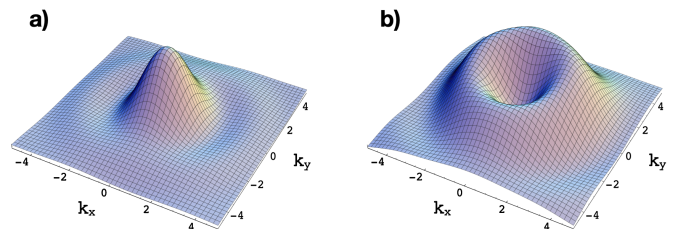


FIG. 5 TOF expansion of a ring shaped condensate pierced by an effective magnetic field. The figure display momentum distribution of a lattice system in the plane of the ring: $n(\mathbf{k}) = |w(\mathbf{k})|^2 \sum_{i,j} e^{-i(\mathbf{x}_i - \mathbf{x}_j) \cdot \mathbf{k}} \langle n \rangle$. The vector $\mathbf{k} = (k_x, k_y)$ and $w(\mathbf{k})$ are Fourier transform of Wannier functions. a) and b) correspond to non-rotating and rotating condensate respectively. Adapted from Amico *et al.*, 2005

An important readout of the current state of the system is provided by heterodyne phase detection protocol (Corman *et al.*, 2014; Eckel *et al.*, 2014a; Mathew *et al.*, 2015). In this case, the ring condensate co-expands with a concentric disk condensate fixing a reference for the phase. The resulting image shows a characteristic spiral interferogram whose details (number of arms and sense of rotation) depend on the direction of circulation of the currents. The spiral interferograms are also sensitive to the possible phase fluctuations along the ring (Corman *et al.*, 2014; Roscilde *et al.*, 2016): in this case, they display dislocations associated to phase slips - see Fig.4-b) and Fig.4-c). A minimally invasive technique based on Doppler shift of the phonon modes of the condensate has been demonstrated to be effective to measure the winding number (Kumar *et al.*, 2016b).

For correlated systems on lattices, the phase information can be achieved by studying noise correlations in the expanding density (Haug *et al.*, 2018b).

3. Persistent current in fermionic rings

The first cold fermionic atoms persistent current's analysis is carried out in (Amico *et al.*, 2005). In this study, the fermions repel each other with an Hubbard interaction (see Eq.III.A.2). Persistent currents of Fermi particles are subjected to parity effects: the currents behave diamagnetically or paramagnetically depending on

the parity of the number of particles on the ring (Leggett, 1991). The effect is due to the periodic boundary conditions imposed on the wavefunction. Explicit calculation with bosonization shows subtle effects of interactions and the effect of temperature (Loss, 1992). There is a critical temperature for the disappearance of the oscillations of the current as $k_B T = \hbar^2 m R^2$. In the case of interacting bosons, no parity effect occurs. In this case, the response is always paramagnetic (Pecci *et al.*, 2021a).

Readout of current states by interferometric means for fermions requires some attention (Pecci *et al.*, 2021b) as compared to the bosonic case since all fermionic orbitals contribute to the interference pattern, giving rise to dislocations in the spiral interferograms. Also, the time-of-flight images of circulating current states display a visible hole only if the circulating current is large enough to displace the whole Fermi sphere in momentum space (Pecci *et al.*, 2021b).

In the case when attractive interactions occur among the particles, pairing or formation of higher-order bound states (quartets, many-body bound states) directly affects the persistent currents (Byers and Yang, 1961): the periodicity of the persistent currents scales as Φ_0/n where n is the number of bound particles (Naldesi *et al.*, 2022). The curvature of the free energy at zero flux also displays a parity effect (Waintal *et al.*, 2008): in this case, it arises from a new branch in the ground-state energy (Pecci *et al.*, 2021a).

Like the attractive bosons, the periodicity of the persistent current of repulsive fermions in the strongly correlated regime is reduced by $1/N$. This effect is demonstrated through Bethe Ansatz analysis for $SU(2)$ (Yu and Fowler, 1992) and $SU(\kappa)$ Fermi gases (Chetcuti *et al.*, 2022a). Such behavior is due to the remarkable phenomenon of spinons-production in the ground state: spinons compensate the increasing effective flux; since the spinons are quantized and the magnetic flux changes continuously, the compensation can be only partial. Therefore, an energy oscillations with characteristic periods smaller than the bare flux quantum Φ_0 is displayed. Eventhough the same $1/N$ reduction of the ground state periodicity is found in strongly correlated attracting bosons (occurring as result of formation of N -particle bound states in the ‘charge’ quasi-momenta), here we note that the ‘effective attraction from repulsion’ resulting in $SU(\kappa)$ systems arises because of the spin-spin correlations. (Naldesi *et al.*, 2022). Finite temperature can affect the periodicity of persistent current as result of interplay between thermal fluctuatuions and interaction (Pâțu and Averin, 2022).

We finally note that, although the persistent current is mesoscopic in nature, it is demonstrated to display critical behavior when undergoing the quantum phase transition from superfluid to Mott phases that, for $\kappa > 2$, occurs at a finite value of the interaction (Chetcuti *et al.*, 2022a). Mott transitions in multi-orbital $SU(\kappa)$ Hubbard models were investigated in Richaud *et al.*, 2021, 2022. The first experimental demonstration of persistent cur-

rent states in fermionic rings has been reported recently (Cai *et al.*, 2022; Del Pace *et al.*, 2022). Focusing on attractive interactions, both homodyne and heterodyne interference in the BEC regime have been obtained. An in-depth theoretical analysis of interference fringes of $SU(\nu)$ fermions was carried out in (Chetcuti *et al.*, 2022b).

C. Two terminal quantum transport in cold atom mesoscopic structures

In a typical two terminals configuration, a *mesoscopic* region, eg a channel or a ring, features quantum mechanical processes such as tunneling and interferences, and large leads characterized by their thermodynamic phases (which can be normal or superfluid) are connected to it to drive currents (Imry and Landauer, 1999) - see Fig. 6a).

1. Double well systems

Two-terminal systems have been used with Bose-Einstein condensates (BEC) to observe and manipulate phase coherence (Andrews *et al.*, 1997) (see (Dalfovo *et al.*, 1999) for a detailed review). Conceptually, the simplest instance is a zero-temperature BEC in a double well potential, as originally proposed in (Smerzi *et al.*, 1997). This system is of considerable interest from many perspectives, ranging from quantum metrology (Pezzè *et al.*, 2018) to quantum information processing (Haroche and Raimond, 2006). We restrict the discussion to atomic transport and refer the reader to these reviews for an in-depth discussions of these other aspects.

a. Tunnel regime In this regime, we focus on the dynamics of the population imbalance in the two wells (Smerzi *et al.*, 1997), which is relevant for high barrier (LeBlanc *et al.*, 2011; Spagnolli *et al.*, 2017). In the unbiased, non-interacting regime, the dynamics reduces to Rabi oscillations of the population across the barrier at the tunnel period (Spagnolli *et al.*, 2017). For increasing interactions and weak population imbalance, Rabi oscillations smoothly evolve into plasma oscillations, with a frequency controlled by the repulsion between atoms (Albiez *et al.*, 2005; LeBlanc *et al.*, 2011; Levy *et al.*, 2007; Pigneur *et al.*, 2018). For the largest imbalances, tunneling cannot compensate the effect of the non-linear interaction, leading to macroscopic quantum self-trapping (Albiez *et al.*, 2005; Levy *et al.*, 2007; Pigneur *et al.*, 2018; Spagnolli *et al.*, 2017). This dynamics occurs in the absence of dissipation, which is true in the two-mode regime at zero temperature (Gati *et al.*, 2006). For attractive interactions, the plasma oscillation mode softens down to zero frequency at a critical attraction (Trenkwalder *et al.*, 2016).

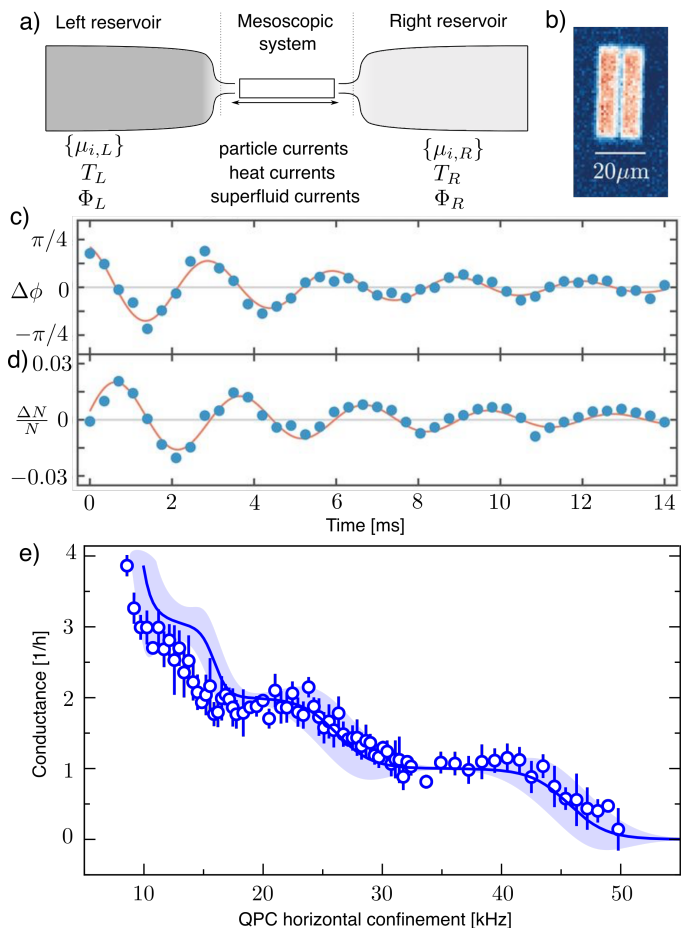


FIG. 6 a) A two terminal system comprises a mesoscopic system connected to reservoirs (L, R), with a set of control parameters: chemical potentials for species i μ_i , temperatures T or superfluid phase Φ . b) Two-terminal Josephson junction in a strongly interacting two-dimensional Fermi gas. Phase difference c) and atom number difference d) as a function of time in the junction, after imprinting a relative phase difference of $\pi/4$. Adapted from Luick *et al.*, 2020 e) Quantized conductance in a quantum point contact for weakly interacting Fermions. Conductance is measured as a function of the QPC trap frequency (ν_x). Solid lines: predictions of the Landauer formula. Adapted from Krinner *et al.*, 2015a

The tunneling and interaction strength parameters of the two-mode model can be derived from the microscopic, mean-field Gross-Pitaevskii equation (Giovanazzi *et al.*, 2008; LeBlanc *et al.*, 2011), and depend on the details of the trap configuration. The predictions of this model are in good agreement with experiment (Ryu *et al.*, 2013). The fluctuations due to the discrete nature of atoms allows us to describe quantum fluctuations of the phase, similar to phase noise in a non-linear interferometer (Pezzè *et al.*, 2018). Beyond the mean-field approximation in the strongly interacting regime, a rich phenomenology has been predicted (Zöllner *et al.*, 2008). Further quantum effects can also arise also from continuous quantum measurements of the atom numbers

(Uchino *et al.*, 2018).

b. Extended reservoirs While the two-mode approximation captures the essence of superfluid atomic currents through a tunnel junction, it disregards processes that take place within the reservoirs. Large reservoirs feature excitations that can couple to the current. The double-well structure is a very powerful configuration in which two identical systems can be produced and compared using interferometry. The internal dynamics of each system is then revealed in the phase relation between the two condensates. The latter has been used, in particular, for the study of one-dimensional gases in parallel wire configuration (Betz *et al.*, 2011; Gring *et al.*, 2012; Hofferberth *et al.*, 2007, 2008; Langen *et al.*, 2015). These landmark experiments reveal very fine details of the effective field-theory describing the one-dimensional reservoirs, including high-order correlations (Schweigler *et al.*, 2021). Interestingly, allowing for a finite tunnel coupling between the two reservoirs modifies the effective Sine-Gordon model describing the low-energy physics (Gritsev *et al.*, 2007). In head-to-tail geometry (Binanti *et al.*, 2021; Polo *et al.*, 2018; Tononi *et al.*, 2020), corresponding to the realization of the Boundary Sine-Gordon model, the Josephson oscillations are damped by the phonon bath in each wire, realizing the Caldeira-Leggett model (Caldeira and Leggett, 1983).

The Josephson dynamics coupled with that of the reservoirs is captured phenomenologically by the resistively-shunted Josephson junction model (RSJJ) (Tinkham, 2012), inspired from the condensed matter physics context and applied to atomtronics circuits in (Burchianti *et al.*, 2018; Eckel *et al.*, 2016; Luick *et al.*, 2020). In this model, the reservoirs are described by an effective capacitance, corresponding to the compressibility of the gas $C = \frac{\partial N}{\partial \mu_r}$, with μ_r the reservoirs chemical potential and N its atom number, derived from the equation of state and geometry.

Large reservoirs are also described by a kinetic inductance due to the finite mass of the atoms, which adds to that of the junction to form the total inductance L . The frequency $\omega_0 = (LC)^{-1/2}$ represents the first normal mode of the system, reducing to the dipole mode of in a purely harmonic trap or to the plasma frequency in the two-modes model. The tunnel barrier itself is described by its critical current I_c , and the dissipative effects are captured by the parallel 'shunt' resistance R . The superfluid character of the system is encoded in the current-phase relation of the tunnel barrier $I = I_c \sin \phi$ and the Josephson-Anderson equation relating the chemical potential difference $\Delta\mu$ to the phase $\phi = \Delta\mu$ (Packard, 1998).

In this framework, the intrinsic properties of the superfluid junction can be studied independently of the dissipation by imposing a quasi-DC current (Kwon *et al.*, 2020; Levy *et al.*, 2007). Alternatively, imprinting a phase difference across the junction by applying an ex-

ternal bias for a short time and measuring the current response through the junction realizes the equivalent of the DC Josephson effect (Luick *et al.*, 2020).

At non-zero temperature, thermally excited atoms serve as a natural source of dissipation justifying a finite value for R (Levy *et al.*, 2007; Marino *et al.*, 1999; Ruostekoski and Walls, 1998; Zapata *et al.*, 1998). Even at zero temperature, a finite damping arises as the current couples to the internal dynamics of the reservoirs. In weakly interacting BECs and in Fermi gases in the BEC-BCS crossover, the physics captured by the resistance is related to the nucleation of topological defects (Burchianti *et al.*, 2018; Eckel *et al.*, 2016; Jendrzejewski *et al.*, 2014; Li *et al.*, 2016; Valtolina *et al.*, 2015; Wright *et al.*, 2013a; Khani *et al.*, 2020) or phase slips in one dimension (Dubessy *et al.*, 2021; Polo *et al.*, 2019). The current also couples to Bogoliubov excitations in BECs and superfluid Fermi gases (Luick *et al.*, 2020; Singh *et al.*, 2020), competing with the coupling to vortices at higher temperature (Singh *et al.*, 2020). The coupling of tunneling with the Bogoliubov spectrum is theoretically studied in (Meier and Zwirger, 2001; Uchino, 2020; Uchino and Brantut, 2020), predicting a finite DC resistance at zero temperature.

Fermi superfluids also feature pair-breaking excitations, which have spectacular effects on the transport properties (Averin and Bardas, 1995). Indirect evidences for such effects have been reported with cold Fermi gases in a point contact (Husmann *et al.*, 2015). Remarkably, the Ambegaokar-Baratoff formula, relating pair-breaking excitations to the critical current in weakly interacting fermionic superfluids is shown to smoothly interpolate with dissipation induced by Bogoliubov excitations in the crossover from BCS to BEC (Zaccanti and Zwirger, 2019). Deeply within the scopes of atomtronics, the Josephson dynamics can be used to probe bulk quantum properties of the materials such as the superfluid order parameter (Kwon *et al.*, 2020) or flat-band superconductivity (Pyykkönen *et al.*, 2021).

c. Weak links in interacting systems In this regime, both the junction and the reservoirs have macroscopic size compared with the coherence or healing length of the gas. In such a weak link an appropriate description of transport can be obtained using superfluid hydrodynamics. It incorporates the transport of non-interacting thermal excitations (Papoular *et al.*, 2014). A lump element model can be derived from the microscopic hydrodynamics in a rigorous way for weakly interacting bosons, leading to accurate predictions for the dynamics of two-terminal systems (Gauthier *et al.*, 2019). In general, the population oscillations between reservoirs (Papoular *et al.*, 2014) and that of the superfluid phase closely matches the plasma oscillation in the two-mode approximation. There, dissipation arises due to phase slippage mechanisms occurring within the weak link, and no qualitative difference emerges for long channels compared with tunnel-like bar-

riers (Beattie *et al.*, 2013; Burchianti *et al.*, 2018; Eckel *et al.*, 2016; Jendrzejewski *et al.*, 2014; Wright *et al.*, 2013a; Khani *et al.*, 2020).

The case of superfluid Fermi gases has been studied in this context through a direct comparison between the unitary gas and a non-interacting Fermi gas, showing two-orders magnitude differences in the conductance (Stadler *et al.*, 2012). Furthermore, long channels can feature sections exposed to a tailored potential such as disorder. In a strongly interacting superfluid, a crossover is observed between a low disorder regime with superfluid transport and a disorder-dominated regime with low conductance (Krimmer *et al.*, 2013, 2015b).

2. Conductance measurements and incoherent reservoirs

In situations where quantum coherence is either non-existent, or can be neglected such as in junctions dominated by dissipation, transport is captured by the conductance $G = I/\Delta\mu$, where $\Delta\mu$ is the chemical potential difference between the two reservoirs.

a. Non-interacting atoms For reservoirs of non-interacting particles or quasi-particles, the current is determined by the energy-dependent transmission coefficients of the junction \mathcal{T}_n , where n labels the transverse modes of the junctions, through the Landauer formalism (Cuevas and Scheer, 2017)

$$I = \frac{1}{h} \int d\epsilon \sum_n \mathcal{T}_n(\epsilon) (f_1(\epsilon) - f_2(\epsilon)) \quad (8)$$

where f_1 and f_2 are the energy distribution of particles in the two reservoirs. For Fermi gases and liquids, f is the Fermi-Dirac distribution corresponding to the reservoir chemical potential μ_i and temperatures T_i . The formalism also applies to weakly interacting bosons above the critical temperature (Kolovsky *et al.*, 2018; Nietner *et al.*, 2014; Papoular *et al.*, 2016). The strength of the Landauer paradigm is the separation between the quantum coherent part and the incoherent reservoirs, the latter featuring fast dissipation processes that are not described microscopically. The atomtronics Landauer setup, with control over the reservoir properties, has motivated detailed theoretical studies of the dissipation dynamics through a comparison of the various microscopic descriptions (Chien *et al.*, 2014; Gallego-Marcos *et al.*, 2014; Ivanov *et al.*, 2013; Kolovsky, 2017; Nietner *et al.*, 2014).

The Landauer paradigm has been proposed for cold atoms in (Bruderer and Belzig, 2012; Gutman *et al.*, 2012) and independently realized experimentally in (Brantut *et al.*, 2012) using weakly interacting fermions in two reservoirs connected by a mesoscopic, quasi-two-dimensional constriction. For tight constrictions, the system behaves as a simple RC circuit, with capacitors modeling the reservoirs, and the constriction the resistance.

Measuring the decay constants of an initially prepared particle-number imbalance between the two reservoirs, and inferring the compressibility from the equation of state allowed to extract the conductance of the constriction. Early experiments focused on variations of conductance induced by changes of shape of the constriction or the introduction of disorder (Brantut *et al.*, 2012). In very recent experiments a similar system was used to investigate Anderson localization effects in two dimensions (White *et al.*, 2020).

At zero temperature and low chemical potential difference, Eq. (8) yields $I = \Delta\mu/hj$, j an integer. Each mode energetically accessible in the conductor contributes independently by $1/h$ to the conductance. In experiments, this is manifested in jumps of the conductance by $1/h$ as the Fermi energy reaches the successive transverse modes of the constriction, as observed in condensed matter devices (van Wees *et al.*, 1988; Wharam *et al.*, 1988) and in the atomtronics context (Krinner *et al.*, 2015a), as shown in figure 6.

On top of such an ideal one dimensional conductor, high-resolution optical methods allowed for the projection of structures as described in section II.C.3, such as point-like scatterers. Measuring the conductance as a function of the scatterer's location produces a high resolution spatial map of the transport process, akin to scanning gate microscopy in the condensed matter context (Häusler *et al.*, 2017). Disposing several scatterers in a regular fashion produced a mesoscopic lattice that exhibits a band structure directly observed in the transport properties, demonstrating the ability to observe and control quantum interferences at the single scatterer level (Lebrat *et al.*, 2018).

The notions of reservoirs and channels can be interpreted in a more abstract way through the concept of synthetic dimension, using internal states of atoms (Celi *et al.*, 2014) or vibrational states of traps (Price *et al.*, 2017). The two-terminal transport concept has also found a generalization through this mapping: a spin imbalanced Fermi gas provides a realization of two terminals in the spin space, and an impurity with engineered spin-changing collisions provide the counterpart of a point contact (You *et al.*, 2019). The use of vibrational states of reservoirs and constrictions as a synthetic dimensions then allows us to envision synthetic multi-terminal situations, where transport would be sensitive to chirality (Salerno *et al.*, 2019).

b. Incoherent transport of interacting atoms The situation of quantum point contacts and one dimensional constrictions in the presence of interactions has been heavily investigated in the condensed matter physics context (Cuevas and Scheer, 2017; Imry, 2002). For two-terminal atomtronics systems this situation has been envisioned theoretically for bosons in (Gutman *et al.*, 2012) with ideal reservoirs and in (Simpson *et al.*, 2014) with superfluid reservoirs, in the framework of Luttinger liquid

physics. For fermions, the point contacts and wires have been investigated experimentally in the deep superfluid regime for a unitary Fermi gas (Husmann *et al.*, 2015), showing non-linear current-bias relations that could be traced back to multiple Andreev reflections (Krinner *et al.*, 2017). This regime is expected to interpolate continuously with the Josephson regime as the transmission in the point contact is reduced (Averin and Bardas, 1995; Yao *et al.*, 2018). This is further investigated by continuously increasing interactions from the free Fermi gas, showing quantized conductance, up to unitarity with non-linear response (Krinner *et al.*, 2016). In the intermediate regime, the conductance plateau is observed to increase continuously from $1/h$ up to values as high as $4/h$ before disappearing close to unitarity, which could be either due to confinement induced pairing within the contact (Kanász-Nagy *et al.*, 2016; Liu *et al.*, 2017) or superfluid fluctuations in the reservoirs (Uchino and Ueda, 2017).

Transport in the one dimensional lattice, featuring a band structure, offers the possibility to explore the fate of metallic and insulating behavior as interactions are varied (Lebrat *et al.*, 2018). It is found that the band insulator evolves smoothly into a correlated insulator comprising of bound pairs with unit filling in the lattice, as interactions are increased providing evidence for the Luther-Emery phase (Giamarchi, 2003).

c. Spin and heat transport Transport in the two-terminal system can be generalized to spin in a two-component Fermi gas, where the total magnetization is conserved, and can be exchanged between two reservoirs. The linear response in currents is expressed through a matrix relating the currents of the two spin components to their respective chemical potential biases, with off-diagonal elements describing spin drag. In contrast with particle conductance, magnetization currents are very sensitive to interactions since collisions do not conserve the total spin current. Even in the absence of a constriction or channel, two clouds of opposite polarization relax very slowly to equilibrium especially at unitarity (Sommer *et al.*, 2011), where the spin diffusion coefficient saturates to a universal value. These experiments have been repeated for a metastable, strongly repulsive Fermi gas, providing evidence for a ferromagnetic instability (Valtolina *et al.*, 2017). In the case of a one dimensional quantum wire, the strongly attractive Fermi gas is found to behave as an ideal spin-insulator, as a consequence of pairing (Krinner *et al.*, 2016). Another possibility to manipulate spin currents is created by the use of spin-dependent potentials, that are used to produce a spin valve from a quantum point contact (Lebrat *et al.*, 2019).

Heat and energy transport can be investigated by introducing a temperature bias between the two reservoirs and observing energy flow through the channel. Heat and particle currents couple both through the thermodynamics of the reservoir due to finite dilation coeffi-

cients, and through genuine thermoelectric effect originating from the energy dependence of the transmission coefficient, as is observed in (Brantut *et al.*, 2013; Häusler *et al.*, 2021). This also opens the perspective of Peltier cooling methods for quantum gases (Grenier *et al.*, 2014, 2016; Sekera *et al.*, 2016). In the case of the unitary Fermi gas, a similar experiment on quasi-one dimensional constrictions was performed, yielding a low heat conductance and a breakdown of the Wiedemann-Franz law, in qualitative agreement with theory (Pershoguba and Glazman, 2019), but a thermopower compatible with that of a non-interacting Fermi gas (Husmann *et al.*, 2018). Such a breakdown is also predicted for strongly interacting bosons within the Luttinger liquid framework (Filippone *et al.*, 2016).

d. Dissipative barriers As opposed to electrons, atomtronic devices allows for the engineering of atom losses. This has been investigated using electron microscopy with the creation of highly localized purely dissipative barriers (Barontini *et al.*, 2013; Labouvie *et al.*, 2015). The non-hermitian character of the resulting Hamiltonian supports the observation of coherent perfect absorption (Müllers *et al.*, 2018). Using an optical barrier involving spontaneous emission also produces dissipation in addition to the optical potential. This is studied in (Corman *et al.*, 2019). The interplay of these effects with interactions and fermionic superfluidity is investigated in (Damanet *et al.*, 2019a).

3. Two terminal transport through ring condensates

Transport in circuits with closed architectures provides a direct way to explore the coherence of the system (Imry, 2002). At the same time, it provides an instance of integrated atomtronic circuits. Consider particles injected from a source into ring-shape circuit pierced by an effective magnetic field, and collected in a drain lead. There, the phase of particles couples with the gauge field and transport displays characteristic Aharonov-Bohm interference patterns (Aharonov and Bohm, 1959; Leggett, 1980; Olariu and Popescu, 1985; Vaidman, 2012), as studied in electronic systems (Büttiker *et al.*, 1984; Gefen *et al.*, 1984; Hod *et al.*, 2006; Jagla and Balseiro, 1993; Lobos and Aligia, 2008; Marquardt and Bruder, 2002; Nitzan and Ratner, 2003; Rincón *et al.*, 2009, 2008; Shmakov *et al.*, 2013; Webb *et al.*, 1985).

Atomtronics allows the study of transport through ring-shaped circuits in new ways, with carriers of various statistics, tunable atom-atom interactions and lead-ring couplings (Haug *et al.*, 2019a,c). Specifically, the non-equilibrium dynamics, described by Bose-Hubbard or discrete Gross-Pitaevskii models, is analyzed by quenching the particles spatial confinement in both closed and open configuration. Depending on the ring-lead coupling, interactions and particle statistics, the system displays

qualitatively distinct non-equilibrium regimes with by different response of the interference pattern to the effective gauge field. In contrast to fermionic systems, the coherent transport of strongly interacting bosons does not display characteristic oscillations as function of the effective magnetic flux. A possible explanation for the suppression of the Aharonov-Bohm oscillations comes as a compensation between the phase of the condensate and Aharonov-Bohm phase. For a field theoretic explanation for the absence of Aharonov-Bohm interference in the circuit see Tokuno *et al.*, 2008.

The transport through lead-ring interface can display a bosonic analogue of Andreev scattering: when a bosonic matterwave hits the lead-ring interface, it is transmitted to the ring with the emission of an matter-wave of negative amplitude, a 'hole', that is reflected backwards (Daley *et al.*, 2008; Watabe and Kato, 2008; Zapata and Sols, 2009). Two-terminal transports through rings and Y-junctions are considered in (Haug *et al.*, 2019a).

A coherent transport can also be achieved through topological pumping, by driving periodically in time a system protected by a band gap (Thouless, 1983; Thouless *et al.*, 1982). Such periodic drives are natural within atomtronics, thanks to the availability of reconfigurable circuits (Gaunt and Hadzibabic, 2012; Gauthier *et al.*, 2016; McGloin *et al.*, 2003). Topological pumping through source-ring-drain atomtronic circuit is addressed in Haug *et al.*, 2019b. This way, topological bands and Aharonov-Bohm effect in interacting bosonic system are intertwined: the Aharonov-Bohm interference affects reflections by inducing specific transitions between topological bands. The system effectively works as a non-linear interferometer, in which the source-ring and the ring-drain act as beam-splitters. Interaction adjusts the transmission and reflection coefficients and entangles the propagating wave-functions in the two arms of the interferometer.

IV. ATOMTRONIC COMPONENTS AND APPLICATIONS

In this section, we discuss the atomtronic circuitual elements that have been considered in the literature. The first sections concern the atomic analogues of some circuit elements in classical electronics. We conclude the section with atomtronic qubits inspired by quantum electronics.

A. Matter wave optics in atomtronic circuits

Transport in atomtronic circuits can be either coherent transmission like in photonic circuits or more like a superfluid similar to superconducting electronics. A classical example is the decay of superfluid currents as described in Sec. III.B. The main stumbling block in observing the coherent transmission of matter waves over macroscopic distances is the degree of roughness of the waveguides that are currently available.

Until recently, except for straight guides formed by collimated laser beams, atomtronics is limited to the latter. This situation changes recently with the first demonstration of coherent guiding over macroscopic distances in a ring-shaped matter wave guide (Pandey *et al.*, 2019). It is now possible to (de)accelerate BECs in an optimal way to speeds of many times the critical superfluid velocity and an angular momentum exceeding $40000 \hbar$ per atom without observable decay over time. Matter-wave lensing or delta-kick cooling (Arnold *et al.*, 2002; Kovachy *et al.*, 2015) has now been demonstrated using gravito-magnetic lenses inside of TAAP matter-wave guides, where BECs and thermal clouds have been collimated, thus reducing their expansion energies by a factor of 46 down to 800 pK (Pandey *et al.*, 2021). Delta-kick cooling with an optical potential is routinely used in waveguide atom interferometers to lower the energy of an expanded and collimated BEC below a few nK (Krzyzanowska *et al.*, 2022).

B. Transistors, diodes, and batteries

The early work in atomtronic devices sought to emulate semiconductor material-based elements by considering neutral atoms in optical lattices, (Pepino *et al.*, 2009; Pepino, 2021; Seaman *et al.*, 2007) but work also sought simply functional duals by considering atoms confined to a small number of potential wells (Stickney *et al.*, 2007). There are substantial differences in underlying physics, as well as practical differences, between these two approaches to device design.

Lattice based devices share clear analogies with electronic systems in periodic potentials characterized by band structure effects. At the same time, bosonic many-particles systems are unavoidably characterized by specific quantum correlations making their dynamics very distinct from the electronic one. Specifically, lattice-based atomtronic components deal with superfluids (instead of conductors) and heavily rely on the possibility to engineer a Mott insulating quantum phase that interacting bosons can undergo to, for integer filling fractions (number of bosons commensurate with the number of lattice points). Another effect without any classical electronics analog is the macroscopic quantum self trapping phenomenon that can hinder the transmission of a bosonic fluid through a potential barrier (Milburn *et al.*, 1997; Smerzi *et al.*, 1997). As a specific example of the semiconductor approach, an atomtronic diode can be conceived in analogy with the electronic P-N junction diode: the different concentration of electrons and holes in the P and N materials set a potential drop that can be modulated by an external voltage bias; the so-called forward (reverse) bias corresponds to a reduction of the potential drop for the electrons (holes) at the junction, and therefore a particles flow takes place. In the atomtronic diode, the junction is realized by facing commensurate and incommensurate lattices of condensates; an abrupt change of the chemical potential at the junction, playing

the role of the voltage bias (Pepino *et al.*, 2009). This way, the control of the chemical potential can make the bosons from the commensurate to the incommensurate lattice of condensate, but not vice-versa. The diode may be connected to two bosonic reservoirs kept at different chemical potential that play the role of the battery. Ultimately, the nonlinear device behavior arises from the *non linearity* of the atom-atom interactions that is a feature specific to the lattice systems.

Here, we note that classical electronic circuits are indeed non-thermal-equilibrium systems whose dynamics is wholly driven by the presence of a battery (or other source of electric potential) supplying power to the circuit. It is also significant to appreciate that a battery is fundamentally associated with an internal resistance, which causes the battery to dissipate energy. In atomtronic circuits, it is a BEC with finite chemical potential and temperature, that serves to provide the 'bias' driving the non-equilibrium dynamics of a circuit. And like the electrical battery, a BEC-based battery providing atom current to a circuit will exhibit an internal resistance. While the classical battery is always associated with a positive resistance, a atomtronic (BEC) battery can exhibit either positive or negative internal resistance, depending on whether the supplied current is thermal or condensed, respectively (Zozulya and Anderson, 2013). An experimental study of atomtronic batteries is carried out in Caliga *et al.*, 2017.

A battery not only powers a circuit, but it is, of course, necessary to provide the gain associated transistor action. Such action has been studied in semi-classical context utilizing a triple-well atomtronic transistor in an oscillator configuration - See Fig. 7 (Caliga *et al.*, 2016b; Stickney *et al.*, 2007). The left-most well acts as source, the middle as gate, and the right as drain, where the nomenclature is taken from the electronic field-effect transistor. Here the system is initialized by placing a BEC at a given temperature and chemical potential in the source well.

The transistor circuit behavior is characterized by a critical feedback parameter given by a normalized difference in barrier height (Caliga *et al.*, 2012): $v = (V_{GD} - V_{GS}) / (k_B T_S)$, in which T_S is the temperature of the source atoms, and V_{GD}, V_{GS} are the barrier heights (see Fig. 7). A semi-classical kinetic treatment has been developed in which the atoms are treated as particles, while they are also allowed to Bose-condense under appropriate conditions. With such an approach, the BEC resulted to spontaneously develop in an initially empty gate well when the feedback exceeds a threshold value (Caliga *et al.*, 2012). This is reflected in the data of Fig. 7 where a high-density of atoms appears in the gate at 10 ms evolution time -in fact the high density is apparent after only 1 ms (Caliga *et al.*, 2016a). The transport semiclassical dynamics of the transistor coupled to the environment, in which the atom steady currents are driven by the chemical potentials, is studied in Caliga *et al.*, 2016b. In particular, by analyzing the gain as function of the operating condition, it is proved that the such

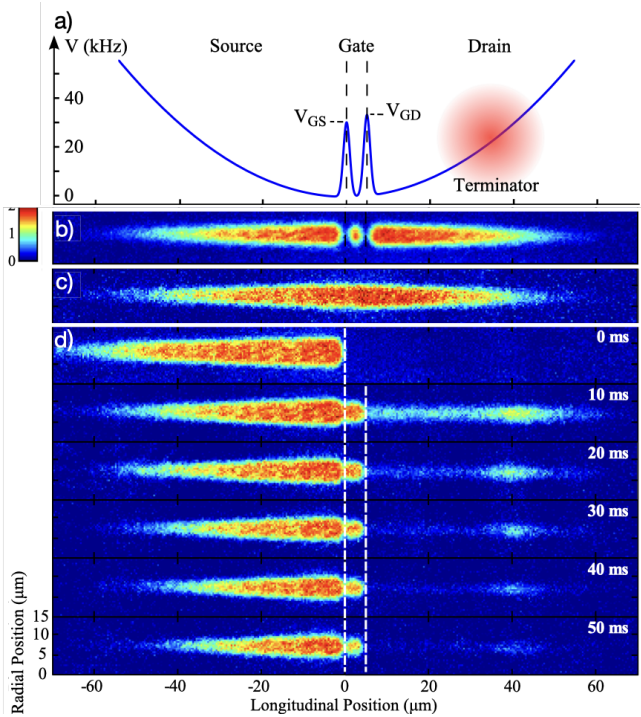


FIG. 7 The atomtronic triple-well transistor. The upper panel a) shows the atomic potential consisting of a hybrid magnetic confinement combined with barriers superimposed by optical projection of a pair of blue-detuned laser beams. A "Terminator" laser beam removes atoms from the drain by pumping them to an untrapped m_F state. The gate width is 4.5μ . Thermal atoms are loaded in the hybrid potential (b) and in absence of the optical barriers (c). Panels d) and below are absorption images of the atoms in the wells at various evolution times starting from $t = 0$ ms and ending at 50ms. Adapted from Caliga *et al.*, 2016a.

atomtronic component can be used to supply power to a given load (therefore acting as an active component).

C. The atomtronic quantum interference device

A toroidal circuit of ultra-cold atoms interrupted by tunnel junctions provides the atomic counterpart of the SQUID: the Atomtronic Quantum Interference Device (AQUID). AQUID's with the characteristic control of noise and interactions and low decoherence of neutral ultracold matter, enclose a great potential both for basic science and technology. AQUID realized by a toroidal shaped superfluid Bose-Einstein condensate obstructed by a rotating weak link is carried out in NIST (Eckel *et al.*, 2014b), Fig.8a). By analogy with the radio frequency SQUID, such rf-AQUID displays hysteresis in angular momentum, Fig.8b). The role of the vortices generated by the stirring barrier (Yakimenko *et al.*, 2015, 2014) or thermal fluctuations (Kumar *et al.*, 2017; Kunitani and Danshita, 2019; Mehdi *et al.*, 2021) have been analysed. Barrier strength and dynamical protocol of

ramping up and down the stirring potential need to be carefully chosen to achieve a controlled and effective realization of the AQUID (Mathey and Mathey, 2016). The read-out of the rf-AQUID in the different regimes of interaction and barrier strength is studied in Haug *et al.*, 2018b by monitoring the dynamics of interference fringes established after the condensate is released.

Toroidal-shape condensates interrupted by two tunnel junctions have been experimentally fabricated by the Los Alamos group through the painting technique described in Sec.II.A.2 (Ryu *et al.*, 2013), Fig.8-c). Such system, providing the atomtronic counterpart of the direct-current SQUID, has dubbed as dc-AQUID. Following (Giovanazzi *et al.*, 2000) the dc Josephson effect in the experiment arises when the atom density (chemical potential) remain constant separately in each sector of the torus despite the two barriers move circumferentially toward each other. Indeed, the current increases with barrier velocity until the critical current of the junctions is reached. At this point the system switches to the ac Josephson regime characterized by an oscillating Josephson current. The frequency of the oscillations turns out proportional to the chemical potential difference across the junction, but no net current across it. Remarkably, the critical current is observed to display characteristic oscillations demonstrating the superposition of superfluid currents, Fig.8d).

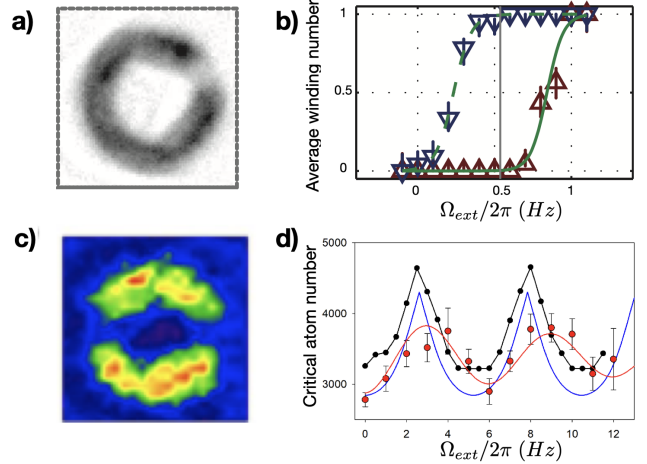


FIG. 8 Fabricated AQUIDs. a) The rf-AQUID of the NIST group. b) The hysteretic property of the rf-AQUID. c) The dc-AQUID realized by the Los Alamos group. d) Oscillations of the critical current demonstrating superposition of superfluid currents. The black and blue curves are theoretical expectations and the error bars are result from the experiment, being the red curve a best fit of it. a) and b) adapted from Eckel *et al.*, 2014b; c) adapted from Ryu *et al.*, 2013 and d) adapted from Ryu *et al.*, 2020.

The interference of persistent currents of dc-AQUIDs is recently carried out experimentally Ryu *et al.*, 2020. By inducing a bias current in a rotating atomic ring interrupted by two weak links, the interference between the Josephson current with the current from the rota-

tion creates a oscillation in the critical current with applied flux. This oscillation is measured experimentally in the transition from the DC to the AC Josephson effect. This experiment has been performed within a dilute Bose-Einstein condensate that is well described within a mean-field description and thus entanglement of currents, which is a key ingredient for the atomic qubit, has not been demonstrated. Nonetheless, it is a major step towards the implementation of the atomic qubit.

D. Atomtronic qubit implementations

Atomtronics qubit implementations have been proposed to combine the logic of cold atoms and superconducting circuits based qubits. The basic idea is to use the persistent currents of cold atoms systems flowing in ring shaped potentials; in order to have two well defined energy levels, the translational invariance of the system needs to be broken by the insertion of suitable weak-links. The presence of the weak-link breaks the axial rotational symmetry of the ring fluid and couples different angular momenta states, opening a gap at the degeneracy point among two angular momentum states (see Sec.III.B.1). This way, the two states of the qubit system are the symmetric and anti-symmetric combinations of the two angular momentum states (Aghamalyan *et al.*, 2015, 2016a; Amico *et al.*, 2014, 2005; Solenov and Mozyrsky, 2010). The nature of the superposition state depends on the system parameters: at weak interactions it is a single-particle superposition, at intermediate interaction a NOON-like state and at very strong interactions a 'Moses state' i.e. a superposition of Fermi seas (Hallwood *et al.*, 2006; Nunnenkamp *et al.*, 2008; Schenke *et al.*, 2011). An important point in this context, is to establish to what extent the cold-atoms quantum technology would be capable to feasibly address the qubit. In particular, the energy gap separating the two energy levels of the qubit displays a specific dependence on the number of atoms in the ring network, atom-atom interaction and atom tunneling rates through the weak link (Nunnenkamp *et al.*, 2011). The numerical analysis based on BHM shows that the limit of a weak barrier and intermediate to strong interactions form the most favorable regime a qubit regime Fig. (9) (Aghamalyan *et al.*, 2016a; Amico *et al.*, 2014). The spectral quality of the qubit is analyzed in (Aghamalyan *et al.*, 2015) as function of the physical parameters of the system. The three weak links architecture (Aghamalyan *et al.*, 2016a), indeed, realizes a two-level effective dynamics in a considerably enlarged parameter space. Machine learning preparation of entangled persistent current is demonstrated in Haug *et al.*, 2021.

Important for the aforementioned feasibility of the qubit dynamics is the analysis based on QPM working in the limit of large number of particles (see Eq. (3)). Here, the two level qubit dynamics emerges analytically (Amico *et al.*, 2014). For the case of a ring-

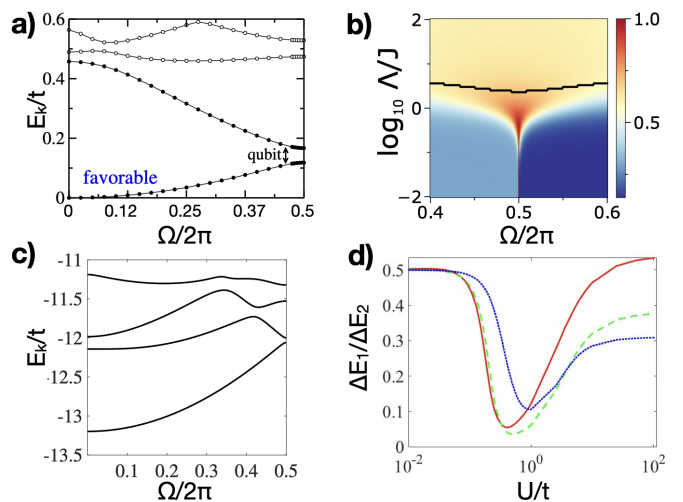


FIG. 9 Atomtronic qubits. a) The upper panels refer to Bose-Hubbard rings interrupted by a single weak link. The bottom panels refer to a flux qubit configuration of a Bose-Hubbard ring interrupted by three weak links. a) and c) display the energy levels E_k . b) shows the noise correlations in the TOF image of the single weak link qubit. Panel d) summarizes the qubit quality factor as provided by the ratio between the energy gaps between the ground state energy and the first two excitation energies ΔE_1 and ΔE_2 . Panel a) adapted from Aghamalyan *et al.*, 2015; panel b) adapted from Haug *et al.*, 2018b; panels c) and d) adapted from Aghamalyan *et al.*, 2016b.

circuit interrupted by a single weak link, the effective Hamiltonian is $\mathcal{H}_{\text{eff}} = \mathcal{H}_{\text{sys}} + \mathcal{H}_{\text{bath}} + \mathcal{H}_{\text{sys-bath}}$ in which $\mathcal{H}_{\text{sys}} = U\mathbf{n}^2 + E_L\varphi^2 - E_J \cos(\theta - \Omega)$ where θ is the phase slip across the weak link, with $E_L = J/M$, and $E_J = J'$. For $\delta \doteq E_J/E_L \geq 1$, \mathcal{H}_{sys} describes a particle in a double well potential. $\mathcal{H}_{\text{bath}}$ respectively describes the dissipative dynamics $\mathcal{H}_{\text{sys-bath}}$ and interaction due to the phase slips occurring in the other lattice sites. See also (Rastelli *et al.*, 2013).

The qubit can be probed through a Rabi-type protocol: By quenching the effective magnetic field to the degeneracy point, characteristic Rabi oscillations occur with a frequency $\propto 1/\Delta E_1$ (Polo *et al.*, 2021; Schenke *et al.*, 2011). The two states of the qubit could be manipulated through a suitable 'pulse' of artificial magnetic field.

The read-out has been studied with various expanding condensate protocols (Aghamalyan, 2015; Haug *et al.*, 2018b). In particular, the two-level system structure and the corresponding specific entanglement between the clockwise and anti-clockwise flows can be quantified through the noise in the momentum distribution: $\langle \hat{n}(\mathbf{k})\hat{n}(\mathbf{k}) \rangle - \langle \hat{n}(\mathbf{k}) \rangle \langle \hat{n}(\mathbf{k}) \rangle$, resulting to be maximum at the degeneracy point - see Fig.9b (Haug *et al.*, 2018b).

Proof of concepts for qubits coupling have been provided in which qubits are imagined to be arranged in stacks (Amico *et al.*, 2014) or in planar (Safaei *et al.*, 2018) configuration. We comment that by relying on recent optical circuit design, much more flexible solutions are feasible

to be implemented (Rubinsztein-Dunlop *et al.*, 2016).

E. Atomtronic interferometers

An interferometer splits a wavefunction into a superposition of two parts and then recombines them in a phase-coherent fashion. If the wavepackets overlap perfectly at the output of the interferometer, the phase difference between the two arms is the difference between the phase shifts imposed by the pulsed beam-splitters and mirrors in each arm plus the propagation phase $\Delta\phi_{prop} = (S^1 - S^2)/\hbar$, where S^i is the classical action computed along path i (Peters *et al.*, 2001). A beam-splitter at the interferometer transforms the phase difference into a population difference, which is easily read out. Most of the atom interferometer solutions demonstrated to date involve free-falling atoms. Traditional atom interferometers involve free-falling atoms. Traditional atom interferometers involve free-falling atoms (Arimondo *et al.*, 2009; Bongs *et al.*, 2019; Geiger *et al.*, 2020, 2011; Müller *et al.*, 2008; Stockton *et al.*, 2011; Sugarbaker, 2014; van Zoest *et al.*, 2010). They have the advantage of decoupling the atoms from many effects which otherwise might cause uncontrollable additional phase shifts, which can lead to a deterioration of contrast or a random shift of the fringes. The main disadvantage is the size of the interferometer: Longer interrogation times lead to larger phase shifts. Therefore free-falling high-precision matter-wave interferometers need to be very tall in order to accommodate the distance that the atoms fall during the interrogation—reaching a size of ten or even one hundred meters (Kovachy *et al.*, 2015; Muntinga *et al.*, 2013). In contrast to this, atomtronic interferometers use a trapping/guiding potential (usually magnetic or dipole) to compensate gravity and thus can achieve a much increased detection time with much reduced space requirements. This comes, however, at the cost of an increased risk of noise and systematic effects due to fluctuations in the guiding potential.

a. Sagnac effect based atomtronic sensors: An important application of waveguide atom interferometer gyro-technology is inertial navigation in the absence of position information provided by a Global Navigation Satellite System (GNSS). An inertial navigation system (INS) contains three accelerometers, whose output is integrated twice to get displacement, along with three gyros that track the orientation of the accelerometers. It turns out that the navigation accuracy of current INS over timescales of hours and longer is limited by the drift in the zero of the gyros. These sensors are usually fiberoptic gyros (FOGs). Free-space atom interferometer gyros have already demonstrated extremely low drift (Gustavson *et al.*, 1997, 2000; Helm *et al.*, 2015), with their main disadvantage for some applications being the large physical size required to accommodate free fall of atoms being interrogated over several seconds. Guided atom

interferometer gyros, analogous to the FOG, would be much more compact, making them attractive for navigation if they can be engineered to have low drift.

In a typical rotation-sensing configuration, atomtronic high-precision gyros are based on the Sagnac effect: two input quantum waves propagating along two different arms of a closed path circuit of enclosed area A produce interference fringes at the interferometer output; if the circuit is rotated at rate Ω , the interference fringes will be shifted by

$$\Phi_{\text{Sagnac}} = \frac{4\pi E}{hc^2} \mathbf{A} \cdot \boldsymbol{\Omega} \quad (9)$$

where E is the energy of the traveling wave, and \mathbf{A} and $\boldsymbol{\Omega}$ are respectively the enclosed area and the rotation vector. For frequency ν photon-based Sagnac interferometers $E_{\text{ph}} = h\nu$ and for matter-waves it is $E_{\text{mw}} = mc^2$ instead, yielding $\Phi_{\text{Sagnac}} = \frac{4\pi}{h/m} \mathbf{A} \cdot \boldsymbol{\Omega}$. For equal particle flux and enclosed area, the difference in sensitivity between photon and matter wave interferometers is thus the ratio between the energies $E_{\text{mw}}/E_{\text{ph}} = 10^{10}$. Light-based interferometers typically contain orders of magnitude more photons than the matter wave interferometers contain atoms. They also tend to enclose a much larger area. Nevertheless, matter wave interferometers are expected to outperform their photon counterparts, e.g., where long-term stability is required.

b. Bright soliton rotation sensors: A BEC with attractive interactions (e.g. ^{85}Rb or ^7Li) in a ring shaped guide can realize bright soliton interferometry: A localized barrier can split the solitons into two waves propagating in clockwise and anticlockwise directions that can ultimately recombine after traveling two semicircles. Even though (perfect) bright solitons can go through each other without changing their density profiles, the two waves can provide a Sagnac phase shift (Helm *et al.*, 2012, 2015; McDonald *et al.*, 2014; Polo and Ahufinger, 2013). The splitting of bright solitons scattering on a localized barrier is analyzed in (Helm *et al.*, 2014; Marchukov *et al.*, 2019; Weiss and Castin, 2009). In such process, superposition states are predicted to occur (Streltsov *et al.*, 2009). The roles of both quantum noise and interactions for rotation sensing with bright solitons described by a many-body Schrödinger equation have been analyzed by a variational principle (Haine, 2018). Because of the formation of solitons, enhanced control on the number of atoms N in the experiments can be reached, that is expected to be beneficial for the sensitivity of the interferometry.

The equivalent of a bright soliton in the fully quantum regime of a ring lattice of attracting bosons described by Bose-Hubbard model was studied in Naldesi *et al.*, 2019. Because of the lattice, the soliton and the number of atoms are protected by a finite gap. A barrier can split such 'quantum soliton' depending on the interplay between interaction, number of particles, and bar-

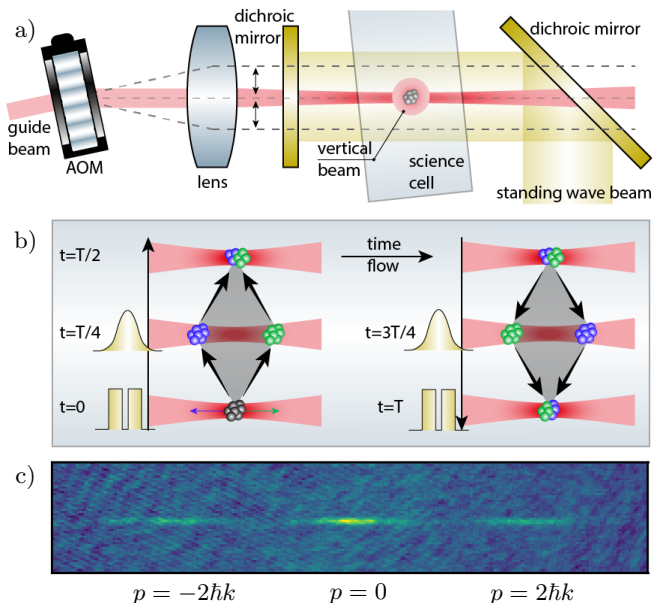


FIG. 10 a) Experimental setup. b) Moving waveguide interferometer. Blue and green colors of atoms correspond to the $+2\hbar k$ and $-2\hbar k$ momentum components respectively. The time flow follows the black arrows. c) Experimental data acquired $\Delta t = 12\text{msec}$ after the recombination pulse, with atoms in two channels: $|p = 0\rangle$ and $|p = \pm 2\hbar k\rangle$. Reproduced from Krzyzanowska *et al.*, 2022

rier strength. For ring-shaped confinement, it is demonstrated that the elementary flux quantum is reduced by $1/N$, where N is the number of particles (Naldesi *et al.*, 2022). Such an effect potentially yields a N -factor enhancement in the sensitivity of attracting bosons to an external field that can reach the Heisenberg limit (Naldesi *et al.*, 2022; Polo *et al.*, 2021).

c. Demonstrated atomtronic interferometers: The first compact atom interferometers utilized stationary clouds of ultracold atoms. These devices and some of the notable physics resulting from experiments with them are discussed in (Böhi *et al.*, 2009; Günther *et al.*, 2007; Jo *et al.*, 2007; Riedel *et al.*, 2010; Schumm *et al.*, 2005). More recently, atomtronic interferometers with moving atoms have been realized in both optical and magnetic traps.

An early example is a Michelson interferometer using a BEC propagating over $120\ \mu\text{m}$ in a magnetic waveguide on an atom chip (Wang *et al.*, 2005). Smoother waveguides obtained with larger coils have been used to realize atom interferometers with thermal atoms (Qi *et al.*, 2017; Wu *et al.*, 2007) and BECs (Burke *et al.*, 2008; Burke and Sackett, 2009; Garcia *et al.*, 2006). This approach has been used to measure the ground state polarizability of ^{87}Rb (Deissler *et al.*, 2008). In optical waveguides (Akatsuka *et al.*, 2017; Ryu and Boshier, 2015) linear interferometers extending up to 1 mm have been demonstrated

(McDonald *et al.*, 2013b). A number of area enclosing interferometers have been realized in macroscopic magnetic traps (Burke and Sackett, 2009; Moan *et al.*, 2020; Qi *et al.*, 2017; Wu *et al.*, 2007).

Recently, an atomtronic Sagnac rotation sensor based on a moving linear waveguide formed by a collimated laser beam is demonstrated (Krzyzanowska *et al.*, 2022). The 3.5mm^2 enclosed by the atomtronic circuit is the largest value realized to date.

In area-enclosing waveguide atom interferometers the signal can be increased by allowing the wavepackets to make multiple orbits around the waveguide loop to increase the enclosed area. The maximum number of round trips is usually limited by atom loss when the counter-propagating wavepackets move through each other. It has recently been shown that this limitation can be removed in an interferometer based on a non-interacting ^{39}K BEC, allowing for over 200 round trips in the guide (Kim *et al.*, 2022).

It is interesting to note that an atomtronic interferometer can be based on free propagation in a guide (Akatsuka *et al.*, 2017; Wang *et al.*, 2005) or on moving fully-trapped atom clouds (clock type interferometers) (Navez *et al.*, 2016; Stevenson *et al.*, 2015). The first case can be pictured as the atoms functioning as an inertial reference much like a flywheel. The phase shift occurred by the fully trapped matter waves is perhaps best understood as being based on the relativistic time gains of an atom clock (Hafele and Keating, 1972).

Finally, we note that several other schemes for novel types of atomtronic interferometers have been proposed (Halkyard *et al.*, 2010; Helm *et al.*, 2018, 2015; Japha *et al.*, 2007; Marti *et al.*, 2015; Moukouri *et al.*, 2021; Pelegri *et al.*, 2018).

V. REMARKS AND FUTURE PERSPECTIVES

Atomtronics defines micrometer-scale coherent networks to address both technology and basic science. It combines bottom-up and a top-down approaches: On one hand, the circuit elements can be designed to implement the microscopic theory in an experimental realization of unprecedented precision. Then, just like in electronics, different circuit elements can be assembled using a hierarchy of heuristic principles. On the other hand, a circuit or even a single circuitual element in its own can be used as a current-based quantum simulator to probe the correlated matter.

Important domains of quantum many-body physics in restricted geometries, ranging from intermediate to extended spatial scales, now become accessible: Analogous to the analysis of current-voltage characteristics in solid state physics, atomtronic circuits have the potential to define current-based emulators and simulators, effectively widening the scope of the existing ones. Currents in particular are the natural quantity to explore not only superflows but also transport in disordered and complex

media as well as topological properties and edge states. An interesting direction to go is to exploit atomtronic circuits to address important questions of high energy physics, such as the phase diagram of quark-gluon plasma (Cazalilla *et al.*, 2009; Chetcuti *et al.*, 2021; He *et al.*, 2006; Ozawa and Baym, 2010; Rapp *et al.*, 2007) or various scattering process in elementary particles physics (Clark *et al.*, 2017; Fu *et al.*, 2020; Surace and Lerose, 2021). Bosonic rings can be employed to study the dynamics of the expanding universe (Eckel *et al.*, 2018).

Atomtronic circuitry has a practical potential as well — a potential that can be realized in part by leveraging the know-how and heuristic design principles of electronics. Atomtronic triple-well transistors are in many respects close analogs of their electronic field-effect transistor counterparts and can be utilized in matter wave oscillators, for example, to produce matter waves with high spatial coherence (Anderson, 2021), which in turn can carry modulated signals or be used in sensing applications. In the future, one can expect many of the familiar elemental functions of electronic circuitry such as amplifiers, switches, oscillators, and so forth, to be carried over to the quantum regime. In another direction, coupled ring circuits, ring-rectilinear wave guides etc have been considered as simple instances of integrated atomtronic circuits (Pérez-Obiol *et al.*, 2021; Polo *et al.*, 2016b; Ryu and Boshier, 2015; Safaei *et al.*, 2019)

Building on the theoretically demonstrated qubit dynamics of specific matter wave circuits (see Sect. IV.D), it will be certainly important to explore atomtronics as a platform for quantum gates. At the same time, matter-wave circuits provide a valuable route to realize high precision compact interferometers working on a wide range of sensitivity and very controllable physical conditions. Such devices are of considerable technological importance in different contexts ranging from inertial navigation (Bongs *et al.*, 2019) to geophysics (Jaroszewicz *et al.*, 2016). Unlike their classical or quantum electronic counterparts, atomtronic circuits can operate a regime in which quantum effects can be dominant and long coherence times are possible with a much simpler cryogenics. In this context, experimental, theoretical and technological inputs are envisaged to be combined together to realize the optimal building block circuit from which complex structures forming actual devices and sensors can be constructed. An important challenge to face in the years to come is to integrate the atomtronic circuits with other existing technologies such as photonic or superconducting integrated circuits (Cano *et al.*, 2008; Mukai *et al.*, 2007; Müller *et al.*, 2010a,b; Nirrengarten *et al.*, 2006; Tosto *et al.*, 2019; Zhang *et al.*, 2012) (for hybrid circuits specifically relevant for quantum information, see (Bernon *et al.*, 2013; Fortágh and Zimmermann, 2007; Hattermann *et al.*, 2017; Petrosyan *et al.*, 2019; Verdú *et al.*, 2009; Xiang *et al.*, 2013; Yu *et al.*, 2017a,b, 2018a,b, 2016a,b,c)). Such hybrid networks may provide a valuable route for the fabrication of integrated 3D matter-wave circuits in which rectilinear, ring guides,

beam splitters etc, together with the fields for the control and read-out of the quantum states and the lasers needed for cooling and manipulation of the cold atoms are built into a single chip. Such an approach can be important to achieve scalable matter-wave circuits.

Both for studies in fundamental science and circuit design with wider specifications, an interesting future direction is to expand the investigations to fermionic atomtronic circuits (Cai *et al.*, 2022; Del Pace *et al.*, 2022) or to open the research in the field to new platforms, as e.g. fermionic systems with N spin components (Chetcuti *et al.*, 2022a,b, 2021) and Rydberg atoms. In the latter platform, bath engineering (Damanet *et al.*, 2019a,b; Keck *et al.*, 2018; Uchino and Brantut, 2020) together with the achieved control of the Rydberg blockade phenomenon (Archimi *et al.*, 2019; Simonelli *et al.*, 2017; Valado *et al.*, 2016) can be explored to start currents with novel specifications. Such a solution may grant the access to the realization of fast atomtronic circuits.

Acknowledgments

We acknowledge the late Frank Hekking for the important contribution given to the Atomtronics field from the earliest stages. We thank G. Birkl, P. Bouyer, W.J. Chetcuti, C. Clark, J. Dalibard, R. Dumke, R. Folman, B. Garraway, T. Giamarchi, T. Haug, T. Neely, S. Pandey, H. Perrin, J. Polo-Gomez, C. Sackett, and J. Schmiedmayer for comments and suggestions on the manuscript. We acknowledge fruitful discussions with J.I. Latorre, A.J. Leggett, C. Miniatura, P. Naldesi, G. Pecci, and K. Wright.

References

- Abad, M., 2016, Physical Review A **93**, 033603.
- Abad, M., A. Sartori, S. Finazzi, and A. Recati, 2014, Physical Review A **89**, 053602.
- Affleck, I., 1988, Nuclear Physics B **305**(4), 582.
- Aghamalyan, D., 2015, *Atomtronics: Quantum technology with cold atoms in ring shaped optical lattices*, Ph.D. thesis, National University of Singapore.
- Aghamalyan, D., L. Amico, and L. C. Kwek, 2013, Physical Review A **88**(6), 063627.
- Aghamalyan, D., M. Cominotti, M. Rizzi, D. Rossini, F. Hekking, A. Minguzzi, L. C. Kwek, and L. Amico, 2015, New Journal of Physics **17**(4), 045023.
- Aghamalyan, D., N. Nguyen, F. Auzsztol, K. Gan, M. M. Valado, P. Condylis, L. Kwek, R. Dumke, and L. Amico, 2016a, New Journal of Physics **18**(7), 075013.
- Aghamalyan, D., N. T. Nguyen, F. Auzsztol, K. S. Gan, M. M. Valado, P. C. Condylis, L.-C. Kwek, R. Dumke, and L. Amico, 2016b, New Journal of Physics **18**(7), 075013.
- Aharonov, Y., and D. Bohm, 1959, Physical Review **115**, 485.
- Akatsuka, T., T. Takahashi, and H. Katori, 2017, Applied Physics Express **10**(11), 112501.
- Albiez, M., R. Gati, J. Fölling, S. Hunsmann, M. Cristiani, and M. K. Oberthaler, 2005, Physical Review Letters **95**(1), 010402.

- Amico, L., 2000, *Modern Physics Letters B* **14**(21), 759.
- Amico, L., D. Aghamalyan, F. Aukstol, H. Crepaz, R. Dumke, and L. C. Kwek, 2014, *Scientific Reports* **4**, 4298.
- Amico, L., G. Birkel, M. Boshier, and L.-C. Kwek, 2017, *New Journal of Physics* **19**(2), 020201.
- Amico, L., M. Boshier, G. Birkel, A. Minguzzi, C. Miniatura, L. C. Kwek, D. Aghamalyan, V. Ahufinger, D. Anderson, N. Andrei, A. S. Arnold, M. Baker, *et al.*, 2021, *AVS Quantum Science* **3**(3), 039201.
- Amico, L., and V. Korepin, 2004, *Annals of Physics* **314**(2), 496.
- Amico, L., A. Osterloh, and F. Cataliotti, 2005, *Physical Review Letters* **95**(6), 063201.
- Amico, L., and V. Penna, 2000, *Physical Review B* **62**(2), 1224.
- Anderson, D. Z., 2021, ArXiv e-prints , 2106.10550.
- Andersson, E., T. Calarco, R. Folman, M. Andersson, B. Hessmo, and J. Schmiedmayer, 2002, *Physical Review Letters* **88**(10), 100401.
- Andrei, N., 1995, *Low-Dimensional Quantum Field Theories for Condensed Matter Physicists* (World Scientific Publishing Co, 2013) pp , 457.
- Andrews, M. R., C. G. Townsend, H.-J. Miesner, D. S. Durfee, D. M. Kurn, and W. Ketterle, 1997, *Science* **275**(5300), 637.
- Anoshkin, K., Z. Wu, and E. Zaremba, 2013, *Physical Review A* **88**, 013609.
- Arabahmadi, E., D. Schumayer, and D. A. W. Hutchinson, 2021, *Physical Review A* **103**, 043319.
- Archimi, M., C. Simonelli, L. Di Virgilio, A. Greco, M. Ciccanti, E. Arimondo, D. Ciampini, I. Ryabtsev, I. Beterov, and O. Morsch, 2019, *Physical Review A* **100**(3), 030501.
- Arimondo, E., W. Ertmer, W. Schleich, and E. Rasel, 2009, *Atom Optics and Space Physics: Proceedings of the International School of Physics " Enrico Fermi", Course CLXVIII, Varenna on Lake Como, Villa Monastero, 3-13 July 2007*, volume 168 (IOS Press).
- Arlt, J., T. Hitomi, and K. Dholakia, 2000, *Applied Physics B* **71**(4), 549.
- Arnold, A. S., C. S. Garvie, and E. Riis, 2006, *Physical Review A* **73**(4), 041606.
- Arnold, A. S., C. MacCormick, and M. G. Boshier, 2002, *Physical Review A* **65**, 031601.
- Averin, D., and A. Bardas, 1995, *Physical Review Letters* **75**, 1831.
- Baeriswyl, D., D. K. Campbell, J. M. Carmelo, F. Guinea, and E. Louis, 2013, *The Hubbard model: its physics and mathematical physics*, volume 343 (Springer Science & Business Media).
- Baiborodov, Y. T., M. S. Ioffe, V. M. Petrov, and R. I. Sobolev, 1963, *Journal of Nuclear Energy. Part C, Plasma Physics, Accelerators, Thermonuclear Research* **5**(6), 409, URL <https://doi.org/10.1088/0368-3281/5/6/315>.
- Barontini, G., R. Labouvie, F. Stubenrauch, A. Vogler, V. Garrera, and H. Ott, 2013, *Physical Review Letters* **110**, 035302.
- Barredo, D., V. Lienhard, S. De Leseleuc, T. Lahaye, and A. Browaeys, 2018, *Nature* **561**(7721), 79.
- Beattie, S., S. Moulder, R. J. Fletcher, and Z. Hadzibabic, 2013, *Physical Review Letters* **110**(2).
- Bell, T. A., G. Gauthier, T. W. Neely, H. Rubinsztein-Dunlop, M. J. Davis, and M. A. Baker, 2018, *Physical Review A* **98**(1), 013604.
- Bell, T. A., J. A. P. Glidden, L. Humbert, M. W. J. Bromley, S. A. Haine, M. J. Davis, T. W. Neely, M. A. Baker, and H. Rubinsztein-Dunlop, 2016, *New Journal of Physics* **18**(3), 035003.
- Bentine, E., T. L. Harte, K. Luksch, A. J. Barker, J. Muret, B. Yuen, and C. J. Foot, 2017, *Journal of Optics B* **50**(9), 094002.
- Bernon, S., H. Hattermann, D. Bothner, M. Knufinke, P. Weiss, F. Jessen, D. Cano, M. Kemmler, R. Kleiner, D. Koelle, *et al.*, 2013, *Nature Communications* **4**(1), 1.
- Betz, T., S. Manz, R. Bücken, T. Berrada, C. Koller, G. Kazakov, I. E. Mazets, H.-P. Stimming, A. Perrin, T. Schumm, and J. Schmiedmayer, 2011, *Physical Review Letters* **106**, 020407.
- Binanti, F., K. Furutani, and L. Salasnich, 2021, *Physical Review A* **103**(6).
- Birkel, G., F. Buchkremer, R. Dumke, and W. Ertmer, 2001, *Optics Communications* **191**(1-2), 67.
- Bleszynski-Jayich, A., W. Shanks, B. Peaudecerf, E. Ginossar, F. Von Oppen, L. Glazman, and J. Harris, 2009, *Science* **326**(5950), 272.
- Bloch, I., 2005, *Nature Physics* **1**(1), 23.
- Bloch, I., J. Dalibard, and W. Zwerger, 2008, *Reviews of Modern Physics* **80**(3), 885.
- Böhi, P., M. F. Riedel, J. Hoffrogge, J. Reichel, T. W. Hänsch, and P. Treutlein, 2009, *Nature Physics* **5**(8), 592.
- Bongs, K., S. Burger, S. Dettmer, D. Hellweg, J. Arlt, W. Ertmer, and K. Sengstock, 2001, *Physical Review A* **63**, 031602(R).
- Bongs, K., M. Holynski, J. Vovrosh, P. Bouyer, G. Condon, E. Rasel, C. Schubert, W. P. Schleich, and A. Roura, 2019, *Nature Reviews Physics* **1**(12), 731.
- Boyer, V., C. M. Chandrashekar, C. J. Foot, and Z. J. Laczik, 2004, *Journal of Modern Optics* **51**(14), 2235.
- Boyer, V., R. M. Godun, G. Smirne, D. Cassettari, C. M. Chandrashekar, A. B. Deb, Z. J. Laczik, and C. J. Foot, 2006, *Physical Review A* **73**(3), 031402.
- Brantut, J.-P., C. Grenier, J. Meineke, D. Stadler, S. Krinner, C. Kollath, T. Esslinger, and A. Georges, 2013, *Science* **342**(6159), 713.
- Brantut, J.-P., J. Meineke, D. Stadler, S. Krinner, and T. Esslinger, 2012, *Science* **337**(6098), 1069.
- Bruderer, M., and W. Belzig, 2012, *Physical Review A* **85**, 013623.
- Buluta, I., and F. Nori, 2009, *Science* **326**(5949), 108.
- Burchianti, A., F. Scazza, A. Amico, G. Valtolina, J. A. Semman, C. Fort, M. Zaccanti, M. Inguscio, and G. Roati, 2018, *Physical Review Letters* **120**, 025302.
- Burke, J. H. T., B. Deissler, K. J. Hughes, and C. A. Sackett, 2008, *Physical Review A* **78**(2).
- Burke, J. H. T., and C. A. Sackett, 2009, *Physical Review A* **80**, 061603.
- Büttiker, M., Y. Imry, and M. Y. Azbel, 1984, *Physical Review A* **30**(4), 1982.
- Büttiker, M., Y. Imry, and R. Landauer, 1983, *Physics Letters A* **96**(7), 365.
- Byers, N., and C. Yang, 1961, *Physical Review Letters* **7**(2), 46.
- Cai, Y., D. G. Allman, P. Sabharwal, and K. C. Wright, 2022, *Physical Review Letters* **128**(15), 150401.
- Caldeira, A. O., and A. J. Leggett, 1983, *Physica A: Statistical mechanics and its Applications* **121**(3), 587.
- Caliga, S. C., C. J. Straatsma, and D. Z. Anderson, 2016a, *New Journal of Physics* **18**(2), 025010.

- Caliga, S. C., C. J. Straatsma, and D. Z. Anderson, 2017, *New Journal of Physics* **19**(1), 013036.
- Caliga, S. C., C. J. Straatsma, A. A. Zozulya, and D. Z. Anderson, 2016b, *New Journal of Physics* **18**(1), 015012.
- Caliga, S. C., C. J. E. Straatsma, A. A. Zozulya, and D. Z. Anderson, 2012, *ArXiv e-prints*, 1208.3109.
- Calogero, F., and A. Degasperis, 1975, *Physical Review A* **11**, 265.
- del Campo, A., M. G. Boshier, and A. Saxena, 2014, *Scientific Reports* **4**.
- Cano, D., B. Kasch, H. Hattermann, R. Kleiner, C. Zimmermann, D. Koelle, and J. Fortágh, 2008, *Physical Review Letters* **101**, 183006.
- Cappellini, G., M. Mancini, G. Pagano, P. Lombardi, L. Livi, M. S. de Cumis, P. Cancio, M. Pizzocaro, D. Calonico, F. Levi, *et al.*, 2014, *Physical Review Letters* **113**(12), 120402.
- Capponi, S., P. Lecheminant, and K. Totsuka, 2016, *Annals of Physics* **367**, 50.
- Cassettari, D., B. Hessmo, R. Folman, T. Maier, and J. Schmiedmayer, 2000, *Physical Review Letters* **85**(26), 5483, ISSN 0031-9007.
- Cazalilla, M. A., R. Citro, T. Giamarchi, E. Orignac, and M. Rigol, 2011, *Reviews of Modern Physics* **83**, 1405.
- Cazalilla, M. A., A. Ho, and M. Ueda, 2009, *New Journal of Physics* **11**(10), 103033.
- Cazalilla, M. A., and A. M. Rey, 2014, *Reports on Progress in Physics* **77**(12), 124401.
- Celi, A., P. Massignan, J. Ruseckas, N. Goldman, I. B. Spielman, G. Juzeliūnas, and M. Lewenstein, 2014, *Physical Review Letters* **112**, 043001.
- Chakraborty, T., and P. Pietiläinen, 1994, *Physical Review B* **50**(12), 8460.
- Chetcuti, W. J., T. Haug, L. C. Kwek, and L. Amico, 2022a, *SciPost Physics* **12**(1).
- Chetcuti, W. J., A. Osterloh, L. Amico, and J. Polo, 2022b, *arXiv preprint arXiv:2206.02807*.
- Chetcuti, W. J., J. Polo, A. Osterloh, P. Castorina, and L. Amico, 2021, *arXiv preprint arXiv:2112.06950*.
- Chien, C.-C., M. Di Ventra, and M. Zwolak, 2014, *Physical Review A* **90**, 023624.
- Choy, T., and F. Haldane, 1982, *Physics Letters A* **90**(1-2), 83.
- Cirac, J. I., and P. Zoller, 2012, *Nature Physics* **8**(4), 264.
- Clark, L. W., A. Gaj, L. Feng, and C. Chin, 2017, *Nature* **551**(7680), 356.
- Cohen-Tannoudji, C., and S. Reynaud, 1977, *Journal of Optics B* **10**(3), 345.
- Colombe, Y., E. Knyazchyan, O. Morizot, B. Mercier, V. Lorent, and H. Perrin, 2004, *Europhysics Letters* **467**, 593.
- Cominotti, M., M. Rizzi, D. Rossini, D. Aghamalyan, L. Amico, L. C. Kwek, F. Hekking, and A. Minguzzi, 2015, *The European Physical Journal Special Topics* **224**(3), 519.
- Cominotti, M., D. Rossini, M. Rizzi, F. Hekking, and A. Minguzzi, 2014, *Physical Review Letters* **113**(2), 025301.
- Corman, L., L. Chomaz, T. Bienaimé, R. Desbuquois, C. Weitenberg, S. Nascimbene, J. Dalibard, and J. Beugnon, 2014, *Physical Review Letters* **113**(13), 135302.
- Corman, L., P. Fabritius, S. Häusler, J. Mohan, L. H. Dogra, D. Husmann, M. Lebrat, and T. Esslinger, 2019, *Physical Review A* **100**, 053605.
- Cornell, E. A., and C. E. Wieman, 2002, *Reviews of Modern Physics* **74**(3), 875.
- Couvert, A. Couvert, M. Jeppesen, T. Kawalec, G. Reinaudi, R. Mathevet, and D. Guéry-Odelin, 2008, *EPL* **83**(5), 6 pages.
- Crompvoets, F. M., H. L. Bethlem, R. T. Jongma, and G. Meijer, 2001, *Nature* **411**(6834), 174.
- Cronin, A. D., J. Schmiedmayer, and D. E. Pritchard, 2009, *Reviews of Modern Physics* **81**(3), 1051.
- Cuevas, J. C., and E. Scheer, 2017, *Molecular Electronics*, volume Volume 15 (World Scientific).
- Curtis, J. E., B. A. Koss, and D. G. Grier, 2002, *Optics Communications* **207**(1), 169.
- Daley, A., P. Zoller, and B. Trauzettel, 2008, *Physical Review Letters* **100**(11), 110404.
- Dalfovo, F., S. Giorgini, L. P. Pitaevskii, and S. Stringari, 1999, *Reviews of Modern Physics* **71**(3), 463.
- Dalibard, J., F. Gerbier, G. Juzeliūnas, and P. Öhberg, 2011, *Reviews of Modern Physics* **83**(4), 1523.
- Dall, R. G., S. S. Hodgman, M. T. Johnsson, K. G. H. Baldwin, and A. G. Truscott, 2010, *Physical Review A* **81**(1), 011602.
- Damanet, F., E. Mascarenhas, D. Pekker, and A. J. Daley, 2019a, *Physical Review Letters* **123**, 180402.
- Damanet, F., E. Mascarenhas, D. Pekker, and A. J. Daley, 2019b, *New Journal of Physics* **21**(11), 115001.
- Danshita, I., and A. Polkovnikov, 2012, *Physical Review A* **85**, 023638.
- David, T., Y. Japha, V. Dikovsky, R. Salem, C. Henkel, and R. Folman, 2008, *The European Physical Journal D* **48**(3), 321.
- Davis, T. J., 1999, *Journal of Optics B* **1**(4), 408.
- Deaver, B. S., and W. M. Fairbank, 1961, *Physical Review Letters* **7**, 43.
- Degen, C. L., F. Reinhard, and P. Cappellaro, 2017, *Reviews of Modern Physics* **89**(3), 035002.
- Deissler, B., K. Hughes, J. Burke, and C. Sackett, 2008, *Physical Review A* **77**(3), 031604.
- Dekker, N. H., C. S. Lee, V. Lorent, J. H. Thywissen, S. P. Smith, M. Drndić, R. M. Westervelt, and M. Prentiss, 2000, *Physical Review Letters* **84**(6), 1124.
- Del Pace, G., W. J. Kwon, M. Zaccanti, G. Roati, and F. Scazza, 2021, *Physical Review Letters* **126**, 055301.
- Del Pace, G., K. Khani, A. M. Falconi, M. Fedrizzi, N. Grani, D. H. Rajkov, M. Inguscio, F. Scazza, W. Kwon, and G. Roati, 2022, *arXiv preprint arXiv:2204.06542*.
- Denschlag, J., D. Cassettari, A. Chenet, S. Schneider, and J. Schmiedmayer, 1999a, *Applied Physics B* **69**(4), 291.
- Denschlag, J., D. Cassettari, and J. Schmiedmayer, 1999b, *Physical Review Letters* **82**(10), 2014.
- Dikovsky, V., Y. Japha, C. Henkel, and R. Folman, 2005, *The European Physical Journal D* **35**(1), 87.
- Diot, D., Y.-J. Wang, D. Anderson, E. Cornell, R. Saravanan, V. Bright, and M. Prentiss, 2004, *International Quantum Electronics Conference, 2004. (IQEC)*, 60.
- Dowling, J. P., and G. J. Milburn, 2003, *Philosophical Transactions of the Royal Society of London A* **361**(1809), 1655.
- Dubessy, R., T. Liennard, P. Pedri, and H. Perrin, 2012, *Physical Review A* **86**, 011602.
- Dubessy, R., J. Polo, H. Perrin, A. Minguzzi, and M. Olshanii, 2021, *Physical Review Research* **3**, 013098.
- Dumke, R., T. Mütter, M. Volk, W. Ertmer, and G. Birkl, 2002, *Physical Review Letters* **89**(22), 220402.
- Dutta, O., M. Gajda, P. Hauke, M. Lewenstein, D.-S.

- Lühhmann, B. A. Malomed, T. Sowiński, and J. Zakrzewski, 2015, Reports on Progress in Physics **78**(6), 066001.
- Eckel, S., F. Jendrzejewski, A. Kumar, C. J. Lobb, and G. K. Campbell, 2014a, Physical Review X **4**(3), 031052.
- Eckel, S., A. Kumar, T. Jacobson, I. B. Spielman, and G. K. Campbell, 2018, Physical Review X **8**, 021021.
- Eckel, S., J. G. Lee, F. Jendrzejewski, C. J. Lobb, G. K. Campbell, and W. T. Hill, 2016, Physical Review A **93**, 063619.
- Eckel, S., J. G. Lee, F. Jendrzejewski, N. Murray, C. W. Clark, C. J. Lobb, W. D. Phillips, M. Edwards, and G. K. Campbell, 2014b, Nature **506**(7487), 200–203.
- Eller, B., O. Oladehin, D. Fogarty, C. Heller, C. W. Clark, and M. Edwards, 2020, Physical Review A **102**(6), 063324.
- Essler, F. H., H. Frahm, F. Göhmann, A. Klümper, and V. E. Korepin, 2005, *The one-dimensional Hubbard model* (Cambridge University Press).
- Fabre, C. M., P. Cheiney, G. L. Gattobigio, F. Vermersch, S. Faure, R. Mathevet, T. Lahaye, and D. Guéry-Odelin, 2011, Physical Review Letters **107**(23), 230401.
- Faddeev, L., and L. Takhtajan, 2007, *Hamiltonian methods in the theory of solitons* (Springer Science & Business Media).
- Fazio, R., and H. Van Der Zant, 2001, Physics Reports **355**(4), 235.
- Fernholz, T., R. Gerritsma, S. Whitlock, I. Barb, and R. J. C. Spreeuw, 2008, Physical Review A **77**(3).
- Filippone, M., F. Hekking, and A. Minguzzi, 2016, Physical Review A **93**, 011602.
- Fisher, M. P., P. B. Weichman, G. Grinstein, and D. S. Fisher, 1989, Physical Review B **40**(1), 546.
- Folman, R., P. Krüger, D. Cassettari, B. Hessmo, T. Maier, and J. Schmiedmayer, 2000, Physical Review Letters **84**(20), 4749.
- Folman, R., P. Krüger, J. Schmiedmayer, J. Denschlag, and C. Henkel, 2002, in *Advances In Atomic, Molecular, and Optical Physics* (Elsevier), pp. 263–356.
- Fortágh, J., and C. Zimmermann, 2007, Reviews of Modern Physics **79**(1), 235.
- Franke-Arnold, S., J. Leach, M. Padgett, V. Lembessis, D. Ellinas, A. Wright, J. Girkin, P. Ohberg, and A. Arnold, 2007, Optics Express **15**(14), 8619.
- Friedman, N., A. Kaplan, D. Carasso, and N. Davidson, 2001, Physical Review Letters **86**(8), 1518.
- Frye, K., S. Abend, W. Bartosch, A. Bawamia, D. Becker, H. Blume, C. Braxmaier, S.-W. Chiow, M. A. Efremov, W. Ertmer, P. Fierlinger, T. Franz, *et al.*, 2021, EPJ Quantum Technology **8**(1), 1.
- Fu, H., Z. Zhang, K.-X. Yao, L. Feng, J. Yoo, L. W. Clark, K. Levin, and C. Chin, 2020, Physical Review Letters **125**(18), 183003.
- Gallego-Marcos, F., G. Platero, C. Nietner, G. Schaller, and T. Brandes, 2014, Physical Review A **90**, 033614.
- Gallé, A., M. Guilleumas, M. Richard, and A. Minguzzi, 2018, Physical Review B **98**, 104502.
- Garcia, O., B. Deissler, K. J. Hughes, J. M. Reeves, and C. A. Sackett, 2006, Physical Review A **74**(3), 031601.
- Garraway, B. M., and H. Perrin, 2016, Journal of Optics B **49**(17), 172001.
- Gati, R., B. Hemmerling, J. Fölling, M. Albiez, and M. K. Oberthaler, 2006, Physical Review Letters **96**(13), 130404.
- Gattobigio, G. L., A. Couvert, G. Renaudi, B. Georgeot, and D. Guéry-Odelin, 2012, Physical Review Letters **109**(3), 030403.
- Gaunt, A. L., and Z. Hadzibabic, 2012, Scientific Reports **2**, 721.
- Gauthier, G., T. A. Bell, A. B. Stilgoe, M. Baker, H. Rubinsztein-Dunlop, and T. W. Neely, 2021, Advances In Atomic, Molecular, and Optical Physics , 1.
- Gauthier, G., I. Lenton, N. M. Parry, M. Baker, M. Davis, H. Rubinsztein-Dunlop, and T. Neely, 2016, Optica **3**(10), 1136.
- Gauthier, G., S. S. Szigeti, M. T. Reeves, M. Baker, T. A. Bell, H. Rubinsztein-Dunlop, M. J. Davis, and T. W. Neely, 2019, Physical Review Letters **123**, 260402.
- Gefen, Y., Y. Imry, and M. Y. Azbel, 1984, Physical Review Letters **52**(2), 129.
- Gehr, R., J. Volz, G. Dubois, T. Steinmetz, Y. Colombe, B. L. Lev, R. Long, J. Esteve, and J. Reichel, 2010, Physical Review Letters **104**(20), 203602.
- Geiger, R., A. Landragin, S. Merlet, and F. Pereira Dos Santos, 2020, AVS Quantum Science **2**(2), 024702.
- Geiger, R., V. Ménotet, G. Stern, N. Zahzam, P. Cheinet, B. Battelier, A. Villing, F. Moron, M. Lours, Y. Bidet, *et al.*, 2011, Nature communications **2**(1), 1.
- Giamarchi, T., 2003, *Quantum physics in one dimension*, volume 121 (Clarendon press).
- Giovanazzi, S., J. Esteve, and M. K. Oberthaler, 2008, New Journal of Physics **10**(4), 045009.
- Giovanazzi, S., A. Smerzi, and S. Fantoni, 2000, Physical review letters **84**(20), 4521.
- Goldman, N., G. Juzeliūnas, P. Öhberg, and I. B. Spielman, 2014, Reports on Progress in Physics **77**(12), 126401.
- Grenier, C., A. Georges, and C. Kollath, 2014, Physical Review Letters **113**, 200601.
- Grenier, C., C. Kollath, and A. Georges, 2016, Comptes Rendus Physique **17**, 1161.
- Grimm, R., M. Weidemüller, and Y. B. Ovchinnikov, 2000, in *Advances In Atomic, Molecular, and Optical Physics*, edited by B. Bederson and H. Walther (Academic Press), volume 42 of *Advances In Atomic, Molecular, and Optical Physics*, pp. 95–170.
- Gring, M., M. Kuhnert, T. Langen, T. Kitagawa, B. Rauer, M. Schreitl, I. Mazets, D. A. Smith, E. Demler, and J. Schmiedmayer, 2012, Science **337**(6100), 1318.
- Gritsev, V., A. Polkovnikov, and E. Demler, 2007, Physical Review B **75**, 174511.
- Guan, X.-W., M. T. Batchelor, and C. Lee, 2013, Reviews of Modern Physics **85**(4), 1633.
- Guarrera, V., R. Moore, A. Bunting, T. Vanderbruggen, and Y. B. Ovchinnikov, 2017, Scientific Reports **7**(1), 4749.
- Guerin, W., J.-F. Riou, J. P. Gaebler, V. Josse, P. Bouyer, and A. Aspect, 2006, Physical Review Letters **97**, 200402.
- Günther, A., S. Kraft, C. Zimmermann, and J. Fortágh, 2007, Physical Review Letters **98**(14), 140403.
- Guo, Y., R. Dubessy, M. d. G. de Herve, A. Kumar, T. Badr, A. Perrin, L. Longchambon, and H. Perrin, 2020, Physical Review Letters **124**(2), 025301.
- Gupta, S., K. Murch, K. Moore, T. Purdy, and D. Stamper-Kurn, 2005, Physical Review Letters **95**(14), 143201.
- Gustavson, T. L., P. Bouyer, and M. A. Kasevich, 1997, Physical Review Letters **78**, 2046.
- Gustavson, T. L., A. Landragin, and M. A. Kasevich, 2000, Classical and Quantum Gravity **17**(12), 2385.
- Gutiérrez-Medina, B., 2013, American Journal of Physics **81**(2), 104, ISSN 0002-9505.
- Gutman, D. B., Y. Gefen, and A. D. Mirlin, 2012, Physical Review B **85**, 125102.

- Gutzwiller, M. C., 1963, *Physical Review Letters* **10**(5), 159.
- Ha, L.-C., L. W. Clark, C. V. Parker, B. M. Anderson, and C. Chin, 2015, *Physical Review Letters* **114**, 055301.
- Hafele, J. C., and R. E. Keating, 1972, *Science* **177**(4044), 168.
- Haine, S. A., 2018, *New Journal of Physics* **20**(3), 033009.
- Haldane, F., 1980, *Physics Letters A* **80**(4), 281.
- Halkyard, P. L., M. P. A. Jones, and S. A. Gardiner, 2010, *Physical Review A* **81**(6), .
- Hallwood, D. W., K. Burnett, and J. Dunningham, 2006, *New Journal of Physics* **8**(9), 180.
- Hallwood, D. W., K. Burnett, and J. Dunningham, 2007, *Journal of Modern Optics* **54**(13-15), 2129.
- Hallwood, D. W., T. Ernst, and J. Brand, 2010, *Physical Review A* **82**(6), 063623.
- Hänsch, W., P. Hommelhoff, T. Hänsch, and J. Reichel, 2001, *Nature* **413**(6855), 498.
- Haroche, S., and J.-M. Raimond, 2006, *Exploring the quantum: atoms, cavities, and photons* (Oxford University Press).
- Hattermann, H., D. Bothner, L. Ley, B. Ferdinand, D. Wiedmaier, L. Sárkány, R. Kleiner, D. Koelle, and J. Fortágh, 2017, *Nature communications* **8**(1), 1.
- Haug, T., L. Amico, R. Dumke, and L.-C. Kwek, 2018a, *Quantum Science and Technology* **3**(3), 035006.
- Haug, T., R. Dumke, L.-C. Kwek, and L. Amico, 2019a, *Quantum Science and Technology* **4**(4), 045001.
- Haug, T., R. Dumke, L.-C. Kwek, and L. Amico, 2019b, *Commun. Phys.* **2**(1), 1.
- Haug, T., R. Dumke, L.-C. Kwek, C. Miniatura, and L. Amico, 2021, *Physical Review Research* **3**, 013034.
- Haug, T., H. Heimonen, R. Dumke, L.-C. Kwek, and L. Amico, 2019c, *Physical Review A* **100**(4), 041601.
- Haug, T., J. Tan, M. Theng, R. Dumke, L.-C. Kwek, and L. Amico, 2018b, *Physical Review A* **97**(1), 013633.
- Häusler, S., P. Fabritius, J. Mohan, M. Lebrat, L. Corman, and T. Esslinger, 2021, *Phys. Rev. X* **11**, 021034, URL <https://link.aps.org/doi/10.1103/PhysRevX.11.021034>.
- Häusler, S., S. Nakajima, M. Lebrat, D. Husmann, S. Krinner, T. Esslinger, and J.-P. Brantut, 2017, *Physical Review Letters* **119**, 030403.
- He, L., M. Jin, and P. Zhuang, 2006, *Physical Review A* **74**(3), 033604.
- Hekking, F., and L. Glazman, 1997, *Physical Review B* **55**(10), 6551.
- Helm, J., S. Rooney, C. Weiss, and S. Gardiner, 2014, *Physical Review A* **89**(3), 033610.
- Helm, J. L., T. P. Billam, and S. A. Gardiner, 2012, *Physical Review A* **85**, 053621.
- Helm, J. L., T. P. Billam, A. Rakonjac, S. L. Cornish, and S. A. Gardiner, 2018, *Physical Review Letters* **120**(6), 063201.
- Helm, J. L., S. L. Cornish, and S. A. Gardiner, 2015, *Physical Review Letters* **114**(13), 134101.
- Henderson, K., C. Ryu, C. McCormick, and M. G. Boshier, 2009, *New Journal of Physics* **11**(4), 043030.
- Henkel, C., P. Kruger, R. Folman, and J. Schmiedmayer, 2003, *Applied Physics B* **76**(2), 173, URL <http://dx.doi.org/10.1007/s00340-003-1112-z>.
- Hod, O., R. Baer, and E. Rabani, 2006, *Physical Review Letters* **97**(26), 266803.
- Hodby, E., G. Hechenblaikner, O. M. Marago, J. Arlt, S. Hopkins, and C. J. Foot, 2000, *Journal of Physics B* **33**(19), 4087, URL <http://dx.doi.org/10.1088/0953-4075/33/19/319>.
- Hofferberth, S., I. Lesanovsky, B. Fischer, T. Schumm, and J. Schmiedmayer, 2007, *Nature* **449**(7160), 324.
- Hofferberth, S., I. Lesanovsky, B. Fischer, J. Verdu, and J. Schmiedmayer, 2006, *Nature Physics* **2**(10), 710, ISSN 1745-2473.
- Hofferberth, S., I. Lesanovsky, T. Schumm, A. Imambekov, V. Gritsev, E. Demler, and J. Schmiedmayer, 2008, *Nature Physics* **4**(6), 489.
- Houde, O., D. Kadio, and L. Pruvost, 2000, *Physical Review Letters* **85**(26), 5543.
- Hubbard, J., 1963, *Proceedings of the Royal Society of London. Series A. Mathematical and Physical Sciences* **276**(1365), 238.
- Hueck, K., A. Mazurenko, N. Luick, T. Lompe, and H. Moritz, 2017, *Review of Scientific Instruments* **88**(1), 016103.
- Husmann, D., M. Lebrat, S. Häusler, J.-P. Brantut, L. Corman, and T. Esslinger, 2018, *Proceedings of the National Academy of Sciences* .
- Husmann, D., S. Uchino, S. Krinner, M. Lebrat, T. Giamarchi, T. Esslinger, and J.-P. Brantut, 2015, *Science* **350**(6267), 1498.
- Hyafil, P., J. Mozley, A. Perrin, J. Tailleur, G. Noguez, M. Brune, J. M. Raimond, and S. Haroche, 2004, *Physical Review Letters* **93**(10), URL <https://doi.org/10.1103/physrevlett.93.103001>.
- Imry, Y., 2002, *Introduction to mesoscopic physics* (Oxford University Press).
- Imry, Y., and R. Landauer, 1999, *Reviews of Modern Physics* **71**, S306.
- Ivanov, A., G. Kordas, A. Komnik, and S. Wimberger, 2013, *The European Physical Journal B* **86**(8), 345.
- Jagla, E., and C. Balseiro, 1993, *Physical Review Letters* **70**(5), 639.
- Jaksch, D., C. Bruder, J. I. Cirac, C. W. Gardiner, and P. Zoller, 1998, *Physical Review Letters* **81**(15), 3108.
- Japha, Y., O. Arzouan, Y. Avishai, and R. Folman, 2007, *Physical Review Letters* **99**(6), 060402.
- Jaroszewicz, L. R., A. Kurzych, Z. Krajewski, P. Marć, J. K. Kowalski, P. Bobra, Z. Zembaty, B. Sakowicz, and R. Jankowski, 2016, *Sensors* **16**(12), 2161.
- Jendrzejewski, F., S. Eckel, N. Murray, C. Lanier, M. Edwards, C. J. Lobb, and G. K. Campbell, 2014, *Physical Review Letters* **113**(4), 045305.
- Jo, G. B., J. H. Choi, C. A. Christensen, T. A. Pasquini, Y. R. Lee, W. Ketterle, and D. E. Pritchard, 2007, *Physical Review Letters* **98**(18), 180401.
- Jördens, R., N. Strohmaier, K. Günter, H. Moritz, and T. Esslinger, 2008, *Nature* **455**(7210), 204.
- Kanamori, J., 1963, *Progress of Theoretical Physics* **30**(3), 275.
- Kanász-Nagy, M., L. Glazman, T. Esslinger, and E. A. Demler, 2016, *Physical Review Letters* **117**, 255302.
- Keck, M., D. Rossini, and R. Fazio, 2018, *Physical Review A* **98**(5), 053812.
- Keil, M., O. Amit, S. Zhou, D. Groswasser, Y. Japha, and R. Folman, 2016, *Journal of modern optics* **63**(18), 1840.
- Ketterle, W., 2002, *Reviews of Modern Physics* **74**(4), 1131.
- Khondker, A., M. R. Khan, and A. Anwar, 1988, *Journal of applied physics* **63**(10), 5191.
- Kim, H., K. Krzyzanowska, K. C. Henderson, C. Ryu, E. Timmermans, and M. Boshier, 2022, *ArXiv e-prints eprint 2201.11888*.

- Kim, S. J., H. Yu, S. T. Gang, and J. B. Kim, 2017, *Applied Physics B* **123**(5), 154, ISSN 0946-2171.
- Kolovsky, A. R., 2017, *Physical Review A* **96**, 011601.
- Kolovsky, A. R., Z. Denis, and S. Wimberger, 2018, *Physical Review A* **98**, 043623.
- Korepin, V. E., N. M. Bogoliubov, and A. G. Izergin, 1997, *Quantum inverse scattering method and correlation functions*, volume 3 (Cambridge university press).
- Kovachy, T., J. M. Hogan, A. Sugarbaker, S. M. Dickerson, C. A. Donnelly, C. Overstreet, and M. A. Kasevich, 2015, *Physical Review Letters* **114**, 143004.
- Kraft, S., A. Günther, H. Ott, D. Wharam, C. Zimmermann, and J. Fortágh, 2002, *Journal of Optics B* **35**(21), L469.
- Kreutzmann, H., U. V. Poulsen, M. Lewenstein, R. Dumke, W. Ertmer, G. Birkl, and A. Sanpera, 2004, *Physical Review Letters* **92**(16).
- Krinner, S., T. Esslinger, and J.-P. Brantut, 2017, *Journal of Physics: Condensed Matter* **29**(34), 343003.
- Krinner, S., M. Lebrat, D. Husmann, C. Grenier, J.-P. Brantut, and T. Esslinger, 2016, *Proceedings of the National Academy of Sciences* **113**(29), 8144.
- Krinner, S., D. Stadler, D. Husmann, J.-P. Brantut, and T. Esslinger, 2015a, *Nature* **517**(7532), 64.
- Krinner, S., D. Stadler, J. Meineke, J.-P. Brantut, and T. Esslinger, 2013, *Physical Review Letters* **110**, 100601.
- Krinner, S., D. Stadler, J. Meineke, J.-P. Brantut, and T. Esslinger, 2015b, *Physical Review Letters* **115**, 045302.
- Krüger, P., L. M. Andersson, S. Wildermuth, S. Hofferberth, E. Haller, S. Aigner, S. Groth, I. Bar-Joseph, and J. Schmiedmayer, 2007, *Physical Review A* **76**(6).
- Krzyzanowska, K., J. Ferreras, C. Ryu, E. C. Samson, and M. Boshier, 2022, *ArXiv e-prints* eprint 2201.12461.
- Kuga, T., Y. Torii, N. Shiokawa, T. Hirano, Y. Shimizu, and H. Sasada, 1997, *Physical Review Letters* **78**(25), 4713.
- Kumar, A., N. Anderson, W. D. Phillips, S. Eckel, G. K. Campbell, and S. Stringari, 2016a, *New Journal of Physics* **18**(2), 025001.
- Kumar, A., N. Anderson, W. D. Phillips, S. Eckel, G. K. Campbell, and S. Stringari, 2016b, *New Journal of Physics* **18**(2), 025001.
- Kumar, A., S. Eckel, F. Jendrzejewski, and G. K. Campbell, 2017, *Physical Review A* **95**(2), 021602.
- Kunimi, M., and I. Danshita, 2017, *Physical Review A* **95**, 033637.
- Kunimi, M., and I. Danshita, 2019, *Physical Review A* **99**, 043613.
- Kwon, W. J., G. Del Pace, R. Panza, M. Inguscio, W. Zwirger, M. Zaccanti, F. Scazza, and G. Roati, 2020, *Science* **369**(6499), 84.
- Labouvie, R., B. Santra, S. Heun, S. Wimberger, and H. Ott, 2015, *Physical Review Letters* **115**, 050601.
- Lacki, M., M. Baranov, H. Pichler, and P. Zoller, 2016, *Physical review letters* **117**(23), 233001.
- Lamata, L., A. Mezzacapo, J. Casanova, E. Solano, T. H. Johnson, S. R. Clark, D. Jaksch, K. V. Krutitsky, P. Navez, F. Queisser, *et al.*, 2014, *Quantum* **1**(1).
- Langen, T., R. Geiger, and J. Schmiedmayer, 2015, *Annual Review of Condensed Matter Physics* **6**(1), 201.
- Lau, J. W. Z., K. S. Gan, R. Dumke, L. Amico, L.-C. Kwek, and T. Haug, 2022, *arXiv preprint arXiv:2205.01636*.
- Leanhardt, A., A. Chikkatur, D. Kielpinski, Y. Shin, T. Gustavson, W. Ketterle, and D. Pritchard, 2002, *Physical Review Letters* **89**(4), 040401.
- LeBlanc, L. J., A. B. Bardson, J. McKeever, M. H. T. Extavour, D. Jervis, J. H. Thywissen, F. Piazza, and A. Smerzi, 2011, *Physical Review Letters* **106**, 025302.
- Lebrat, M., S. Häusler, P. Fabritius, D. Husmann, L. Corman, and T. Esslinger, 2019, *Physical Review Letters* **123**, 193605.
- Lebrat, M., P. Grišins, D. Husmann, S. Häusler, L. Corman, T. Giamarchi, J.-P. Brantut, and T. Esslinger, 2018, *Physical Review X* **8**, 011053.
- Lee, T. D., K. Huang, and C. N. Yang, 1957, *Physical Review* **106**, 1135.
- Leggett, A., 2006, *Quantum Fluids* (Oxford University Press Oxford).
- Leggett, A. J., 1980, *Progress of Theoretical Physics Supplement* **69**, 80.
- Leggett, A. J., 1991, *NATO ASI Ser. B* **251**, 297.
- Lesanovsky, I., and W. von Klitzing, 2007, *Physical Review Letters* **99**(8), 083001.
- Lévy, L. P., G. Dolan, J. Dunsmuir, and H. Bouchiat, 1990, *Physical Review Letters* **64**, 2074.
- Levy, S., E. Lahoud, I. Shomroni, and J. Steinhauer, 2007, *Nature* **449**(7162), 579.
- Lewenstein, M., A. Sanpera, and V. Ahufinger, 2012, *Ultracold Atoms in Optical Lattices: Simulating quantum many-body systems* (Oxford University Press).
- Li, A., S. Eckel, B. Eller, K. E. Warren, C. W. Clark, and M. Edwards, 2016, *Physical Review A* **94**, 023626.
- Li, G., M. D. Fraser, A. Yakimenko, and E. A. Ostrovskaya, 2015, *Physical Review B* **91**(18), 184518.
- Lieb, E. H., and W. Liniger, 1963, *Physical Review* **130**(4), 1605.
- Lieb, E. H., and F. Wu, 1968, *Physical Review Letters* **21**(3), 192.
- Lim, Y., J. Goo, H. Kwak, and Y. Shin, 2021, *Physical Review A* **103**(6), 063319.
- Liu, B., H. Zhai, and S. Zhang, 2017, *Physical Review A* **95**, 013623.
- Lobos, A., and A. Aligia, 2008, *Physical Review Letters* **100**(1), 016803.
- Long, R., T. Rom, W. Hansel, T. W. Hansch, and J. Reichel, 2005, *European Physical Journal D* **35**, 125.
- Loss, D., 1992, *Physical Review Letters* **69**(2), 343.
- Luick, N., L. Sobirey, M. Bohlen, V. P. Singh, L. Mathey, T. Lompe, and H. Moritz, 2020, *Science* **369**(6499), 89.
- Lukoshkin, V. A., V. K. Kalevich, M. M. Afanasiev, K. V. Kavokin, Z. Hatzopoulos, P. G. Savvidis, E. S. Sedov, and A. V. Kavokin, 2018, *Physical Review B* **97**, 195149.
- Mahan, G. D., 2013, *Many-particle physics* (Springer Science & Business Media).
- Majorana, E., 1932, *Il Nuovo Cimento* **9**, 43.
- Manmana, S. R., K. R. Hazzard, G. Chen, A. E. Feiguin, and A. M. Rey, 2011, *Physical Review A* **84**(4), 043601.
- Marchukov, O. V., B. A. Malomed, V. A. Yurovsky, M. Olshanii, V. Dunjko, and R. G. Hulet, 2019, *Physical Review A* **99**(6).
- Marino, I., S. Raghavan, S. Fantoni, S. R. Shenoy, and A. Smerzi, 1999, *Physical Review A* **60**, 487.
- Marquardt, F., and C. Bruder, 2002, *Physical Review B* **65**(12), 125315.
- Marti, G. E., R. Olf, and D. M. Stamper-Kurn, 2015, *Physical Review A* **91**(1), 013602.
- Mas, H., S. Pandey, G. Vasilakis, and W. von Klitzing, 2019, *New Journal of Physics* **21**, 123039.
- Mathew, R., A. Kumar, S. Eckel, F. Jendrzejewski, G. K. Campbell, M. Edwards, and E. Tiesinga, 2015, *Physical*

- Review A **92**, 033602.
- Mathey, A. C., C. W. Clark, and L. Mathey, 2014, Physical Review A **90**(2), 023604.
- Mathey, A. C., and L. Mathey, 2016, New Journal of Physics **18**(5), 055016.
- Matveev, K., A. Larkin, and L. Glazman, 2002, Physical Review Letters **89**(9), 096802.
- McDonald, G. D., H. Keal, P. A. Altin, J. E. Debs, S. Bennetts, C. C. N. Kuhn, K. S. Hardman, M. T. Johnsson, J. D. Close, and N. P. Robins, 2013a, Physical Review A **87**(1), 013632.
- McDonald, G. D., C. C. N. Kuhn, K. S. Hardman, S. Bennetts, P. J. Everitt, P. A. Altin, J. E. Debs, J. D. Close, and N. P. Robins, 2014, Physical Review Letters **113**(1), 013002.
- McDonald, G. D., C. C. N. Kuhn, S. Bennetts, J. E. Debs, K. S. Hardman, M. Johnsson, J. D. Close, and N. P. Robins, 2013b, Physical Review A **88**(5), 053620.
- McGloin, D., G. C. Spalding, H. Melville, W. Sibbett, and K. Dholakia, 2003, Optics Express **11**(2), 158.
- Mehdi, Z., A. S. Bradley, J. J. Hope, and S. S. Szigeti, 2021, SciPost Phys. **11**, 80.
- Meier, F., and W. Zwerger, 2001, Physical Review A **64**, 033610.
- Mielke, A., 2015, Many Body Physics: From Kondo to Hubbard. Modeling and Simulation **5**.
- Milburn, G., J. Corney, E. M. Wright, and D. Walls, 1997, Physical Review A **55**(6), 4318.
- Milner, V., J. L. Hanssen, W. C. Campbell, and M. G. Raizen, 2001, Physical Review Letters **86**(8), 1514.
- Moan, E. R., R. A. Horne, T. Arpornthip, Z. Luo, A. J. Fallon, S. J. Berl, and C. A. Sackett, 2020, Physical Review Letters **124**(12).
- Mohanty, P., 1999, Annalen der Physik **8**(7-9), 549.
- Morizot, O., Y. Colombe, V. Lorent, H. Perrin, and B. M. Garraway, 2006, Physical Review A **74**(2), 023617.
- Moukouri, S., Y. Japha, M. Keil, T. David, D. Groswasser, M. Givon, and R. Folman, 2021, Multi-pass guided atomic sagnac interferometer for high-performance rotation sensing, eprint 2107.03446.
- Moulder, S., S. Beattie, R. P. Smith, N. Tammuz, and Z. Hadzibabic, 2012, Physical Review A **86**(1), 013629.
- Mukai, T., C. Hufnagel, A. Kasper, T. Meno, A. Tsukada, K. Semba, and F. Shimizu, 2007, Physical Review Letters **98**(26), 260407.
- Müller, D., D. Z. Anderson, R. J. Grow, P. D. D. Schwindt, and E. A. Cornell, 1999, Physical Review Letters **83**(25), 5194.
- Müller, D., E. A. Cornell, D. Z. Anderson, and E. R. I. Abraham, 2000, Physical Review A **61**(3), 033411.
- Muller, D., E. A. Cornell, M. Prevedelli, P. Schwindt, A. Zozulya, and D. Z. Anderson, 2000, Optics Letters **25**(18), 1382-1384, ISSN 0146-9592.
- Müller, H., S.-w. Chiow, Q. Long, S. Herrmann, and S. Chu, 2008, Physical Review Letters **100**(18), 180405.
- Müller, T., B. Zhang, R. Fermini, K. Chan, M. Lim, and R. Dumke, 2010a, Physical Review A **81**(5), 053624.
- Müller, T., B. Zhang, R. Fermini, K. Chan, Z. Wang, C. Zhang, M. Lim, and R. Dumke, 2010b, New Journal of Physics **12**(4), 043016.
- Müllers, A., B. Santra, C. Baals, J. Jiang, J. Benary, R. Labouvie, D. A. Zezyulin, V. V. Konotop, and H. Ott, 2018, Science Advances **4**(8), eaat6539.
- Muntinga, H., H. Ahlers, M. Krutzik, A. Wenzlawski, S. Arnold, D. Becker, K. Bongs, H. Dittus, H. Duncker, N. Gaaloul, C. Gherasim, E. Giese, *et al.*, 2013, Physical Review Letters **110**, 093602.
- Murray, N., M. Krygier, M. Edwards, K. C. Wright, G. K. Campbell, and C. W. Clark, 2013, Physical Review A **88**, 053615.
- Naldesi, P., J. P. Gomez, B. Malomed, M. Olshanii, A. Minguzzi, and L. Amico, 2019, Physical Review Letters **122**, 053001.
- Naldesi, P., J. Polo, V. Dunjko, H. Perrin, M. Olshanii, L. Amico, and A. Minguzzi, 2022, SciPost Physics **12**(4), 138.
- Navez, P., S. Pandey, H. Mas, K. Poullos, T. Fernholz, and W. von Klitzing, 2016, New Journal of Physics **18**(7), 075014.
- Nazarov, Y. V., and Y. M. Blanter, 2009, *Quantum Transport: Introduction to Nanoscience* (Cambridge University Press).
- Nicolau, E., J. Mompart, B. Juliá-Díaz, and V. Ahufinger, 2020, Physical Review A **102**, 023331.
- Nietner, C., G. Schaller, and T. Brandes, 2014, Physical Review A **89**, 013605.
- Nirrengarten, T., A. Qarry, C. Roux, A. Emmert, G. Nogues, M. Brune, J.-M. Raimond, and S. Haroche, 2006, Physical Review Letters **97**(20), 200405.
- Nitzan, A., and M. A. Ratner, 2003, Science **300**(5624), 1384.
- Nogrette, F., H. Labuhn, S. Ravets, D. Barredo, L. Béguin, A. Vernier, T. Lahaye, and A. Browaeys, 2014, Physical Review X **4**, 021034.
- Nunnenkamp, A., A. M. Rey, and K. Burnett, 2008, Physical Review A **77**(2), 023622.
- Nunnenkamp, A., A. M. Rey, and K. Burnett, 2011, Physical Review A **84**(5), 053604.
- Oelkers, N., and J. Links, 2007, Physical Review B **75**, 115119.
- Olariu, S., and I. I. Popescu, 1985, Reviews of Modern Physics **57**, 339.
- Oliinyk, A., A. Yakimenko, and B. Malomed, 2019, Journal of Physics B: Atomic, Molecular and Optical Physics **52**(22), 225301.
- Olson, S. E., M. L. Terraciano, M. Bashkansky, and F. K. Fatemi, 2007, Physical Review A **76**(6), 061404.
- Onofrio, R., D. S. Durfee, C. Raman, M. Kohl, C. E. Kulewicz, and W. Ketterle, 2000, Physical Review Letters **84**(5), 810.
- Ozawa, T., and G. Baym, 2010, Physical Review A **82**(6), 063615.
- Packard, R. E., 1998, Reviews of Modern Physics **70**, 641.
- Pagano, G., M. Mancini, G. Cappellini, L. Livi, C. Sias, J. Catani, M. Inguscio, and L. Fallani, 2015, Physical Review Letters **115**(26), 265301.
- Pandey, S., H. Mas, G. Drougakis, P. Thekkepatt, V. Bolpasi, G. Vasilakis, K. Poullos, and W. von Klitzing, 2019, Nature **570**(7760), 1.
- Pandey, S., H. Mas, G. Vasilakis, and W. von Klitzing, 2021, Physical Review Letters **126**(17).
- Papoular, D. J., L. P. Pitaevskii, and S. Stringari, 2014, Physical Review Letters **113**, 170601.
- Papoular, D. J., L. P. Pitaevskii, and S. Stringari, 2016, Physical Review A **94**, 023622.
- Pătu, O. I., and D. V. Averin, 2022, Physical Review Letters **128**(9), 096801.
- Pecci, G., P. Naldesi, L. Amico, and A. Minguzzi, 2021a, Physical Review Research **3**(3).
- Pecci, G., P. Naldesi, A. Minguzzi, and L. Amico, 2021b, ArXiv e-prints, 2105.10408.

- Peierls, R., 1933, *Zeitschrift für Physik* **80**(11-12), 763.
- Pelegri, G., J. Mompert, and V. Ahufinger, 2018, *New Journal of Physics* **20**(10), 103001.
- Penna, V., and A. Richaud, 2017, *Physical Review A* **96**(5), 053631.
- Pepino, R., J. Cooper, D. Anderson, and M. Holland, 2009, *Physical Review Letters* **103**(14), 140405.
- Pepino, R. A., 2021, *Entropy* **23**(5), 534.
- Pérez-Obiol, A., J. Polo, and L. Amico, 2021, arXiv preprint arXiv:2112.08072 .
- Perrin, H., and B. M. Garraway, 2017, *Advances In Atomic, Molecular, and Optical Physics* .
- Pershoguba, S. S., and L. I. Glazman, 2019, *Physical Review B* **99**, 134514.
- Peters, A., K. Y. Chung, and S. Chu, 2001, *Metrologia* **38**(1), 25.
- Petrich, W., M. H. Anderson, J. R. Ensher, and E. A. Cornell, 1995, *Physical Review Letters* **74**(17), 3352, URL <https://doi.org/10.1103/PhysRevLett.74.3352>.
- Petrosyan, D., K. Mølmer, J. Fortágh, and M. Saffman, 2019, *New Journal of Physics* **21**(7), 073033.
- Pezzè, L., A. Smerzi, M. K. Oberthaler, R. Schmied, and P. Treutlein, 2018, *Reviews of Modern Physics* **90**, 035005.
- Piazza, F., L. A. Collins, and A. Smerzi, 2009, *Physical Review A* **80**(2), 021601(R).
- Pigneur, M., T. Berrada, M. Bonneau, T. Schumm, E. Demler, and J. Schmiedmayer, 2018, *Physical Review Letters* **120**, 173601.
- Polo, J., and V. Ahufinger, 2013, *Physical Review A* **88**(5), 053628.
- Polo, J., V. Ahufinger, F. W. Hekking, and A. Minguzzi, 2018, *Physical Review Letters* **121**(9), 090404.
- Polo, J., A. Benseny, T. Busch, V. Ahufinger, and J. Mompert, 2016a, *New Journal of Physics* **18**(1), 015010.
- Polo, J., R. Dubessy, P. Pedri, H. Perrin, and A. Minguzzi, 2019, *Physical Review Letters* **123**, 195301.
- Polo, J., J. Mompert, and V. Ahufinger, 2016b, *Physical Review A* **93**(3), 033613.
- Polo, J., P. Naldesi, A. Minguzzi, and L. Amico, 2021, *Quantum Science and Technology* **7**(1), 015015.
- Price, H. M., T. Ozawa, and N. Goldman, 2017, *Physical Review A* **95**, 023607.
- Pritchard, D. E., 1983, *Physical Review Letters* **51**(15), 1336.
- Pritchard, J. D., A. N. Dinkelaker, A. S. Arnold, P. F. Griffin, and E. Riis, 2012, *New Journal of Physics* **14**(10), 103047.
- Pyykkönen, V. A. J., S. Peotta, P. Fabritius, J. Mohan, T. Esslinger, and P. Törmä, 2021, *Physical Review B* **103**, 144519.
- Qi, L., Z. Hu, T. Valenzuela, Y. Zhang, Y. Zhai, W. Quan, N. Waltham, and J. Fang, 2017, *Applied Physics Letters* **110**(15), 153502.
- Ramanathan, A., K. C. Wright, S. R. Muniz, M. Zelan, W. T. Hill, C. J. Lobb, K. Helmerson, W. D. Phillips, and G. K. Campbell, 2011, *Physical Review Letters* **106**(13), 130401.
- Rapp, A., G. Záránd, C. Honerkamp, and W. Hofstetter, 2007, *Physical Review Letters* **98**(16), 160405.
- Rastelli, G., I. M. Pop, and F. W. Hekking, 2013, *Physical Review B* **87**(17), 174513.
- Read, N., and N. Cooper, 2003, *Physical Review A* **68**(3), 035601.
- Reichel, J., 2002, *Applied Physics B* **74**(6), 469.
- Reichel, J., W. Hänsel, and T. W. Hänsch, 1999, *Physical Review Letters* **83**(17), 3398.
- Reichel, J., and V. Vuletić, 2011, *Atom Chips* (Wiley-VCH Verlag GmbH and Co. KGaA).
- Renn, M. J., E. A. Donley, E. A. Cornell, C. E. Wieman, and D. Z. Anderson, 1996, *Physical Review A* **53**(2), R648.
- Rhodes, D. P., G. P. T. Lancaster, J. Livesey, D. McGloin, J. Arlt, and K. Dholakia, 2002, *Optics Communications* **214**(1-6), 247.
- Richaud, A., M. Ferraretto, and M. Capone, 2021, *Physical Review B* **103**(20), 205132.
- Richaud, A., M. Ferraretto, and M. Capone, 2022, *Condensed Matter* **7**(1), 18.
- Richaud, A., and V. Penna, 2017, *Physical Review A* **96**(1), 013620.
- Riedel, E. K., and F. von Oppen, 1993, *Physical Review B* **47**(23), 15449.
- Riedel, M. F., P. Böhi, Y. Li, T. W. Hänsch, A. Sinatra, and P. Treutlein, 2010, *Nature* **464**(7292), 1170.
- Rincón, J., A. Aligia, and K. Hallberg, 2009, *Physical Review B* **79**(3), 035112.
- Rincón, J., K. Hallberg, and A. Aligia, 2008, *Physical Review B* **78**(12), 125115.
- Roscilde, T., M. F. Faulkner, S. T. Bramwell, and P. C. W. Holdsworth, 2016, *New Journal of Physics* **18**(7), 075003.
- Rubinsztein-Dunlop, H., A. Forbes, M. V. Berry, M. R. Dennis, D. L. Andrews, M. Mansuripur, C. Denz, C. Alpmann, P. Banzer, T. Bauer, E. Karimi, L. Marrucci, *et al.*, 2016, *Journal of Optics* **19**(1), 013001.
- Ruostekoski, J., and D. F. Walls, 1998, *Physical Review A* **58**, R50.
- Ryu, C., P. Blackburn, A. Blinova, and M. Boshier, 2013, *Physical Review Letters* **111**(20), 205301.
- Ryu, C., and M. G. Boshier, 2015, *New Journal of Physics* **17**(9), 092002.
- Ryu, C., K. C. Henderson, and M. G. Boshier, 2014, *New Journal of Physics* **16**(1), 013046.
- Ryu, C., E. C. Samson, and M. G. Boshier, 2020, *Nature Communications* **11**(1), 3338.
- Safaei, S., B. Grémaud, R. Dumke, L.-C. Kwek, L. Amico, and C. Miniatura, 2018, *Physical Review A* **97**(4), 042306.
- Safaei, S., L.-C. Kwek, R. Dumke, and L. Amico, 2019, *Physical Review A* **100**(1), 013621.
- Salerno, G., H. M. Price, M. Lebrat, S. Häusler, T. Esslinger, L. Corman, J.-P. Brantut, and N. Goldman, 2019, *Physical Review X* **9**, 041001.
- Salim, E. A., S. C. Caliga, J. B. Pfeiffer, and D. Z. Anderson, 2013, *Applied Physics Letters* **102**(8), 084104.
- Saminadayar, L., C. Bauerle, and D. Mailly, 2004, *Enc. Nanosci. Nanotech* **4**, 267.
- Sanvitto, D., F. Marchetti, M. Szymańska, G. Tosi, M. Baudisch, F. P. Laussy, D. Krizhanovskii, M. Skolnick, L. Marrucci, A. Lemaitre, *et al.*, 2010, *Nature Physics* **6**(7), 527.
- Sauer, J. A., M. D. Barrett, and M. S. Chapman, 2001, *Physical Review Letters* **87**(27), 270401.
- Schenke, C., A. Minguzzi, and F. W. J. Hekking, 2011, *Physical Review A* **84**, 053636.
- Schmiedmayer, J., 1995a, *Physical Review A* **52**(1), R13.
- Schmiedmayer, J., 1995b, *Applied Physics B* **60**(2), 169.
- Schmiedmayer, J., and A. Scrinzi, 1996a, *Quantum and Semi-classical Optics: Journal of the European Optical Society Part B* **8**(3), 693.
- Schmiedmayer, J., and A. Scrinzi, 1996b, *Physical Review A* **54**(4), R2525.
- Schneble, D., M. Hasuo, T. Anker, T. Pfau, and J. Mlynek, 2003, *Journal of the Optical Society of America B* **20**(4), 648.

- Schnelle, S. K., E. D. Van Ooijen, M. J. Davis, N. R. Heckenberg, and H. Rubinsztein-Dunlop, 2008, *Optics Express* **16**(3), 1405.
- Schumm, T., S. Hofferberth, L. M. Andersson, S. Wildermuth, S. Groth, I. Bar-Joseph, J. Schmiedmayer, and P. Krüger, 2005, *Nature Physics* **1**(1), 57.
- Schweigler, T., M. Gluza, M. Tajik, S. Sotiriadis, F. Cataldini, S.-C. Ji, F. S. Møller, J. Sabino, B. Rauer, J. Eisert, and J. Schmiedmayer, 2021, *Nature Physics* **17**(5), 559.
- Seaman, B., M. Krämer, D. Anderson, and M. Holland, 2007, *Physical Review A* **75**(2), 023615.
- Sekera, T., C. Bruder, and W. Belzig, 2016, *Physical Review A* **94**, 033618.
- Sherlock, B. E., M. Gildemeister, E. Owen, E. Nugent, and C. J. Foot, 2011, *Physical Review A* **83**(4), 043408, URL <http://dx.doi.org/10.1103/PhysRevA.83.043408>.
- Shmakov, P., A. Dmitriev, and V. Y. Kachorovskii, 2013, *Physical Review B* **87**(23), 235417.
- Simonelli, C., M. Archimi, L. Asteria, D. Capecci, G. Masella, E. Arimondo, D. Ciampini, and O. Morsch, 2017, *Physical Review A* **96**(4), 043411.
- Simpson, D., D. Gangardt, I. Lerner, and P. Krüger, 2014, *Physical review letters* **112**(10), 100601.
- Sinclair, C. D. J., E. A. Curtis, I. L. Garcia, J. A. Retter, B. V. Hall, S. Eriksson, B. E. Sauer, and E. A. Hinds, 2005, *Physical Review A* **72**, 031603.
- Singh, V. P., N. Luick, L. Sobirey, and L. Mathey, 2020, *Physical Review Research* **2**, 033298.
- Sinuco-León, G. A., K. A. Burrows, A. S. Arnold, and B. M. Garraway, 2014, *Nature Communications* **5**(1).
- Smerzi, A., S. Fantoni, S. Giovanazzi, and S. Shenoy, 1997, *Physical Review Letters* **79**(25), 4950.
- Solenov, D., and D. Mozysky, 2010, *Physical Review A* **82**(6), 061601.
- Sommer, A., M. Ku, G. Roati, and M. W. Zwierlein, 2011, *Nature* **472**(7342), 201.
- Spagnolli, G., G. Semeghini, L. Masi, G. Ferioli, A. Trenkwalder, S. Coop, M. Landini, L. Pezzè, G. Modugno, M. Inguscio, A. Smerzi, and M. Fattori, 2017, *Physical Review Letters* **118**, 230403.
- Spehner, D., L. Morales-Molina, and S. A. Reyes, 2021, *New Journal of Physics* .
- Stadler, D., S. Krinner, J. Meineke, J.-P. Brantut, and T. Esslinger, 2012, *Nature* **491**(7426), 736.
- Stevenson, R., M. R. Hush, T. Bishop, I. Lesanovsky, and T. Fernholz, 2015, *Physical Review Letters* **115**, 163001.
- Stickney, J. A., D. Z. Anderson, and A. A. Zozulya, 2007, *Physical Review A* **75**(1), 013608.
- Stockton, J., K. Takase, and M. Kasevich, 2011, *Physical Review Letters* **107**(13), 133001.
- Streltsov, A. I., O. E. Alon, and L. S. Cederbaum, 2009, *Physical Review A* **80**(4), 043616.
- Sugarbaker, A., 2014, *Atom interferometry in a 10 m fountain* (Stanford University).
- Sun, K., K. Padavić, F. Yang, S. Vishveshwara, and C. Lannert, 2018, *Physical Review A* **98**(1).
- Surace, F. M., and A. Lerose, 2021, *New Journal of Physics* **23**(6), 062001.
- Sutherland, B., 1968, *Physical Review Letters* **20**(3), 98.
- Sutherland, B., 1975, *Physical Review B* **12**, 3795.
- Tajik, M., B. Rauer, T. Schweigler, F. Cataldini, J. Sabino, F. S. Møller, S.-C. Ji, I. E. Mazets, and J. Schmiedmayer, 2019, *Optics Express* **27**(23), 33474.
- Thouless, D., 1983, *Physical Review B* **27**(10), 6083.
- Thouless, D. J., M. Kohmoto, M. P. Nightingale, and M. den Nijs, 1982, *Physical Review Letters* **49**(6), 405.
- Tinkham, M., 2012, *Introduction to superconductivity* (Courier Dover Publications).
- Tokuno, A., M. Oshikawa, and E. Demler, 2008, *Physical Review Letters* **100**(14), 140402.
- Tollett, J. J., C. C. Bradley, C. A. Sackett, and R. G. Hulet, 1995, *Physical Review A* **51**, R22.
- Tononi, A., F. Toigo, S. Wimberger, A. Cappellaro, and L. Salasnich, 2020, *New Journal of Physics* **22**(7), 073020.
- Tosto, F., P. Baw Swe, N. T. Nguyen, C. Hufnagel, M. Mart'inez Valado, L. Prigozhin, V. Sokolovsky, and R. Dumke, 2019, *Applied Physics Letters* **114**(22), 222601.
- Trebbia, J.-B., C. L. Garrido Alzar, R. Cornelussen, C. I. Westbrook, and I. Bouchoule, 2007, *Physical Review Letters* **98**, 263201.
- Trenkwalder, A., G. Spagnolli, G. Semeghini, S. Coop, M. Landini, P. Castilho, L. Pezzè, G. Modugno, M. Inguscio, A. Smerzi, and M. Fattori, 2016, *Nature Physics* **12**(9), 826.
- Turpin, A., J. Polo, Y. V. Loiko, J. Küber, F. Schmaltz, T. K. Kalkandjiev, V. Ahufinger, G. Birkl, and J. Mompert, 2015, *Optics Express* **23**(2), 1638.
- Uchino, S., 2020, *Physical Review Research* **2**, 023340.
- Uchino, S., and J.-P. Brantut, 2020, *Physical Review Research* **2**, 023284.
- Uchino, S., and M. Ueda, 2017, *Physical Review Letters* **118**, 105303.
- Uchino, S., M. Ueda, and J.-P. Brantut, 2018, *Physical Review A* **98**, 063619.
- Vaidman, L., 2012, *Physical Review A* **86**, 040101.
- Valado, M., C. Simonelli, M. Hoogerland, I. Lesanovsky, J. P. Garrahan, E. Arimondo, D. Ciampini, and O. Morsch, 2016, *Physical Review A* **93**(4), 040701.
- Valtolina, G., A. Burchianti, A. Amico, E. Neri, K. Khani, J. A. Seman, A. Trombettoni, A. Smerzi, M. Zaccanti, M. Inguscio, and G. Roati, 2015, *Science* **350**(6267), 1505.
- Valtolina, G., F. Scazza, A. Amico, A. Burchianti, A. Recati, T. Enss, M. Inguscio, M. Zaccanti, and G. Roati, 2017, *Nature Physics* **13**(7), 704.
- Verdú, J., H. Zoubi, C. Koller, J. Majer, H. Ritsch, and J. Schmiedmayer, 2009, *Physical Review Letters* **103**(4), 043603.
- Victorin, N., T. Haug, L.-C. Kwek, L. Amico, and A. Minguzzi, 2019, *Physical Review A* **99**(3), 033616.
- Waintal, X., G. Fleury, K. Kazymyrenko, M. Houzet, P. Schmitteckert, and D. Weinmann, 2008, *Physical Review Letters* **101**(10), 106804.
- Wang, Y., S. Subhankar, P. Bienias, M. Lacki, T.-C. Tsui, M. A. Baranov, A. V. Gorshkov, P. Zoller, J. V. Porto, and S. L. Rolston, 2018, *Physical Review Letters* **120**(8), 083601, ISSN 0031-9007.
- Wang, Y.-H., A. Kumar, F. Jendrzejewski, R. M. Wilson, M. Edwards, S. Eckel, G. K. Campbell, and C. W. Clark, 2015, *New Journal of Physics* **17**, 125012.
- Wang, Y.-J., D. Z. Anderson, V. M. Bright, E. A. Cornell, Q. Diot, T. Kishimoto, M. Prentiss, R. A. Saravanan, S. R. Segal, and S. Wu, 2005, *Physical Review Letters* **94**(9), 090405.
- Watabe, S., and Y. Kato, 2008, *Physical Review A* **78**(6), 063611.
- Webb, R. A., S. Washburn, C. Umbach, and R. Laibowitz, 1985, *Physical Review Letters* **54**(25), 2696.
- van Wees, B. J., H. van Houten, C. W. J. Beenakker, J. G.

- Williamson, L. P. Kouwenhoven, D. van der Marel, and C. T. Foxon, 1988, *Physical Review Letters* **60**, 848.
- Weiss, C., and Y. Castin, 2009, *Physical Review Letters* **102**(1), 010403.
- Wharam, D. A., T. J. Thornton, R. Newbury, M. Pepper, H. Ahmed, J. E. F. Frost, D. G. Hasko, D. C. Peacock, D. A. Ritchie, and G. A. C. Jones, 1988, *Journal of Physics C* **21**(8), L209.
- White, D. H., T. A. Haase, D. J. Brown, M. D. Hoogerland, M. S. Najafabadi, J. L. Helm, C. Gies, D. Schumayer, and D. A. W. Hutchinson, 2020, *Nature Communications* **11**(1).
- Wright, E., J. Arlt, and K. Dholakia, 2000, *Physical Review A* **63**(1), 013608.
- Wright, K. C., R. B. Blakestad, C. J. Lobb, W. D. Phillips, and G. K. Campbell, 2013a, *Physical Review Letters* **110**(2), 025302.
- Wright, K. C., R. B. Blakestad, C. J. Lobb, W. D. Phillips, and G. K. Campbell, 2013b, *Physical Review A* **88**(6), 063633.
- Wu, S., E. Su, and M. Prentiss, 2007, *Physical Review Letters* **99**(17).
- Wu, S., Y.-J. Wang, Q. Diot, and M. Prentiss, 2005, *Physical Review A* **71**(4), 043602.
- Xhani, K., E. Neri, L. Galantucci, F. Scazza, A. Burchianti, K.-L. Lee, C. F. Barenghi, A. Trombettoni, M. Inguscio, M. Zaccanti, G. Roati, and N. P. Proukakis, 2020, *Physical Review Letters* **124**, 045301.
- Xiang, Z.-L., S. Ashhab, J. Q. You, and F. Nori, 2013, *Reviews of Modern Physics* **85**(2), 623.
- Yakimenko, A., Y. Bidasyuk, M. Weyrauch, Y. Kuriatnikov, and S. Vilchinskii, 2015, *Physical Review A* **91**(3), 033607.
- Yakimenko, A., S. Vilchinskii, Y. Bidasyuk, Y. Kuriatnikov, K. Isaieva, and M. Weyrauch, 2014, *ArXiv e-prints*, 1411.3490.
- Yao, J., B. Liu, M. Sun, and H. Zhai, 2018, *Physical Review A* **98**, 041601.
- You, J.-S., R. Schmidt, D. A. Ivanov, M. Knap, and E. Demler, 2019, *Physical Review B* **99**, 214505.
- Yu, D., L. C. Kwek, L. Amico, and R. Dumke, 2017a, *Quantum Science and Technology* **2**(3), 035005.
- Yu, D., L. C. Kwek, L. Amico, and R. Dumke, 2017b, *Physical Review A* **95**(5), 053811.
- Yu, D., L. C. Kwek, L. Amico, and R. Dumke, 2018a, *Physical Review A* **98**, 033833.
- Yu, D., A. Landra, L. C. Kwek, L. Amico, and R. Dumke, 2018b, *New Journal of Physics* **20**(2), 023031.
- Yu, D., A. Landra, M. M. Valado, C. Hufnagel, L. C. Kwek, L. Amico, and R. Dumke, 2016a, *Physical Review A* **94**(6), 062301.
- Yu, D., M. M. Valado, C. Hufnagel, L. C. Kwek, L. Amico, and R. Dumke, 2016b, *Physical Review A* **93**(4), 042329.
- Yu, D., M. M. Valado, C. Hufnagel, L. C. Kwek, L. Amico, and R. Dumke, 2016c, *Scientific Reports* **6**, 38356.
- Yu, N., and M. Fowler, 1992, *Physical Review B* **45**, 11795.
- Zabow, G., R. S. Conroy, and M. G. Prentiss, 2004, *Physical Review Letters* **92**(18), 180404.
- Zaccanti, M., and W. Zwerger, 2019, *Physical Review A* **100**, 063601.
- Zapata, I., and F. Sols, 2009, *Physical Review Letters* **102**(18), 180405.
- Zapata, I., F. Sols, and A. J. Leggett, 1998, *Physical Review A* **57**, R28.
- Zhang, B., M. Siercke, K. S. Chan, M. Beian, M. J. Lim, and R. Dumke, 2012, *Physical Review A* **85**, 013404.
- Zobay, O., and B. M. Garraway, 2001, *Physical Review Letters* **86**(7), 1195.
- van Zoest, T., N. Gaaloul, Y. Singh, H. Ahlers, W. Herr, S. Seidel, W. Ertmer, E. Rasel, M. Eckart, E. Kajari, *et al.*, 2010, *Science* **328**(5985), 1540.
- Zöllner, S., H.-D. Meyer, and P. Schmelcher, 2008, *Physical Review Letters* **100**, 040401.
- Zou, Y. Q., E. Le Cerf, B. Bakkali-Hassani, C. Maury, G. Chauveau, P. C. M. Castilho, R. Saint-Jalm, S. Nascimbene, J. Dalibard, and J. Beugnon, 2021, *Journal of Optics B* **54**(8), 08LT01.
- Zozulya, A. A., and D. Z. Anderson, 2013, *Physical Review A* **88**(4).
- Zupancic, P., P. M. Preiss, R. Ma, A. Lukin, M. E. Tai, M. Rispoli, R. Islam, and M. Greiner, 2016, *Optics Express* **24**(13), 13881.
- Zvyagin, A. A., and I. V. Krive, 1995, *Low Temperature Physics* **21**, 533.